

The Role of Plant Growth Promoting Hormones in Phytoplankton-Bacteria Interactions

by Abeeha Khalil

Thesis submitted in fulfilment of the requirements for
the degree of

Doctor of Philosophy

under the supervision of Prof. Justin Seymour and Dr. Jean-Baptiste Raina

University of Technology Sydney
Faculty of Science

October 2024

Certificate of Original Authorship:

I, Abeeza Khalil, declare that this thesis, is submitted in fulfilment of the requirements for the award of Doctorate of Philosophy, in the Faculty of Science at the University of Technology Sydney.

This thesis is wholly my own work unless otherwise referenced or acknowledged. In addition, I certify that all information sources and literature used are indicated in the thesis.

This document has not been submitted for qualifications at any other academic institution.

This research is supported by the Australian Government Research Training Program.

Production Note:

Signature: Signature removed prior to publication.

Date: 07/10/24

Thesis Acknowledgements:

First and foremost, I would like to thank my supervisors, **Prof. Justin Seymour** and **Dr. Jean-Baptiste Raina**, for taking me on as an Honours student and then as a PhD candidate. My journey as a PhD student over the last four years has, at times, been difficult, but with their guidance, mentoring, and encouragement, I have become a better scientist. They have shown immense dedication in helping me achieve what you are reading today. I am extremely grateful for the long hours both of them have devoted to helping me, from teaching me in the labs to editing my manuscripts. Thank you for pushing me to reach my fullest potential. I truly couldn't have asked for better supervisors.

A special thank you to **Dr. Alen Faiz** for assisting me with my CRISPR experiments and sharing your extensive knowledge about genetic engineering. I would also like to thank **Dr. Anna Bramucci** for her support during the first few months of my PhD. A big thank you to the UTS staff, including **Phil Doughty** for taking care of all the labs, and **Chris Songsomboon** for helping me with R codes and for always being a ray of sunshine whenever I needed assistance.

Thank you to all the members of the Ocean Microbiology Group, particularly **Dr. Amaranta Focardi** for assisting me with all thing's bioinformatics, **Dr. Nahshon Siboni** for helping me run my Python scripts, and **Dr. Maeva Brunet** for answering the millions of questions I had.

I would like to thank my mum, **Farhat Naveed**, for always taking care of me, my dad, **Khalil Awan**, for inspiring me to become a doctor just like him, my brother, **Raakin Awan**, for laughing with me until we cry and for picking me up from the station every day after university, my sister, **Sadaf Khalil**, and brother-in-law, **Dan Kew**, for always listening to me talk about my PhD and for giving me the cutest niece, **Ayla Kew**, who has made the difficult days easier. Finally, my husband, **Shawn Price**, for always being by my side. This thesis is dedicated to all of them, their support has been invaluable.

Table of Contents

Certificate of Original Authorship:	i
Thesis Acknowledgements:	iii
Preface.....	xiii
General Abstract:.....	xiv
Chapter 1: General Introduction:	1
1.1 Life in the ocean: The essential role of phytoplankton in marine ecosystems	1
1.2 Microbes of the ocean: understanding phytoplankton and bacteria interactions.....	1
1.2.1 The phycosphere: A microscopic microcosm in the Ocean	2
1.3 Plant growth promoting hormones in terrestrial systems:	5
1.4 Plant growth promoting hormones in phytoplankton-bacteria interactions:	6
Chapter 2:	9
2.2 Materials and Methods:.....	12
2.2.1 Diatom – Bacteria model system:	12
2.2.2 Genome sequencing and genomic survey of PGPH biosynthesis pathway genes in bacterial isolates:.....	12
2.2.3 Extraction protocol for PGPH quantification:	13
2.3.4 Chemical characterisation using LC MS-MS analysis:	15
2.3.5 PGPH and cell density index correlation analysis:	15
2.3.6 Measuring the effect of PGPH on diatom growth:	16
2.3 Results:.....	18
2.3.1 Genomic survey of PGPH biosynthesis pathway genes in bacterial isolates:	18
2.3.2 Indole-3 acetic acid biosynthesis pathway:	18
2.3.4 Trans-zeatin, Abscisic acid and Jasmonic acid Brassinosteroid Pathways:	22
2.3.5 Quantification of PGPH production by bacterial isolates:.....	22
2.3.6 Relationship between phytoplankton growth and PGPH concentrations:	24
2.3.7 Measuring the effect of PGPH on <i>Actinocyclus</i> sp. growth:	25
2.4 Discussion:	29
2.4.1 Widespread production of bacterial-produced PGPHs:	29
2.4.2 Effect of bacterial-produced PGPH on marine diatoms:	30
2.5 Conclusion:	32
3.1 Introduction:	35
3.2 Methods:	37
3.2.1 Diatom and bacteria culturing:	37
3.2.2 CRISPR – Cas9 editing in <i>A. mediterranea</i>:	37
3.2.3 Vector Design:	38

3.2.4 Expression Vector Construction:	39
3.2.5 Transformation and Screening:	39
3.2.6 Gene Knockout:	39
3.2.7 IAA characterisation using LC-MS/MS analysis:	41
3.2.8 Cogrowth experiments:	42
3.3 Results:	44
3.3.1 CRISPR-Cas9 mediated knockout of IAA in <i>A. mediterranea</i>:	44
3.3.2 Quantification of IAA production by bacterial and phytoplankton isolates:	46
3.3.3 Co-growth experiments:	47
3.4 Discussion:	50
3.4.1 Understanding single-metabolite interactions through genetic engineering:	50
3.4.2 The role of IAA in phytoplankton-bacteria interactions:	51
3.4.3 Effects of IAA on other phytoplankton species:	51
3.5 Conclusion:	53
Chapter 4:	54
4.1 Introduction:	55
4.2 Methods:	57
4.2.1 IAA and GA gene collation and <i>Tara Oceans</i> metagenomic data:	57
4.2.2 Bacteria-phytoplankton network analysis:	57
4.2.3 Statistical analysis:	58
4.3 Results:	59
4.3.1 Taxonomy and relative abundance of bacteria harbouring IAA biosynthesis gene homologues in the ocean:	59
4.3.2 Geographical abundance of bacterial-IAA genes:	61
4.3.2.1 Presence IAA genes in sea surface samples:	61
4.3.2.2 Presence of IAA genes in deep chlorophyll maximum samples:	61
4.3.3 Taxonomy and relative abundance of bacteria harbouring GA biosynthesis gene homologues in the ocean:	64
4.3.4 Geographical distribution of bacterial-GA genes:	65
4.3.4.1 Presence of GA genes in sea surface samples:	65
4.3.4.2 Presence of GA genes in deep chlorophyll maximum samples:	65
4.3.5 Correlations between environmental variables and abundance of IAA and GA genes:	68
4.3.6 Bacteria-phytoplankton network analysis:	68
4.4 Discussion:	70
4.4.1 Bacterial groups that possess IAA and GA biosynthesis genes:	70
4.4.2 Widespread presence of IAA and GA genes in the global ocean:	71

4.4.3 Associations between phytoplankton and PGPH-synthesising bacteria:	72
4.5 Conclusion:	73
Chapter 5: General Discussion	74
5.1 Phytoplankton-associated bacteria produce many PGPHs:	75
5.2 PGPH-producing bacteria are taxonomically divers:	75
5.3 PGPHs have an impact on phytoplankton growth:	76
5.4 Genomic potential for PGPHs production is widespread in the ocean:	77
5.5 PGPH-synthesising bacteria form putative associations with phytoplankton in the marine environment:	77
5.6 Future directions:	78
Conclusion:	78
Appendix:	80
References:	91

List of Figures:

Figure 1.1: Chemical exchanges in the phycosphere and rhizosphere. A) Chemical exchanges between roots and bacteria in the rhizosphere (colour gradient around the roots where plant-bacteria interactions occur). Bacteria can get access to plant-derived nutrients through root exudations and initiate reciprocal exchanges of micronutrients affecting plant growth and function. Examples of mutualistic interactions are shown with curved arrows. Plant growth promoting hormones (PGPH) such as Abscisic acid and Brassinosteroid can be produced by bacteria in exchange for photosynthates. **B)** Chemical exchanges between phytoplankton and bacteria within the phycosphere (colour gradient around the cells where phytoplankton-bacteria interactions occur). Example of mutualistic interactions occurring between bacteria cells and phytoplankton are shown with curved arrows. The brown bacterium (right) depicts the exchange of bacteria-derived PGPHs in exchange of phytoplankton-produced DOC.4

Figure 2.1: Indole-3 acetic acid biosynthesis pathway and production potential in the 14 bacteria isolates. A) Tryptophan dependent IAA pathways in bacteria. Five main IAA biosynthesis pathways, including the Indole-3 acetonitrile (red), Indole-3-acetamide (blue), Tryptophan side chain oxidase (purple), Indole-3-pyruvate (yellow), and Tryptamine (green) pathways are depicted. Intermediate molecules are depicted with black bold text. IAOx, Indole-3-acetaldoxime; IAN, Indole-3-acetonitrile; IAM, indole-3-acetamide; IPyA, Indole-3-pyruvate; TrypA, Tryptamine; IAld, indole-3-acetaldehyde. Enzymes are depicted un-bold black text and lines. CYP79B2/3, cytochrome P450; IAOxD, Indole-acetaldoxime dehydratase; NIT, Nitrilase; NH, Nitrile hydrolase; IaaM, Tryptophan-2-monooxygenase; IaaH, Indole-3-acetamide hydrolase; TSO, Tryptophan side-chain oxidase; IPDC, TDC, Tryptophan decarboxylase; Indole-3-pyruvate decarboxylase; AO, Amine oxidase; IAaldD, indole-3-acetaldehyde dehydrogenase. **B)** Heatmap of the presence of orthologues for IAA biosynthesis in the 14 bacterial strains tested. Grey squares depict the detection of orthologues of IAA synthesis genes (bottom) in the bacteria (left), as indicated by a BLASTp search (e-value < 10⁻¹⁰, Supplementary Table S2 19

Figure 2.2: Gibberellic acid biosynthesis pathway and production potential in the 14 bacteria isolates. A) GA pathway in bacteria. Each stage of the pathway is categorised by red (stage 1), blue (stage 2) and green (stage 3) coloured arrows. GA biosynthesis pathway intermediate molecules are depicted with black bold text. GGDP, Geranylgeranyl diphosphate; CCP, Copalyl diphosphate; KA, Ent-kaurene; GA₁₂-ald, Gibberellic acid-12-aldehyde; GA,

Gibberellic acid. Genes and enzymes are depicted with un-bold black text. CPS, Copalyl diphosphate synthase; KS, Kaurene synthase; KO, Kaurene oxidase KAO, Kaurenoic acid oxidase 20ox, 20-oxoglutarate-dependent dioxygenase; 3ox, 3-oxidase. **B)** The presence of orthologues for GA biosynthesis in the 14 bacterial strain tested. Grey squares depict the detection of orthologues of GA synthesis genes (bottom) in the bacteria (left), as indicated by a BLASTn and BLASTp search (e-value $< 10^{-10}$, Supplementary Table S4).....21

Figure 2.3: Quantification of intracellular concentrations of plant growth promoting hormones (μg/cell) in the 14 bacterial strains tested. A heat map illustrating the intracellular concentration (coloured squares) of the plant growth promoting hormones Indole -3 acetic acid (IAA), Indole -3 butyric acid (IBA), Abscisic acid (ABA), Gibberellic acid (GA), Jasmonic acid (JA), Trans-zeatin (TZ) and Brassinolide (BSN) of the 14 bacteria tested.....23

Figure 2.4: Quantification of plant growth promoting hormones (μg/cell) exuded by the 14 bacterial strains tested. A heat map illustrating the concentration (coloured squares) of the plant growth promoting hormones Indole -3 acetic acid (IAA), Indole -3 butyric acid (IBA), Abscisic acid (ABA), Gibberellic acid (GA), Jasmonic acid (JA), and Trans-zeatin (TZ) released into the surrounding media from the 14 bacteria tested. Extracellular quantification of BSN was not conducted as extraction protocols to detect released concentrations of BSN have not yet been developed.....24

Figure 2.5: Correlation analysis between extracellularly-released PGPHs and maximum Actinocyclus growth-enhancement in co-culture experiments. As reported in Le Reun et. al. 2023, Actinocyclus growth enhancement (cell density index) was calculated by calculating the area under the curve (AUC) for each bacteria co-culture **A)** Correlogram for each PGPH tested (the size and colour of each bubble is proportional to the strength of the correlation). Only statistically significant correlations are not crossed (Pearson's correlation, $p < 0.05$). **B)** Linear regression of the only statistically supported correlation. The x-axis represents released IAA concentrations measured for each bacterial isolate (μg/cell) while the y-axis represents the maximum growth enhancement of Actinocyclus cells for 12 out of the 14 bacteria isolates when co-grown with Actinocyclus (Le Reun et al., 2023). R-square and p-value (Pearson's correlation) are displayed in italic.....25

Figure 2.6: Growth over the course of 11 days of Actinocyclus inoculated with IAA, GA, IBA, ABA, JA, TZ, BSN and the average PGPH concentration released by the 14 bacteria. **A)** Actinocyclus cell numbers per millilitre in response to three different IAA concentrations (chosen based on quantifications data, see methods). **B)** Actinocyclus cell numbers per millilitre in response to three different GA concentrations (chosen based on quantifications

data, see methods). Error bars are standard error of the mean (SEM), n = 4. A significant difference between a given concentration and the control is depicted as an empty circle (Repeated-measures ANOVA, p<0.05, Supplementary Table S15) and red arrows depict inoculation times for IAA and GA treatments (2 d and 6 d for both). Number of *Actinocyclus* sp. cells per millilitre (y-axis) when treated with **C**) IBA, **D**) ABA, **E**) JA, **F**) TZ, **G**) BSN at three different concentrations. The blue line, yellow line and red line each represent concentrations of 1×10^{-12} , 1×10^{-11} and 1×10^{-10} $\mu\text{g/mL}$ for IBA, ABA, JA and BSN, 1×10^{-10} , 1×10^{-9} and 1×10^{-8} for BA and 1×10^{-9} , 1×10^{-8} and 1×10^{-7} $\mu\text{g/mL}$ for TZ. *Actinocyclus* sp. axenic control grown solely in F/2 is represented by the black line with filled circles over the course of 11 days (y-axis). The data displays a typical phytoplankton growth curve pattern with a lag, exponential, and stationary phases. Error bars are displayed as black vertical lines on each data point (\pm SEM; n = 4). Significant difference depicted as empty circle data points (Simple Main Effect Test, p<0.05, Supplementary Table S15). H: Average Extracellular PGPHs released by the 14 bacteria. Error bars are SEM, n=56.....28

Figure 3.1: Tryptophan-dependent Indole-3 acetic acid biosynthesis pathway in *A. mediterranea*. A) Homologs of two IAA biosynthesis pathways, Indole-3-acetamide (blue) and Tryptamine (red) pathways were identified in the genome of *A. mediterranea*. Intermediate molecules are depicted with black bold text and the targeted gene is highlighted. IAM, indole-3-acetamide; TrypA, Tryptamine; IAALd, indole-3-acetaldehyde (highlighted in yellow). Enzymes are depicted un-bold black text and lines. IaaM, Tryptophan-2-monooxygenase; IaaH, Indole-3-acetamide hydrolase; TDC, Tryptophan decarboxylase; AO, Amine oxidase; IAALdD, indole-3-acetaldehyde dehydrogenase. **B)** E-values and percentage similarity of *A. mediterranea* homologous proteins to closely related bacteria, using Blastp searches for bacterial homologs. BLASTp hits with an e-value $\geq 10^{-10}$ or less was used as a cut-off. 38

Figure 3. 2: CRISPR-Cas9 knockout protocol. The left side depicts A) preparation of gRNA oligonucleotide sequences specific to IAALdD expression with flanking regions complementary to the pST_140_LVL2_cam plasmid, B) ligation of gRNA to pST_140_LVL2_cam plasmid backbone, C) clone and selection of plasmid with DH5 α *E. coli* colonies and D) transfection of purified plasmid with IAALdD gRNA into *A. mediterranea*. The right side shows the process of the Cas9 protein editing the *A. mediterranea* genome to knockout expression of IAALdD.40

Figure 3.3: Confirmation of IAALdD gene knockout in *A. mediterranea*. A) Aligned IAALdD gene sequences for the wildtype and mutant *A. mediterranea*. The top sequence

displays the gRNA, which corresponds to the first 20 base pairs of the IAALdD gene. The middle sequence shows the wildtype *A. mediterranea* strain, and the bottom sequence represents the mutant *A. mediterranea*, the dashed line indicating the point mutation. Amino acid translation (letters under the sequence) indicate a stop codon at the site of the knockout. **B)** Indel (insertions and deletions) spectrum plot with x-axis depicting the type of indels in the IAALdD-deficient mutant compared to the wildtype, while the y-axis highlights the frequency and proportion of each indel type. **C)** Aberrant sequence signal plot showing the percentage of sequence variance between mutant (test) vs. wildtype (control) *A. mediterranea*. Bars indicate the frequency of aberrant sequences at each base pair, the height of each bar represents the level of sequence variation/deviation from the wildtype sequence.**Error! Bookmark not defined.**

Figure 3.4: Quantification of IAA in *A. mediterranea*. **A)** LC-MS/MS chromatogram depicting peak intensity of wildtype *A. mediterranea* (red), mutant *A. mediterranea* (blue), and Marine Broth control (green). **B)** Biovolume concentration of IAA produced by mutant (blue) and wildtype (red) *A. mediterranea*. Error bars are standard error of the mean (SEM), n = 4.

.....46

Figure 3.5: Quantification of IAA in in three phytoplankton species. **A)** LC-MS/MS chromatogram depicting peak intensity of *Actinocyclus* sp. (orange), *N. oceanica* (blue) and *P. tricornutum* (green). Error bars are standard error of the mean (SEM), n = 4. **B)** Biovolume concentration of IAA produced by *Actinocyclus* sp. (orange), *N. oceanica* (blue) and *P. tricornutum* (green). Error bars are standard error of the mean (SEM), n = 4. Significant differences are depicted with asterisks (*; One-way ANOVA, p<0.05, Table S3.4)......47

Figure 3.6: Growth of three phytoplankton species with wild-type and IAALdD-deficient *A. mediterranea* over the course of 20 days. Phytoplankton cell numbers per millilitre in co-culture with IAALdD-deficient mutant (red), and wild-type (blue) *A. mediterranea*, compared to the axenic controls (green). **A)** Growth dynamics of *Actinocyclus* sp. co-cultures (n = 5); **B)** *P. tricornutum* co-cultures (n = 5); and **C)** *N. oceanica* co-culture (n = 3). A significant difference between a given concentration and the control is depicted as an empty circle (Repeated-measures ANOVA, p<0.05, Supplementary table S3.3)......49

Figure 4.1: Relative abundance (%) of bacteria that harboured IAA biosynthesis gene homologues. Bacteria are coloured based on taxonomy (order), with similar colours associated to closely related bacteria. 60

Figure 4.2: Distribution of indole-3-acetic acid (IAA) gene relative abundances across the Tara Oceans sites. A) IAA gene relative abundance at sea surface. B) IAA gene relative abundance at deep chlorophyll max. Colour-coded circles are representative of the varying abundance proportion of genes at each site. The bar chart on the left of the map illustrates the average abundance of IAA genes within nine different ocean regions (as defined in IHO General Sea Areas 1953), error bars are standard error of the mean (SEM) and significant differences are marked with letters (Wilcoxon pairwise test, $p<0.05$, Supplementary Table S4.1).	63
Figure 4.3: Relative abundance (%) of bacteria that harboured GA biosynthesis gene homologues. Bacteria are coloured based on taxonomy (order), with similar colours associated to closely related bacteria.....	64
Figure 4.4: Distribution of gibberellic acid (GA) gene abundance across the Tara Oceans sites. A) Abundance of GA genes at sea surface. B) Abundance of GA genes at deep chlorophyll max depth. Colour-coded circles are representative of the varying abundance of genes at each site, illustration special variability across different oceanic regions and depths. The bar chart on the left of the map illustrates the average abundance of GA genes within each ocean region, error bars are standard error of the mean (SEM) and significant differences are marked with letters (Wilcoxon pairwise test, $p<0.05$, Supplementary Table S4.1).	67
Figure 4.5: Correlations between environmental factors and abundance of IAA and GA gene homologues. Heatmap illustrating the correlation between the abundance of IAA (bottom) and GA (top) gene homologues and environmental variables. Statistically significant correlations are highlighted in colours (Spearman's correlation).	68
Figure 4.6: Correlative network of phytoplankton ASVs and bacterial MAGs that harbour IAA biosynthesis genes. All correlations are positive, nodes are edge weighted based on strength of Spearman's Rho, the stronger the correlation the thicker the line.....	69
Figure 5.1: Schematic summary of the contributions of my research, spanning the microscale to global ocean scale. 1) Interactions between <i>Actinocyclus</i> sp. (green diatom) and heterotrophic bacteria (red, blue, yellow cells) producing IAA (red halo), GA (green halo), and other PGPHs (purple halo) were examined, revealing that IAA had the largest effect on <i>Actinocyclus</i> growth (large arrow), followed by GA (smaller arrow), while other PGPHs had no measurable effects (dashed arrow). 2) A bacterial mutant unable to synthesize IAA (pink bacteria with a cross) had no effects on <i>Actinocyclus</i> growth, indicating that bacterial-synthesized IAA was responsible for nearly all the growth enhancement measured. 3) Global	

distributions of bacterial IAA and GA biosynthesis gene homologues demonstrating that PGPH-synthesizing bacteria are ubiquitous across the global ocean.....74

List of Tables:

Table 1.1: Main plant growth promoting hormones. For each hormone type, the different subtypes, function in plants, and organism producing them are presented. Hormone sub-types that have been identified in phytoplankton-bacteria interactions are presented in bold.....7

Preface

Thesis format:

This thesis is written in the format of a thesis by compilation—a combination of published chapters and those unpublished but with the intention of publication in a peer reviewed scientific journal in the near future. Given that this thesis is presented as a series of ready to submit manuscripts, there is an element of repetition in the introduction of some chapters.

General Abstract:

The ecological interactions between phytoplankton and bacteria are a fundamentally important inter-species relationship in the marine environment, which shape ecosystem productivity by controlling nutrient cycling at the base of aquatic food webs. The relationship between these microorganisms often involves reciprocal exchanges of metabolites. One potentially important category of chemicals exchanged in these interactions are plant growth promoting hormones (PGPHs), which play vital roles in terrestrial systems and have recently been shown to promote the growth of some planktonic microorganisms. However, the diversity of PGPHs produced by marine bacteria, the distribution of genes involved in their synthesis in the global ocean, and the specific effects of these molecules on phytoplankton growth remain unknown.

I first determined the importance of seven different PGPHs in phytoplankton-bacteria interactions (**Chapter 2**). Very little is known about the diversity of PGPHs produced by marine bacteria and their specific effects on phytoplankton growth. Here, we examined the PGPH synthesis capabilities of 14 bacterial strains that had previously been demonstrated to enhance the growth of the common diatom *Actinocyclus*. PGPHs biosynthesis was ubiquitous among the bacteria tested, with all 14 strains displaying the genomic potential to synthesise multiple hormones, and quantification using mass-spectrometry confirming that each strain produced at least 6 out of the 7 tested PGPHs. Some of the PGPHs identified here, such as Brassinolide and Trans-zeatin, have never before been reported in marine microorganisms. All strains produced the growth hormone Indole-3 acetic acid (IAA) in high concentrations and released it into their surroundings. Furthermore, IAA extracellular concentrations were positively correlated with the ability of the strains to promote *Actinocyclus* growth. When added to axenic *Actinocyclus* cultures, IAA and gibberellic acid enhanced the growth of the diatom, with cultures exposed to IAA exhibiting a two-fold increase in cell numbers. Overall the results of Chapter 2 reveal that marine bacteria produce a much broader range of PGPHs than previously suspected and that some of these compounds enhance the growth of a marine diatom.

I next aimed to determine the relative importance of IAA in phytoplankton growth promotion (**Chapter 3**). IAA is just one of a suite of metabolites produced by heterotrophic bacteria, making it challenging to quantify its specific effects on phytoplankton growth. Here, I used a CRISPR-Cas9 gene knockout approach to eliminate IAA production in the marine bacterium *Alteromonas mediterranea* and subsequently quantified the effect of this deficiency on the

growth of three phytoplankton species: the diatoms *Actinocyclus* sp. and *Phaeodactylum tricornutum*, and the marine microalga *Nannochloropsis oceanica*. My results show that bacterial production of IAA provides significant growth enhancement to *Actinocyclus* cells, whereby IAA indeed contributed to over 98% of the observed growth enhancement caused by wildtype *A. mediterranea* strain. This indicates a key role of this hormone in the mutualistic partnership between *A. mediterranea* and *Actinocyclus*. In contrast, wildtype *A. mediterranea* strains only affected the growth of *P. tricornutum* on 8 d of experimentation and had negligible effects on *N. oceanica* growth in co-culture. These findings reveal that the ability of *A. mediterranea* to enhance *Actinocyclus* growth is primarily due to its synthesis of IAA, highlighting the critical role of IAA bacterial provision in promoting phytoplankton growth.

Due to the importance of bacterial production of PGPHs including IAA and GA in governing phytoplankton growth identified in Chapters 2 and 3, I next aimed to investigate the environmental occurrence and global distribution of these PGPHs (**Chapter 4**). Homologues of genes involved in the biosynthesis IAA were present in over 1000 bacterial metagenome-assembled genomes (MAGs) in the world's oceans, while only 9 MAGs had the genomic potential to synthesize GA. Geographical distributions of bacteria that possessed genes required for IAA and GA biosynthesis highlighted that these bacteria were present across 50% of *Tara* Oceans sites, but gene abundances differ greatly between oceanographic regions, and genes were only present in the photic zone. Bacteria that possessed genes for IAA synthesis correlated with phytoplankton abundance in the Ochrophyta taxon, including *Thalassiosira oceanica* and *Pseudo-nitzshia*, suggesting the importance of IAA in specific phytoplankton-bacteria partnerships across global scales. Our findings reveal the wide geographical distribution of IAA genes in the photic zone of world's ocean and identify some strong correlations between bacterial producers of this hormone and specific phytoplankton species *in situ* for the first time.

In summary, this thesis presents new information on the diversity, prevalence and function of PGPHs in the ocean. This work demonstrates that (i) marine heterotrophic bacteria produce and release a much wider diversity of PGPHs than previously anticipated; (ii) the supplementation of some of these PGPHs enhance diatom growth; (iii) the elimination of IAA in a symbiotic bacteria completely removed the growth-promoting capacity of the bacteria, indicating that IAA is likely the most important growth-enhancing molecule exchanged in this specific diatom-bacteria interaction; (iv) bacteria that possess IAA and GA genes are

ubiquitous and form putative associations with phytoplankton across the world's oceans. Together, this research highlights the significance of PGPH exchanges at the base of marine food webs, indicating that these chemicals have the potential to shape microbial community structure and marine productivity.

Chapter 1: General Introduction:

1.1 Life in the ocean: The essential role of phytoplankton in marine ecosystems

Cumulatively, the ocean microbiome (microalgae, protists, bacteria and viruses) represents more than two-thirds of its biomass (Suttle, 2007). These microorganisms are essential to perform important ecological and biogeochemical roles (Field et al., 1998). A large bulk of these microbes are phytoplankton, unicellular photoautotrophic microorganisms that are responsible for up to 40% of aquatic primary production (Falkowski & Knoll, 2007; Guo, 2015; Paerl et al., 2011). In addition to being the main primary producers in marine ecosystems, they play pivotal roles in the cycling of essential elements (e.g., carbon, nitrogen and sulphur), which influences the stability and productivity of marine food-webs (Reynolds, 2006; Shurin et al., 2013; Smith & McBride, 2015). Phytoplankton growth is governed by a complex suite of abiotic factors, including light, temperature, and dissolved nutrients (e.g., nitrogen, phosphorus, and iron) (Reynolds, 2006). In addition, emerging evidence indicates that their growth can be significantly influenced by ecological interactions with other microorganisms, in particular heterotrophic bacteria (Amin et al., 2012; Buchan et al., 2014; Seymour et al., 2017). While some of these bacteria can be parasitic, pathogenic or have no effect on the growth or development of phytoplankton, others are involved in important mutualistic interactions that promote the growth of their phytoplankton host (Amin et al., 2012; Buchan et al., 2014; Le Reun et al., 2023; Matthews et al., 2023; Seymour et al., 2017; Van Tol et al., 2017). Recent laboratory experiments have revealed that these intimate inter-kingdom interactions are often governed by complex and reciprocal exchanges of chemicals (Croft et al., 2005; Durham et al., 2015; Raina et al., 2023; Seymour et al., 2017), influencing the survival and growth of both organisms. Yet, it is becoming clear that previous research has only just begun to scratch the surface of the diversity of chemicals involved in these sophisticated ecological exchanges.

1.2 Microbes of the ocean: understanding phytoplankton and bacteria interactions

Mutualistic interactions between phytoplankton and bacteria are often species-specific, and while occurring between individual cells at the microscale, can ultimately have ecosystem-scale consequences (Cooper & Smith, 2015; Vardi et al., 2009). These interactions include the provision of dissolved organic carbon (DOC) to bacteria, which in turn provide the phytoplankton with limiting re-mineralised nutrients, minerals and micronutrients, and

vitamins (Amin et al., 2012; Seymour et al., 2017). These exchanges are often facilitated by complex chemical signalling between the partners (Amin et al., 2015; Kim et al., 2022), which can trigger metabolic cascades that allow bacteria to express genes related to the production of specific molecules (Amin et al., 2015; Hughes et al., 2018; Kim et al., 2022). For example, the mutually beneficial interaction between the diatom *Thalassiosira pseudonana* and Roseobacter clade member *Ruegeria pomeroyi* involves the catabolic uptake of *T. pseudonana*-produced 2,3- dihydroxypropane-1-sulfonate by *R. pomeroyi*, while in exchange *R. pomeroyi* provides *T. pseudonana* with vitamin B₁₂, a vitamin essential for diatom growth (Croft et al., 2005; Durham et al., 2015). However, the *T. pseudonana* – *R. pomeroyi* and mutualism is just one of a number of emerging sophisticated mutualistic interactions between phytoplankton and bacteria.

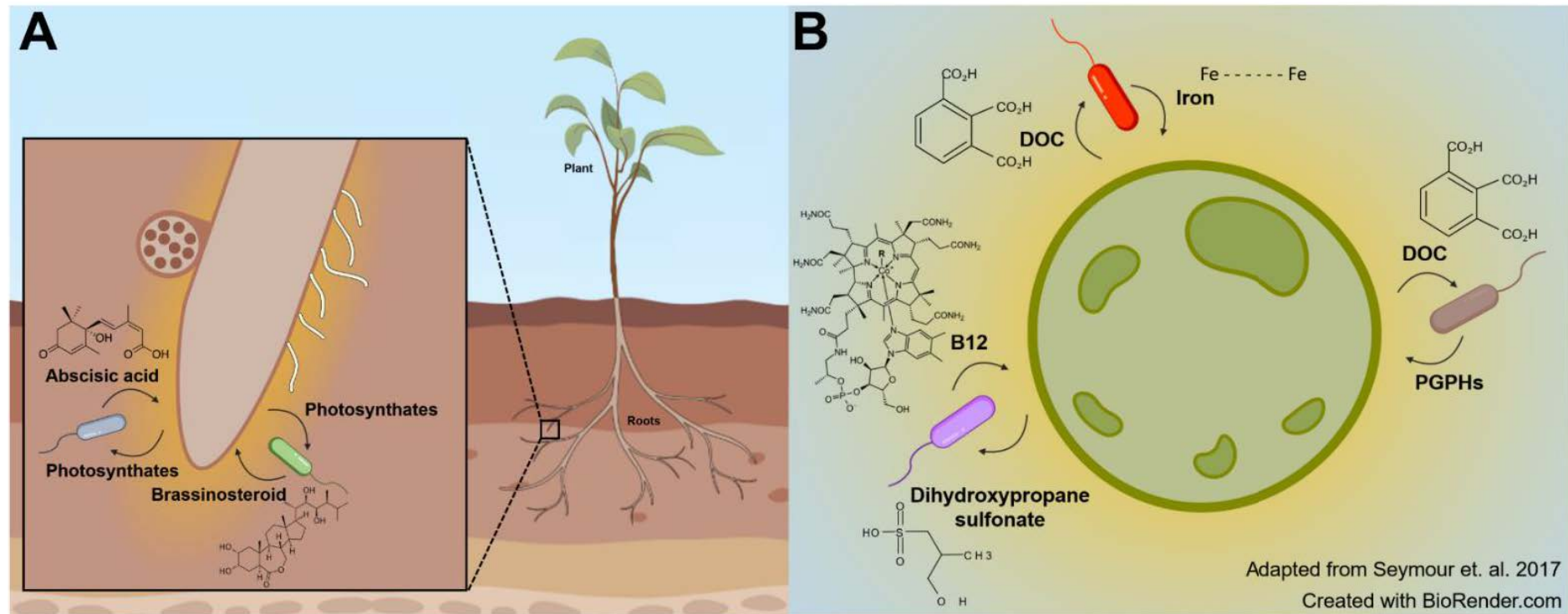
While phytoplankton-bacteria interactions can result in growth benefits for one partner (i.e., commensalism), or both partners (i.e., mutualism), some interactions can be parasitic or antagonistic, leading to growth inhibition or death of the microorganisms (Amin et al., 2012; Seymour et al., 2017a; Cirri and Pohnert, 2019). Antagonistic interactions have been well documented, for instance, the bacterium *Kordia algicida* causes cell lysis in various diatom species, including *Skeletonema costatum*, *Thalassiosira weissflogii*, and *Phaeodactylum tricornutum*, through the release of proteases (Paul and Pohnert, 2011). While, some bacteria kill their algal hosts indirectly, such as *Croceibacter atlanticus*, which inhibit the cell division of *Thalassiosira pseudonana* and benefit from the organic matter released in the process (Van Tol et al., 2017; Bartolek et al., 2022).

1.2.1 The phycosphere: A microscopic microcosm in the Ocean

Intricate chemical exchanges between microbial partners within the vast expanse of the pelagic ocean are perhaps not intuitive, particularly given that, on average, the minimum distance between a bacterium and the nearest phytoplankton in the water column is nearly 1 mm, which is equivalent to a thousand bacterial cell lengths (Bell & Mitchell, 1972; Stocker, 2015). For complex reciprocal exchanges to occur in this setting, phytoplankton and bacteria need to remain in close proximity (Martínez-Pérez et al., 2024), which is believed to occur when bacteria colonise the nutrient rich microenvironment surrounding phytoplankton cells called the phycosphere (Figure 1.1) (Seymour et al., 2017). Phytoplankton derived photosynthates are exuded into the phycosphere through both passive and active transport. For example, most gases and some small molecules can diffuse through the cell membrane passively, while large

or polar molecules typically require active transport (Segev, Wyche, Kim, et al., 2016; Seymour et al., 2017). The constant exudation of photosynthates from phytoplankton generates steep concentration gradients near the cell surface that motile bacteria can exploit through chemotaxis, the capacity of microorganisms to direct their movement up or down chemical gradients (Martínez-Pérez et al., 2024; Seymour et al., 2017). Alternatively, some bacteria attach directly to the surfaces of phytoplankton cells to maximise exposure to phytoplankton-derived metabolites (Martínez-Pérez et al., 2024).

The phycosphere is the aquatic analogue of the well-studied rhizosphere in terrestrial systems, the region of soil directly adjacent to the roots that is chemically influenced by the plant's activity (Figure 1.1) (Curl & Truelove, 1986; Ross et al., 2011; Ross & Reid, 2010). Many parallels exist between the rhizosphere and the phycosphere. For instance, microbial behaviours, such as chemotaxis, are central to the establishment of interactions in both microenvironments (Smriga et al., 2016). Additionally, microorganisms in both environments exchange similar suites of chemicals with their respective hosts (Amin et al., 2015; Seymour et al., 2017). Although the beneficial influence of rhizosphere bacteria on plant biology are well established (Gaskins et al., 1985; Yang et al., 2009), the influence of bacteria inhabiting the phycosphere on phytoplankton growth rate and fitness remains less understood (Attar, 2015; Seymour et al., 2017)



1

2 **Figure 1.1: Chemical exchanges in the phycosphere and rhizosphere. A)** Chemical exchanges between roots and bacteria in the rhizosphere
 3 (colour gradient around the roots where plant-bacteria interactions occur). Bacteria can get access to plant-derived nutrients through root exudations
 4 and initiate reciprocal exchanges of micronutrients affecting plant growth and function. Examples of mutualistic interactions are shown with curved
 5 arrows. Plant growth promoting hormones (PGPH) such as Abscisic acid and Brassinosteroid can be produced by bacteria in exchange for
 6 photosynthates. **B)** Chemical exchanges between phytoplankton and bacteria within the phycosphere (colour gradient around the cells where
 7 phytoplankton-bacteria interactions occur). Example of mutualistic interactions occurring between bacteria cells and phytoplankton are shown
 8 with curved arrows. The brown bacterium (right) depicts the exchange of bacteria-derived PGPHs in exchange of phytoplankton-produced DOC.

1.3 Plant growth promoting hormones in terrestrial systems:

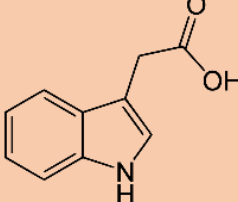
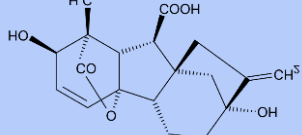
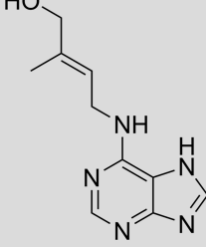
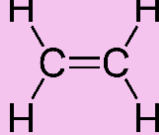
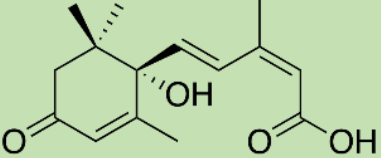
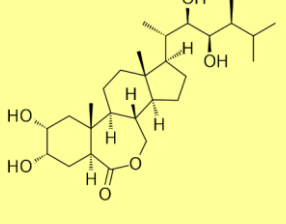
Many rhizosphere-associated bacteria produce hormones that have a positive influence on plant growth (Curl & Truelove, 1986; Ross & Reid, 2010). Five major classes of these ‘plant-growth promoting hormones’ (PGPHs) exist: auxins, gibberellins, cytokinins, ethylenes and abscisic acid, each governing specific cellular mechanism within plants (Table 1.1) (Reynolds, 2006; Wilkinson et. al., 2010). Many PGPHs benefit plant growth by promoting root and stem elongation (Zhao, 2010; Goswami, Thakker and Dhandhukia, 2016), aiding seed germination (Wang and Irving, 2011; Spaepen, 2015; Salazar-Cerezo et al., 2018), promoting cell division (Timmusk et al., 1999; Moubayidin, Di Mambro and Sabatini, 2009; Spaepen, 2015), controlling fruit ripening (Ross et al., 2011; Spaepen, 2015; Yaish, Antony and Glick, 2015), and promoting formation of plant tissues (Wilkinson and Davies, 2010; Wang and Irving, 2011; Spaepen, 2015). More recently, other phytohormones such as Lactones, steroids and Jasmonates have also been discovered, and are believed to play a role in reproductive functions (Smith, Li and Li, 2017; Eng et al., 2018) and plant immunity (Yopp, Mandava and Sasse, 1981; Mandava, 2003; Ross and Reid, 2010). There is evidence that these different PGPHs govern specific mechanisms at the cellular, tissue and organismal level in plants, resulting in beneficial effects on plant health (Ross and Reid, 2010). At the molecular level, these hormones control cellular processes by interacting with specific receptors and activating downstream transcriptional pathways. Indole-3-acetic acid (IAA), for instance, functions by promoting repressor proteins, thereby releasing auxin response factors to regulate gene expression involved in cell elongation and division (Moubayidin et al., 2009; Spaepen et al., 2007). Gibberellins bind to receptors, leading to the degradation of specific transcriptional repressors thereby promoting growth, germination, and developmental transitions (Wang and Irving, 2011; Spaepen, 2015; Salazar-Cerezo et al., 2018)

Among auxins, one of the most prevalent PGPHs, IAA has been extensively studied for its roles in cell enlargement, division and tropism (Labeeuw et al., 2016; Moubayidin et al., 2009; Spaepen et al., 2007). Notably, IAA has also been identified as a potentially important chemical currency in the phycosphere (Amin et al., 2015; Croft et al., 2005; Durham et al., 2015), demonstrating the possible significance of PGPHs in phytoplankton-bacteria interactions.

1.4 Plant growth promoting hormones in phytoplankton-bacteria interactions:

Growing evidence for the involvement of PGPHs in phytoplankton-bacteria interactions has recently been developing. In the symbiotic partnership between the Alphaproteobacterium *Sulfitobacter* sp. and the diatom *Pseudo-nitzschia multiseries*, tryptophan produced and secreted by *P. multiseries* is subsequently used by *Sulfitobacter* to produce IAA, which is then used by *P. multiseries* and enhances the diatoms growth (Amin et al., 2015). Additionally, the provision of IAA by specific bacteria, including *Labrenzia* and *Marinobacter*, has been shown to enhance the growth of dinoflagellate Symbiodiniaceae (Matthews et al., 2023). It has also been demonstrated that when *Methylobacteria* was co-incubated with different phytoplankton (*Chlorella vulgaris*, *Scenedesmus vacuolatus*, and *Haematococcus lacustris*), up to a 14-fold increase in algal biomass occurred, with subsequent analysis of the *Methylobacteria* genome revealing the presence of genes involved in the synthesis of PGPHs (Krug et al., 2020). PGPHs may also have species-specific effects across different phytoplankton species, with some evidence that specific phytohormones promote growth in some species, but hinder growth in others (Cirri & Pohnert, 2019). However, the diversity of PGPHs produced by phytoplankton-associated bacteria, the extent of their influence on the growth of different groups of phytoplankton, and the relative importance of PGPHs compared to other metabolites released by bacteria in the phycosphere are all critical, but unanswered questions.

Table 1.1: Main plant growth promoting hormones. For each hormone type, the different subtypes, function in plants, and organism producing them are presented. Hormone sub-types that have been identified in phytoplankton-bacteria interactions are presented in bold.

Hormone Type	General Hormone Structure	Hormone Sub-types (most to least abundant)	Function in Plants	Producing organism
Auxin		Indole-3-acetic acid 4-Chloroindole-3-acetic acid 2-phenylacetic acid Indole-3-butyric acid Indole-3-propionic acid	Promote stem and root elongation towards nutrients.	Heterotrophic bacteria (<i>Bacillus</i> , <i>Pseudomonas</i> , <i>Escherichia</i> , <i>Micrococcus</i> and <i>Staphylococcus</i>).
Gibberellin		Gibberellic acid	Developmental processes like elongation of stems, seed germination and dormancy.	Fungi and heterotrophic bacteria.
Cytokinin		Zeatin Trans-zeatin Kinetin Benzyl-aminopurine Diphenylurea Thidiazuron	Promote cell division (cytokinesis) in roots and shoots.	Heterotrophic bacteria (<i>Agrobacterium</i> and <i>Pseudomonas</i>).
Ethylene		Ethylene	Controls fruit ripening.	Fungi and heterotrophic bacteria.
Abscisic Acid		Abscisic acid	Promotes development of plant tissue pathways by inhibits cell division.	Fungi and heterotrophic bacteria.
Steroids		Brassinosteroid	Regulates development process and are essential for plant immunity.	Heterotrophic bacteria

Microscale interactions between phytoplankton and bacteria are complex and involve multifaceted chemical communications, and although many studies have explored the presence of bacterial-synthesised metabolites, understanding the relative importance of specific metabolites remains unclear. On a global scale, the distribution and abundance of key metabolites like nitrogen and iron have been thoroughly explored due to their importance in biogeochemical cycles, however, biogeographical studies of emerging important metabolites, like PGPHs, are rare. As PGPHs have the potential to affect oceanic productivity by enhancing phytoplankton growth, a clearer understanding of the diversity of molecules produced by phytoplankton-associated bacteria, the roles of these molecules and the distribution of bacteria producing them is critical. Within this context, the overarching aim of my PhD thesis is to understand the role of PGPHs in phytoplankton-bacteria interactions. To achieve this aim, I will address the following three objectives:

- 1. Identify the capacity of diverse bacterial associates to produce different PGPHs and elucidate the effect of PGPHs on phytoplankton growth.**

In this chapter, I will characterise the genomic and phenotypic capacity of a diverse suite of diatom-associated bacteria to produce different types of PGPHs and determine the effect of identified PGPHs on the growth of the diatom.

- 2. Manipulate PGPH biosynthesis in bacterial symbionts to determine the impact on phytoplankton growth.**

This chapter will investigate the effects of eliminating IAA biosynthesis in a phytoplankton-associated bacterium that normally promotes the growth of its diatom partner, with the goal of defining the relative importance of this PGPH in growth promotion. I will use gene editing tools to knockout the biosynthesis of IAA and explore the effects of growing the impaired bacterium with three different phytoplankton species to quantify for the first time the relative contribution of IAA production in promoting phytoplankton growth.

- 3. Identify the abundance and distribution of PGPH genes across the global ocean and determine the effects of environmental factors on potential PGPH synthesis.**

This chapter will identify the geographical distribution of PGPH genes in the *Tara Oceans* data, determine relationships between abiotic and biotic environmental factors on PGPH gene abundance and link the presence of PGPH synthesis genes in bacteria to specific phytoplankton species.

Chapter 2:

Widespread production of plant growth promoting hormones among marine bacteria and their impacts on the growth of a marine diatom

Abeeha Khalil¹, Anna R. Bramucci¹, Amaranta Focardi¹, Nine Le Reun¹, Nathan L. R. Williams², Unnikrishnan Kuzhiumparambil¹, Jean-Batiste Raina¹, Justin R. Seymour^{1*}

¹Climate Change Cluster, University of Technology Sydney, Ultimo, 2007, NSW, Australia.

² Department of Biological Sciences—Marine and Environmental Biology, University of Southern California, Los Angeles, California, United States.

* Corresponding author: justin.seymour@uts.edu.au

This chapter has been accepted for publication in *Microbiome*.

2.1 Introduction:

Ecological interactions between phytoplankton and bacteria play a key role in structuring the base of aquatic food webs (Cole, 2003). Mutualistic relationships between these two groups of microorganisms often involve tight metabolic linkages that are underpinned by reciprocal exchanges of metabolites (Amin et al., 2012; Grossart, 1999; Seymour et al., 2017). These include the provision of diverse forms of dissolved organic carbon (DOC) from phytoplankton to bacteria, in return for the delivery of re-mineralised micronutrients, vitamins or complex secondary metabolites (Amin et al., 2012, 2015; Seymour et al., 2017). For instance, marine Alphaproteobacteria from the Roseobacter clade provide vitamin B12 to the diatom *Thalassiosira*, while benefiting from the provision of diatom-produced 2,3-dihydroxypropane-1-sulfonate (DHPS) (Durham et al., 2015).

Another group of metabolites called plant growth promoting hormones (PGPHs) may also be key to phytoplankton-bacteria interactions, with Indole-3 acetic acid (IAA) (Amin et al., 2015; J. L. Matthews et al., 2023) and gibberellic acid (GA) (G. Dao et al., 2020) recently reported in cultures. Previously, GA and IAA were only known to affect plants in terrestrial systems, where GA aids germination of seed into seedling (G. Dao et al., 2020) and IAA promotes plant stem and root elongation towards nutrients (Reynolds, 2006; Spaepen, 2015; Zhao, 2010a). However, it has been demonstrated that IAA can be secreted by a range of marine Alpha and Gammaproteobacteria associated with phytoplankton, and this molecule can enhance the growth of the diatom *Pseudo-nitzschia multiseries* (Amin et al., 2015), the coccolithophore *Emiliania huxleyi* (Labeeuw et al., 2016; Segev, Wyche, Kim, et al., 2016) and the dinoflagellates *Symbiodinium microadriaticum* and *Breviolum minutum* (J. L. Matthews et al., 2023). Similarly, GA secreted by bacteria within the Pseudomonadales, Xanthomonadales and Burkholderiales orders induced growth enhancement in the microalgae *Scenedesmus* sp. (G. Dao et al., 2020). Several marine phytoplankton species have recently been shown to benefit from PGPH supplementation (Amin et al., 2015; Buchan et al., 2014; Krug et al., 2020). For instance, inoculation of auxins in *Nannochloropsis oceanica* resulted in an increase in growth rates, lipid production, and the production of omega-3 polyunsaturated fatty acid and eicosapentaenoic acid (Udayan & Arumugam, 2017). Additionally, Jasmonic acid (JA) increased growth rates, influenced the production of fatty acids and alleviated stress in *Chlorella vulgaris* (Czerpak et al., 2006; Jusoh et al., 2015; Piotrowska-Niczyporuk et al.,

2012). These findings suggest that different phytoplankton species may be sensitive to a range of PGPHs.

Notably, further emerging evidence suggests that, beyond interactions featuring IAA and GA, a wider range of PGPHs may be involved in mutualistic interactions between phytoplankton and bacteria (Czerpak et al., 2006; Kumar & Perumal, 2021).

In terrestrial systems, almost all aspects of plant development and responses to their environment are regulated by PGPHs (Foo et al., 2019). Six major classes of PGPHs have been identified: Auxins, Gibberellins, Cytokinin, Ethylene, Jasmonates and Abscisic acid, and each has been linked to specific functions (Eng et al., 2018; Mandava, 2003; Moubayidin et al., 2009; Salazar-Cerezo et al., 2018a; S. M. Smith et al., 2017; Wilkinson & Davies, 2010; Zhao, 2010a). While there is evidence of the presence of PGPHs, such as IAA and GA (Amin et al., 2015; Cirri & Pohnert, 2019; G. Dao et al., 2020) within phytoplankton and bacteria interactions, we still lack a clear understanding of the diversity of bacteria capable of producing PGPHs and, the range of PGPHs they are able to produce.

Given the emerging evidence that PGPHs impact phytoplankton health and productivity, we propose that it is important to determine how many of these molecules can be produced by phytoplankton-associated bacteria and which ones affect phytoplankton. Here, we examined the PGPH-production capacity of 14 bacterial isolates, which have previously been demonstrated to enhance the growth of *Actinocyclus* (Le Reun et al., 2023), a common marine diatom (Koizumi et al., 2003; Smirnova et al., 2015). We subsequently measured the effects of different PGPHs produced by these bacteria on *Actinocyclus* growth.

2.2 Materials and Methods:

2.2.1 Diatom – Bacteria model system:

We examined the potential role of PGPHs within a model diatom-microbiome system, whereby we have previously identified the growth promoting benefits of a set of 14 diatom-associated bacteria (Le Reun et al., 2023). *Actinocyclus* sp. was isolated from an oceanographic reference station (Port Hacking – 34° 05.00 S, 151° 15.00 E) on the east coast of Australia (Brown et al., 2018; Le Reun et al., 2023). *Actinocyclus* sp. cultures were maintained in sterile seawater supplemented with f/2 medium (Ryther & Guillard, 1962), and grown under light conditions of 55-65 µE, 12:12 day/night at 20-22 °C. We previously demonstrated that 14 unique bacterial strains, spanning five different families and 14 genera (*Supplementary Table S1*), promote the growth of *Actinocyclus* sp. in co-culture conditions (Le Reun et al., 2023). Here we screened the capacity of these beneficial diatom-associated bacteria to synthesis PGPHs.

2.2.2 Genome sequencing and genomic survey of PGPH biosynthesis pathway genes in bacterial isolates:

To confirm the presence of genes involved in PGPH synthesis within the 14 isolated bacterial strains, whole genome sequencing was conducted. Each isolate was grown in 20 mL of Marine Broth (Difco Marine Broth 2,216). Cultures grown to exponential phase were centrifuged at 4,000 rpm for 10 min and the pellet was used for DNA extraction, using a physical lysis extraction technique (Bramucci et al., 2021). Briefly, lysis of the cells was achieved by adding a solution of 0.0215 g/mL KOH and 0.008 g/mL dithiothreitol, followed by a freeze-thaw cycle. Free DNA was then purified and eluted using AMPure XP magnetic beads (Beckman Coulter).

Genome libraries were prepared and sequenced on an Illumina MiSeq platform at the Australian Genomic Research Facility (AGRF). Raw sequences were quality checked and adapters trimmed using trimmomatic v0.35 (Bolger et al., 2014), before de novo genome assembly was performed using SPAdes (Bankevich et al., 2012). The resulting contigs were binned using metabat2 (Kang et al., 2019), with the quality of the assembled genomes calculated using checkM2 (Chklovski et al., 2022) Open reading frames (ORFs) were identified with Prodigal (Hyatt et al., 2010) and taxonomy was assigned using Genome Taxonomy Database (GTDB-tk v. 2.2.4). To assess the presence of PGPH biosynthesis pathways for the isolated bacteria, protein sequences, predicted using prodigal, were blasted (e-value < 10⁻¹⁰)

against a custom reference database that contained all genes for IAA, GA and TZ biosynthesis listed in prior literature (Añorga et al., 2020; Fidler et al., 2015; Labeeuw et al., 2016; Salazar-Cerezo et al., 2018a; Spaepen & Vanderleyden, 2011), which were retrieved from NCBI. For the analysis of JA and Brassinosteroid (BSN), for which no bacterial biosynthetic pathways are currently known, we leveraged information from the eukaryotic (plant) alpha-Linoleic and Brassinosteroid reference pathway deposited in the KEGG database. Pathways for Indole-3-butyric acid (IBA) biosynthesis are still completely uncharacterised and were therefore not included in this analysis. A database containing the gene sequences involved in PGPH pathways (present in KEGG; <https://www.genome.jp/kegg/genes.html>), was used to identify homolog sequences. Specifically, PGPH synthesis gene sequences from bacteria closely related to the 14 isolates examined here were collated for the IAA, GA and TZ pathway genes, and eukaryotic (plant) proxy genes were used as query for ABA, JA and BSN (Supplementary Table S2-S7). Reciprocal BLASTp and BLASTn searches were performed using the gene database to identify potential PGPH homologs in the whole genome sequences of the 14 bacterial isolates (used as the query). BLASTp hits with an e-value $\geq 1 \times 10^{-10}$ were not considered.

2.2.3 Extraction protocol for PGPH quantification:

All 14 bacterial strains were phenotypically screened for PGPH biosynthesis, whereby PGPH levels during the exponential growth phase for each of the isolates were measured. For each bacterial isolate, two different PGPH extraction protocols were carried out to quantify: i) intracellular and ii) exuded PGPHs. To prepare cultures for PGPH extraction, 50 ml each bacterial isolate was grown to exponential phase in quadruplicate as described above. A 200 μ l aliquot was collected from each replicate and bacteria counts were enumerated using a CytoFLEX LX flow cytometer (Beckman Coulter). First, cells were stained with SYBR green I (final concentration 1:10000; SYBR-Green I, Invitrogen) and incubated for 15 min at 4 °C then bacterial cells were identified according to side scatter (SSC) and green fluorescence (SYBR-Green) and enumerated. Each replicate was then transferred to a 50 mL Falcon tube (Eppendorf), and centrifuged at 2,000 rpm for 30 min (Eppendorf). The supernatant was collected and transferred into a clean 50 mL Falcon tube. Supernatant and pellet samples were flash frozen in liquid nitrogen and stored at -80°C until PGPH extraction.

2.2.3.1 Intracellular PGPH Extractions:

To quantify intracellular PGPH concentrations within the bacterial cell pellets, each sample was separated into two pellets and two separate extraction protocols were implemented, i) for the quantification of Auxins, Gibberellins, Cytokines, and Zeatins, and ii) for the quantification of Steroids. For the extraction of i) 2 mL of a 14:4:1 solution of 99% methanol (Sigma-Aldrich), ultrapure water, and 99% formic acid (Sigma-Aldrich) was added to each tube, which was then sonicated for 2 min to lyse the cells. The cellular debris was subsequently centrifuged down at 2000 rpm, and quadruplicate samples of supernatant extract were freeze-dried at -80 °C. The sample residues were then reconstituted into 1 mL of 1 M formic acid, and further purified on Evolute express CX columns (Biotage) that had been pre-conditioned with methanol and 1 M formic acid. The samples were first eluted with 3 mL of 99% methanol, then 3 mL of 0.35 M ammonium hydroxide (Sigma-Aldrich), and finally 3 mL of 0.35 M in ammonium hydroxide in 60% methanol. All samples were then freeze dried at -80 °C and reconstituted with 99% ultrapure high-pressure liquid chromatography (UHPLC) grade methanol (Sigma-Aldrich). For the extraction ii) the pellet was freeze dried at -80 °C then reconstituted in 1 mL of 60% Acetonitrile supplemented with 5- α -Cholestane (internal standard 1mg/mL) (Sigma-Aldrich). Samples were then further lysed through bead beating using a mixture of \leq 106 μ m and 425-600 μ m acid-washed glass beads (0.5g of each) (Sigma-Aldrich) and sonication in an ultrasonic cleaner (Unisonic PTY.LTD, Australia) for 3 min at 4 °C. Samples were then centrifuged and the supernatant was collected for LC-MS/MS analysis.

2.2.3.1 Extracellular PGPH Extraction:

To quantify the PGPH concentrations exuded by bacterial cells, the supernatant of the bacterial cultures was first filtered through a 0.22 μ m filter (Sartorius) to remove all bacteria. A sixteen valve SUPELCO manifold and 6 cc 200 mg Oasis HBL cartridge were used to extract PGPH from the samples. The cartridges were pre-conditioned with 20 mL of ultrapure water and then 20 mL of 99% methanol (Sigma-Aldrich). The bacterial supernatant was then loaded into the column 10 mL at a time. The samples were eluted with 3 mL of 20% methanol, then 3 mL of 70% methanol (Sigma-Aldrich). All samples were then freeze dried at -80 °C and reconstituted with 99% UHPLC grade methanol (Sigma-Aldrich). Extracellular quantification of BSN concentration was not conducted as extraction protocols to detect released concentrations of BSN have not yet been developed.

2.3.4 Chemical characterisation using LC MS-MS analysis:

Known standards of IAA, Indole-3 butyric acid (IBA), Abscisic acid (ABA), Gibberellic acid (GA), Jasmonic acid (JA), Trans-zeatin (TZ) and Brassinolide (BSN) were used to calibrate the LC-MS/MS to mobile phase, run time and energy requirements for phytohormone fragmentation. A 10-point standard curve spanning: 50, 25, 12.5, 6.25, 3.12, 2.5, 1.25, 0.624, 0.312, and 0.03 ng/mL was prepared for each PGPH. Quantification of PGPH was performed using a Shimadzu LCMS-8060 (Shimadzu, Kyoto, Japan) instrument with a dual ion source (DUIS) interfaced to Shimadzu Nexera X2 liquid chromatography system. The separation was performed on an Acquity UPLC HSS T3 column (1.8 μ m, 2.1 \times 150 mm) using a binary gradient of milliQ water (A) and methanol (B) for 15 min, at a flow rate of 0.18 mL/min. The linear gradient program was run at: 0–10 min, 20–95% B; 10–11 min, 95–20% B; 11–15 min, 20 % B. Column temperature was maintained at 30 °C. Samples were analysed in the multiple reaction monitoring mode. The following transitions were monitored with a fragmentor voltage of 160 V. Collision energy for each hormone were as follows: IAA -6 eV m/z 174 \rightarrow 130, d₅-IAA m/z 179 \rightarrow 135, IBA -10eV, m/z 202 \rightarrow 116, ABA -9eV, m/z 263 \rightarrow 219, GA -21, m/z 345 \rightarrow 221, JA -25 eV, m/z 209 \rightarrow 59, TZ, -10 eV, m/z 220 \rightarrow 136, BSN -14 eV, m/z 481 \rightarrow 445, The resulting peaks were then quantified using the 10-point calibration curves. Statistical differences in hormone concentrations between the bacteria isolates were assessed using a one-way ANOVA.

2.3.5 PGPH and cell density index correlation analysis:

We next aimed to determine whether the concentrations of bacterial-produced PGPHs measured here could lead to phytoplankton growth enhancement. Specifically, we correlated levels of PGPH production with the growth-promoting effect of 12 out of the 14 bacteria isolates when co-grown with *Actinocyclus*. For each bacterial strain tested, we used Pearson's correlation to investigate the relationship between the extracellular concentration of each PGPH they release and the effect the strain has on *Actinocyclus* growth (using the previously reported cell density index, a metric that integrates the growth-promoting effect of a bacterial strain in co-culture with *Actinocyclus* over time). As reported in Le Reun et. al 2023, to assess the growth-promoting effect of each bacterial strain on the diatom over time, the co-cultures were divided into three time periods: days 0–6, days 8–12, and days 14–16. For each strain and time period, a cell density index (CD) was calculated. This index was determined by calculating the area under the curve (AUC) for each co-culture (using the AUC() function from the

DescTools R package) and then dividing it by the AUC of the axenic culture (Le Reun et al., 2023).

2.3.6 Measuring the effect of PGPH on diatom growth:

To determine the effect of each PGPH on the growth of *Actinocyclus* sp., each hormone identified in the bacterial isolates was added individually to axenic *Actinocyclus* sp. cultures. Axenic cultures of *Actinocyclus* sp. were grown to exponential phase, diluted to 5000 cells/mL and normalised to a 50 mL volume in f/2 medium. Stock solutions of the PGPHs were prepared to concentrations matching those measured in the extracellular production by bacterial isolates. An initial screening of the growth effects was conducted at three different concentrations, including one magnitude above and below the extracellular concentrations measured in our experiment, in order to determine the optimal concentration of PGPH required for growth enhancement. The optimal concentrations were found to be 1×10^{-8} µg/mL for IAA, 1×10^{-9} µg/mL for BA, 1×10^{-10} µg/mL for TZ, GA and BSN, and 1×10^{-11} µg/mL for IBA, ABA, and JA (Sigma-Aldrich). All hormones were dissolved in f/2 medium with the exception of IAA and ABA, which were diluted in ethanol and dimethyl sulfoxide (DMSO) (Sigma-Aldrich). Individual hormones were added at early exponential (2 d) and early stationary (6 d) of *Actinocyclus* sp. growth phases to mimic a supply by associated bacteria.

Axenic *Actinocyclus* sp. cultures were spiked with each hormone in 70 mL sterile tissue culture flasks (n = 4 flasks for each pair). Each tissue culture flask contained 50 mL of *Actinocyclus* sp. at 5000 cells/mL and 5 µL of PGPH diluted to the aforementioned final concentrations. Additionally, quadruplicate controls were maintained alongside the treatments, which consisted of axenic phytoplankton without any hormones added. All flasks were maintained in the same incubation conditions as described above. The cultures were monitored over time using flow cytometry to enumerate diatom cell numbers and to confirm the culture remained axenic. Samples were taken every second day at the same time whereby, 200 µL samples were collected in 1.5 mL microcentrifuge snap-seal Eppendorf tubes and fixed with 2% glutaraldehyde. Cells were enumerated using a CytoFLEX LX flow cytometer (Beckman Coulter). *Actinocyclus* cells were discriminated according to forward scatter (FSC), side scatter (SSC) and red fluorescence (chlorophyll). Samples for enumeration of bacteria were enumerated as mentioned previously.

All data was analysed using repeated-measures ANOVA to identify significant changes in growth between control and treatment cultures. All data was assessed for normality and homogeneity of variance using Shapiro and Levene's test before performing pairwise comparison to assess the overall effect of the PGPH treatments. Differences in cell numbers between the hormone treatment and axenic control at each time point were assessed using a two-way repeated-measure ANOVA (Simple Main Effect test) (Quinn & Keough, 2002).

2.3 Results:

2.3.1 Genomic survey of PGPH biosynthesis pathway genes in bacterial isolates:

Here we examined PGPH biosynthesis capacity in the genomes of 14 unique bacterial strains (*Supplementary Table S1*) that have previously been demonstrated to enhance the growth of the diatom *Actinocyclus* sp. (Le Reun et al., 2023). Our analysis revealed that all 14 of the tested bacteria have the genomic potential to synthesise at least one of the PGPHs investigated.

2.3.2 Indole-3 acetic acid biosynthesis pathway:

Five different IAA biosynthesis pathways have previously been identified, including the Indole-3-acetamide, Indole-3-pyruvate, Indole-3 acetonitrile, Tryptophan side chain oxidase and Tryptamine pathways (Labeeuw et al., 2016; Spaepen & Vanderleyden, 2011). All 14 bacterial isolates possessed clear orthologues of all the enzymes required for one or more pathways for IAA production (*Figure 1, Supplementary Table S2*), with genes involved in the tryptamine and indole-3-acetonitrile pathways the most common. Of the 14 bacteria screened, 92% displayed the genomic capacity to synthesise *Tryptophan decarboxylase (TDC)* a precursor to the Tryptamine dependent pathway (Figure 1; green). In addition, 85% of the bacterial genomes harboured *Amine oxidase (AO)*, a gene required to synthesise Indole-3-acetaldehyde. The capacity to synthesise IAA via the Indole-3-acetonitrile pathway was present in 64% of the bacteria (Figure 1; red), whereby 85% possessed the *Nitrate hydrolase (NH)* gene, and 85% had the *Indole-acetaldoxime dehydratase (NIT)* gene, which is responsible for the last step of the IAA synthesis pathway.

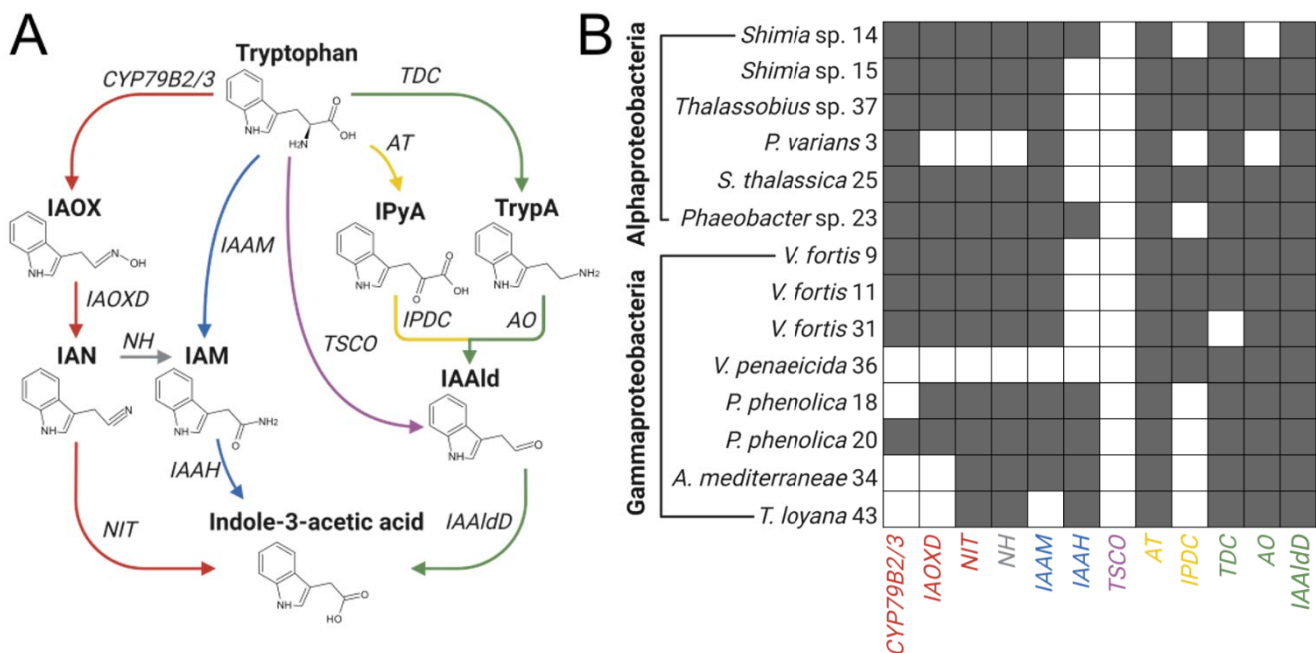


Figure 2.1: Indole-3 acetic acid biosynthesis pathway and production potential in the 14 bacteria isolates. A) Tryptophan dependent IAA pathways in bacteria. Five main IAA biosynthesis pathways, including the Indole-3 acetonitrile (red), Indole-3-acetamide (blue), Tryptophan side chain oxidase (purple), Indole-3-pyruvate (yellow), and Tryptamine (green) pathways are depicted. Intermediate molecules are depicted with black bold text. IAOx, Indole-3-acetaldoxime; IAN, Indole-3-acetonitrile; IAM, indole-3-acetamide; IPyA, Indole-3-pyruvate; TrypA, Tryptamine; IAld, indole-3-acetaldehyde. Enzymes are depicted un-bold black text and lines. *CYP79B2/3*, cytochrome P450; IAOxD, Indole-acetaldoxime dehydratase; NIT, Nitrilase; NH, Nitrile hydrolase; IaAM, Tryptophan-2-monooxygenase; IaAH, Indole-3-acetamide hydrolase; TSO, Tryptophan side-chain oxidase; IPDC, TDC, Tryptophan decarboxylase; Indole-3-pyruvate decarboxylase; AO, Amine oxidase; IAldD, indole-3-acetaldehyde dehydrogenase. **B)** Heatmap of the presence of orthologues for IAA biosynthesis in the 14 bacterial strains tested. Grey squares depict the detection of orthologues of IAA synthesis genes (bottom) in the bacteria (left), as indicated by a BLASTp search (e-value < 10⁻¹⁰, Supplementary Table S2

2.3.3 Gibberellic acid biosynthesis pathway:

GA synthesis is mediated by a single linear pathway categorized into three distinct stages. The first stage involves catalysis by soluble enzymes to form molecules such as ent-kaurene, while the second stage involves oxidation to form precursor GA molecules such as GA12-aldehyde. The final stage involves further catalysis via *mono-oxygenases* to form four bioactive GA molecules (*Figure 2A*) [18]. Only 70% of the targeted bacteria (mainly from the Rhodobacteraceae and Vibrionaceae clades) possessed genes responsible for the second and third stages of the pathway (*Figure 2B*) (*Supplementary Table S4*). Interestingly, none of the genomes of the tested bacteria contained the *Copalyl diphosphate synthase* (*CPS*) or *Kaurene synthase* (*KS*).

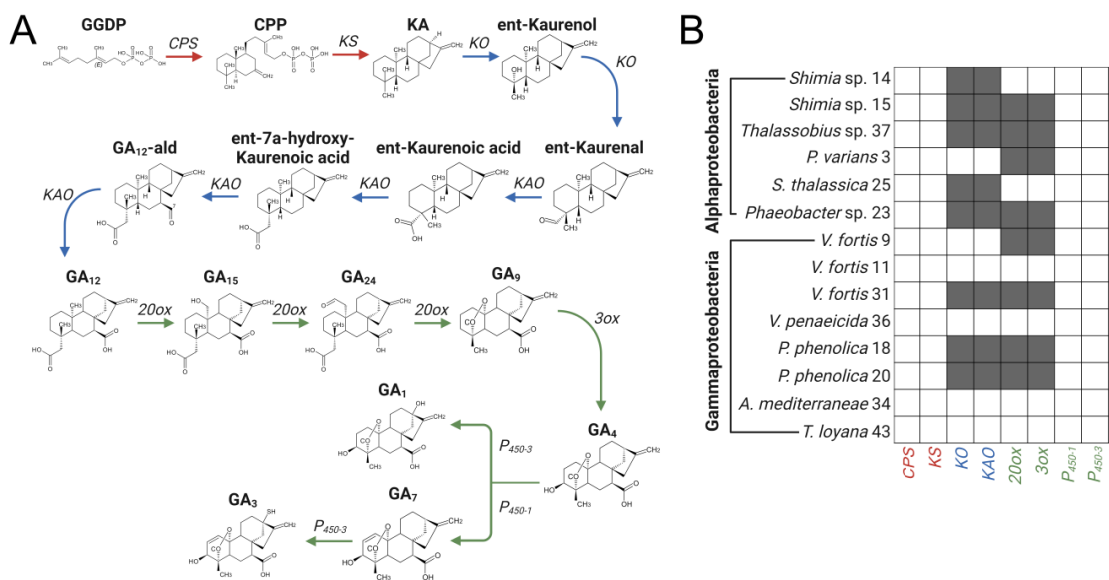


Figure 2.2: Gibberellic acid biosynthesis pathway and production potential in the 14 bacteria isolates. A) GA pathway in bacteria. Each stage of the pathway is categorised by red (stage 1), blue (stage 2) and green (stage 3) coloured arrows. GA biosynthesis pathway intermediate molecules are depicted with black bold text. GGDP, Geranylgeranyl diphosphate; CCP, Copalyl diphosphate; KA, Ent-kaurene; GA₁₂-ald, Gibberellic acid-12-aldehyde; GA, Gibberellic acid. Genes and enzymes are depicted with un-bold black text. CPS, Copalyl diphosphate synthase; KS, Kaurene synthase; KO, Kaurene oxidase KAO, Kaurenoic acid oxidase 20ox, 20-oxoglutarate-dependent dioxygenase; 3ox, 3-oxidase. B) The presence of orthologues for GA biosynthesis in the 14 bacterial strain tested. Grey squares depict the detection of orthologues of GA synthesis genes (bottom) in the bacteria (left), as indicated by a BLASTn and BLASTp search (e-value < 10⁻¹⁰, Supplementary Table S4).

2.3.4 Trans-zeatin, Abscisic acid and Jasmonic acid Brassinosteroid Pathways:

Analysis of homologs for TZ pathway-specific genes revealed that all 14 bacteria examined possessed the putative bacterial pathways via one or more biosynthesis routes (*Supplementary Figure S1 & Table S6*). The TZ synthesis pathway comprises two distinct routes, comprising known and unknown TZ biosynthesis genes. With the exception of *Isopentenyl-diphosphate delta-isomerase (IPP isomerase)*, 100% of the screened bacteria were found to contain all other known genes necessary for synthesizing TZ (*Supplementary Figure S1 & Table S6*). Putative pathways for ABA, JA, and BSN biosynthesis were constructed based on eukaryotic (plant) organisms. Our analysis revealed that the genomes of the screened bacteria include limited gene orthologues for pathways of plant origin. As a result, none of these bacteria have a complete set of known genes necessary for hormone synthesis (*Figure 5, Supplementary Figure S1, S3 and Table S3, S5, S7*).

2.3.5 Quantification of PGPH production by bacterial isolates:

2.3.5.1 Intracellular PGPH Concentrations:

Strikingly, with the exception of IBA, all 14 bacterial strains produced each of the PGPHs tested (*Figure 3*). This result was particularly notable given that the capacity of most strains to produce a wide diversity of PGPHs was not expected based on their genome sequences. On average, the concentrations of BSN were 100 higher than the other hormones tested (One-way ANOVA, $p=0.000271$, *Supplementary Table S14*). This was followed by IAA and ABA (One-way ANOVA, $p=0.000397$ and $p=1.1\times10^{-13}$, *Supplementary Table S8 and S10* respectively), which exceeded that of IBA, JA, GA, and TZ by 10 to 100 orders of magnitude (*Supplementary Figure S5*). Out of the 14 bacterial strains, *Phaeobacter* sp. 23 produced significantly higher concentrations of IBA, ABA, TZ and BSN, which exceeded all other tested bacteria tested by 10 to 1000 orders of magnitude (one-way ANOVA, $p<0.05$, *Supplementary Table S9, S10, S13 and S14*).

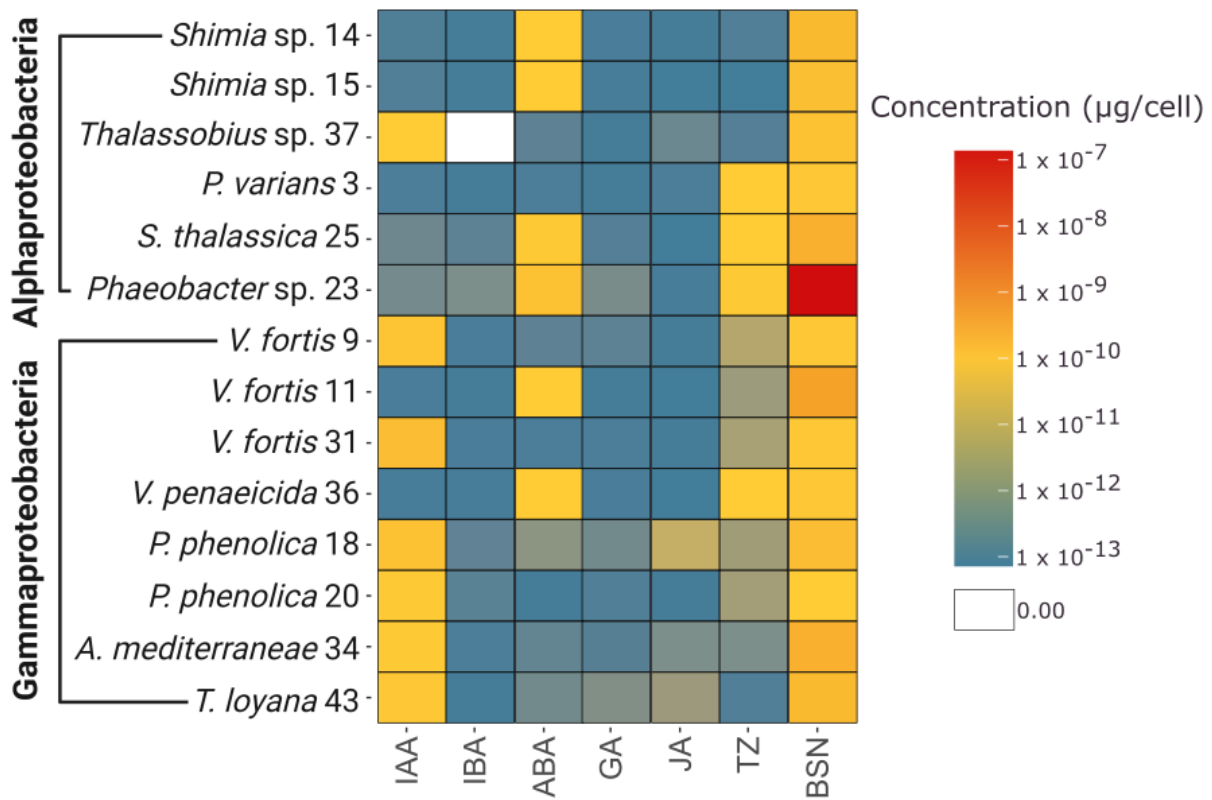


Figure 2.3: Quantification of intracellular concentrations of plant growth promoting hormones (µg/cell) in the 14 bacterial strains tested. A heat map illustrating the intracellular concentration (coloured squares) of the plant growth promoting hormones Indole -3 acetic acid (IAA), Indole -3 butyric acid (IBA), Abscisic acid (ABA), Gibberellic acid (GA), Jasmonic acid (JA), Trans-zeatin (TZ) and Brassinolide (BSN) of the 14 bacteria tested.

2.3.5.2 Extracellular PGPH Concentrations:

Out of the 14 bacterial strains tested, 6 (42%) released all seven of the tested PGPHs into the surrounding medium, while 10 (71%) released at least seven of these compounds (Figure 4). However, there was considerable variation in the concentrations and diversity of PGPHs released among the strains. Of the seven targeted PGPH, only IAA was produced by 13 of the 14 tested bacteria. Production of the six other PGPHs – GA, JA IBA, ABA, TZ and BSN was heterogeneously distributed across the screened strains (Figure 4). On average, out of the seven hormones tested, IAA was exuded at significantly higher concentrations (One-way ANOVA, $p < 0.05$, Supplementary Table S8), closely followed by TZ (One-way ANOVA, $p < 0.05$, Supplementary Table S13), with exuded concentration of IAA exceeding IBA, JA, GA, and ABA by 10 to 1000 orders of magnitude (Figure 5H). *T. loyana* 43 released the highest concentrations of IAA ($2.7 \pm 1 \times 10^{-8}$ µg/cell; One-way ANOVA $p < 0.05$, Supplementary Table S8), while *Phaeobacter* sp. 23 released the highest concentrations of IBA, ABA, GA, and JA

(One-way ANOVA, $p < 0.05$, Supplementary Table S9-S12). Notably, *P. varians* 3 did not exude detectable amounts of any of the tested PGPHs, despite producing all 7 of the hormones intracellularly.

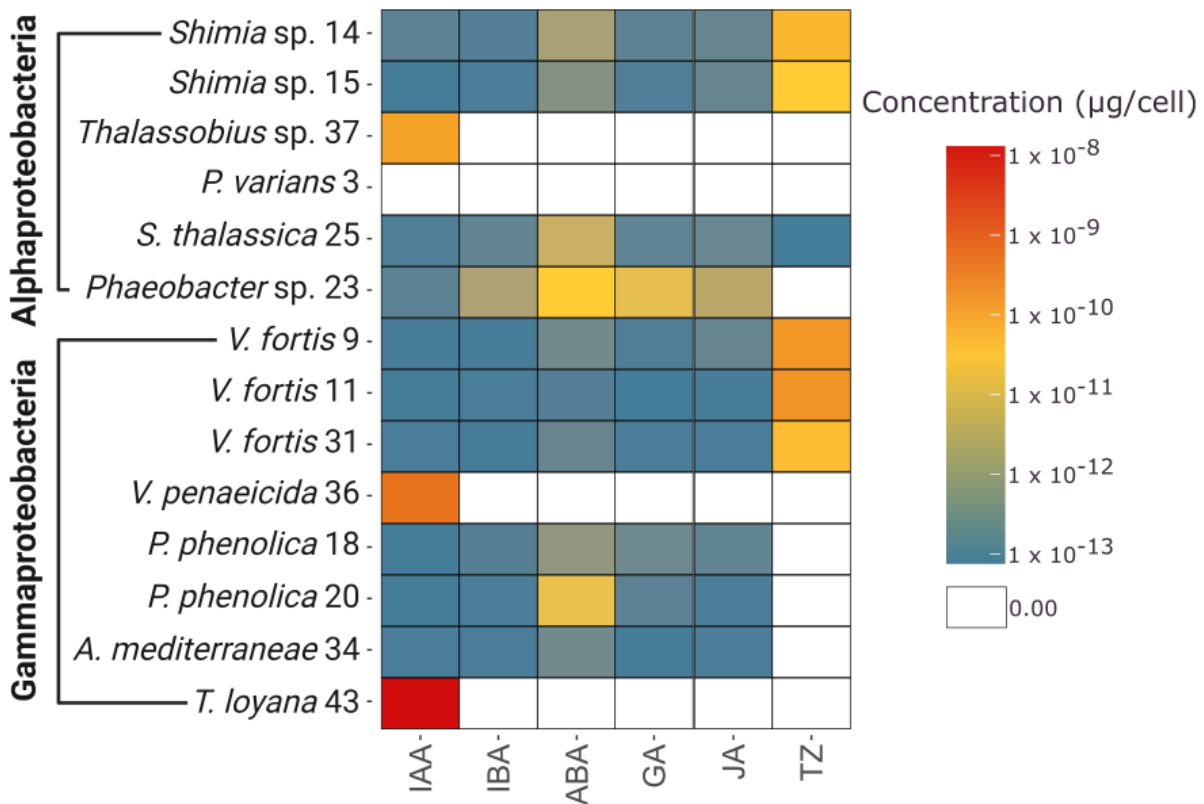


Figure 2.4: Quantification of plant growth promoting hormones (µg/cell) exuded by the 14 bacterial strains tested. A heat map illustrating the concentration (coloured squares) of the plant growth promoting hormones Indole -3 acetic acid (IAA), Indole -3 butyric acid (IBA), Abscisic acid (ABA), Gibberellic acid (GA), Jasmonic acid (JA), and Trans-zeatin (TZ) released into the surrounding media from the 14 bacteria tested. Extracellular quantification of BSN was not conducted as extraction protocols to detect released concentrations of BSN have not yet been developed.

2.3.6 Relationship between phytoplankton growth and PGPH concentrations:

To determine if the production of specific PGPHs may be linked to bacterial augmentation of *Actinocyclus* growth, we used results derived from a previous experiment that quantified the growth-promotion (cell density index) of each of the bacterial isolates during co-culture experiments with *Actinocyclus* (Le Reun et al., 2023). Our results revealed that out of the 7 hormones tested, IAA was the only hormone for which extracellular concentrations were

positively and significantly correlated to increases in *Actinocyclus* cell density (Pearson's correlation, $R = 0.73$; Figure 5).

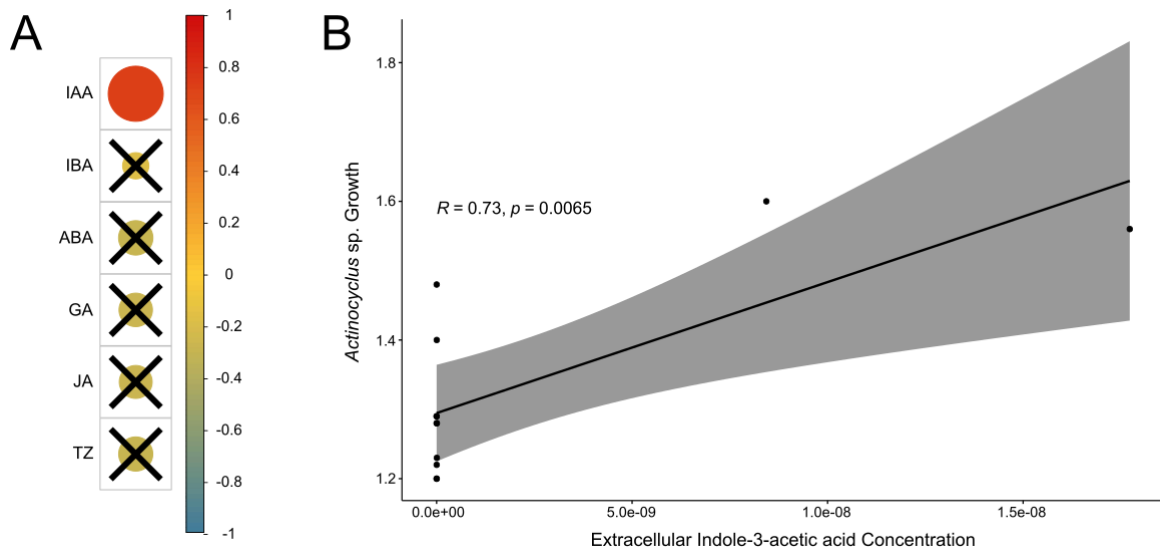


Figure 2.5: Correlation analysis between extracellularly-released PGPHs and maximum *Actinocyclus* growth-enhancement in co-culture experiments. As reported in Le Reun et. al. 2023, *Actinocyclus* growth enhancement (cell density index) was calculated by calculating the area under the curve (AUC) for each bacteria co-culture **A**) Correlogram for each PGPH tested (the size and colour of each bubble is proportional to the strength of the correlation). Only statistically significant correlations are not crossed (Pearson's correlation, $p < 0.05$). **B**) Linear regression of the only statistically supported correlation. The x-axis represents released IAA concentrations measured for each bacterial isolate ($\mu\text{g}/\text{cell}$) while the y-axis represents the maximum growth enhancement of *Actinocyclus* cells for 12 out of the 14 bacteria isolates when co-grown with *Actinocyclus* (Le Reun et al., 2023). R-square and p-value (Pearson's correlation) are displayed in italic.

2.3.7 Measuring the effect of PGPH on *Actinocyclus* sp. growth:

To measure whether the seven detected bacterial PGPHs enhanced the growth of *Actinocyclus*, axenic diatom cultures were inoculated with each hormone at concentrations one order of magnitude higher and lower than the highest PGPH concentrations extracellular released by the bacteria. Provision of IBA, ABA, JA, TZ and BSN did not result in any significant increase in *Actinocyclus* sp. cell numbers (Figure 5(C-G) and Supplementary Table S15). However, the addition of IAA and GA led to significantly higher *Actinocyclus* cell numbers compared to the axenic control (Repeated-measures ANOVA, p -value < 0.05 ; Figure 6, Supplementary Table

S15). All three tested IAA concentrations significantly increased *Actinocyclus* cell numbers compared to the control (Repeated-measures ANOVA, *p*-value < 0.05; Figure 6A, Supplementary Table S15). This effect started after 4 days and lasted until the end of the experiment. The highest IAA concentration tested (10^{-7} $\mu\text{g/mL}$) caused a 2.5 times increase in cell numbers compared to the control after 7 days (Repeated-measures ANOVA, *p*-value < 0.05, Supplementary Table S15). For GA, only the lowest concentration (10^{-11} $\mu\text{g/mL}$) significantly increased the number of *Actinocyclus* cells compared to the control (Repeated-measures ANOVA, *p*-value < 0.05; Figure 6B, Supplementary Table S15). This effect started on 6 d and lasted until the end of the experiment with the largest effect of GA on *Actinocyclus* cell numbers was recorded on 10 d, when a 30% increase in cell abundance occurred (Repeated-measures ANOVA, *p*-value < 0.05; Figure 6B, Supplementary Table S15).

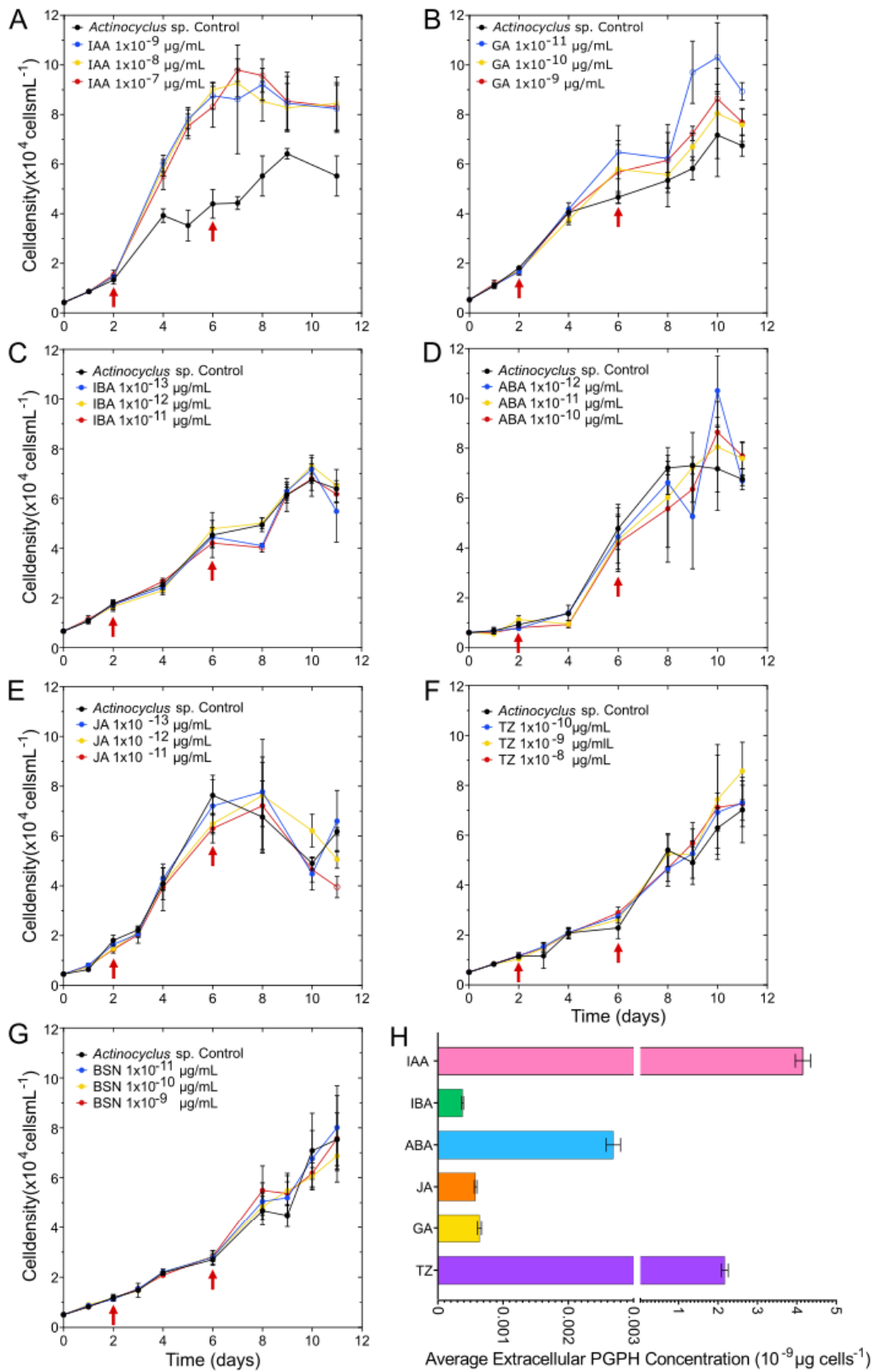


Figure 2.6: Growth over the course of 11 days of *Actinocyclus* inoculated with IAA, GA, IBA, ABA, JA, TZ, BSN and the average PGPH concentration released by the 14 bacteria.

A) *Actinocyclus* cell numbers per millilitre in response to three different IAA concentrations (chosen based on quantifications data, see methods). **B)** *Actinocyclus* cell numbers per millilitre in response to three different GA concentrations (chosen based on quantifications data, see methods). Error bars are standard error of the mean (SEM), n = 4. A significant difference between a given concentration and the control is depicted as an empty circle (Repeated-measures ANOVA, p<0.05, Supplementary Table S15) and red arrows depict inoculation times for IAA and GA treatments (2 d and 6 d for both). Number of *Actinocyclus* sp. cells per millilitre (y-axis) when treated with **C)** IBA, **D)** ABA, **E)** JA, **F)** TZ, **G)** BSN at three different concentrations. The blue line, yellow line and red line each represent concentrations of 1×10^{-12} , 1×10^{-11} and 1×10^{-10} $\mu\text{g/mL}$ for IBA, ABA, JA and BSN, 1×10^{-10} , 1×10^{-9} and 1×10^{-8} for BA and 1×10^{-9} , 1×10^{-8} and 1×10^{-7} $\mu\text{g/mL}$ for TZ. *Actinocyclus* sp. axenic control grown solely in F/2 is represented by the black line with filled circles over the course of 11 days (y-axis). The data displays a typical phytoplankton growth curve pattern with a lag, exponential, and stationary phases. Error bars are displayed as black vertical lines on each data point (\pm SEM; n = 4). Significant difference depicted as empty circle data points (Simple Main Effect Test, p<0.05, Supplementary Table S15). **H:** Average Extracellular PGPHs released by the 14 bacteria (derived from the data presented in Figure 2.4). Error bars are SEM, n=56.

2.4 Discussion:

Diverse chemical currencies are involved in the ecological interactions between phytoplankton and bacteria (Amin et al., 2015; Barak-Gavish et al., 2023; Cirri & Pohnert, 2019; Durham et al., 2015; Seymour et al., 2017). Among these exchanged metabolites, the bacterial production of PGPHs may be a critical regulator of phytoplankton growth (Anam et al., 2021; Kaur et al., 2023), yet the production and effects of PGPHs remain understudied in the marine environment. Here, our goal was to deliver a comprehensive analysis of the PGPH-producing capabilities of a suite of marine bacteria that have previously been demonstrated to enhance the growth of the diatom *Actinocyclus* (Le Reun et al., 2023), and examine the impacts of these hormones on diatom growth. Both analysis of the genomic potential for PGPH synthesis and direct chemical quantification revealed that the diverse range of marine bacteria tested can produce a wide range of PGPHs and that some of these PGPHs enhance the growth of *Actinocyclus*.

2.4.1 Widespread production of bacterial-produced PGPHs:

PGPH biosynthesis was widespread across the tested bacteria, with each of the 14 strains producing at least six different hormones. Surprisingly, 85% of the strains synthesised all seven PGPHs tested, including Brassinolide, which had never been reported in the marine environment before. This result is striking because the simultaneous biosynthesis of more than three PGPHs has not previously been reported in marine bacteria (Muhamarram et al., 2019). In addition, the capacity of most strains to produce a wide diversity of PGPHs was not expected based on their genome sequences. Indeed, despite the absence of genes thought to be required for JA, ABA and BSN biosynthesis and the partial presence of genes required for GA biosynthesis the 14 screened strains still produced quantifiable amounts of each of these PGPHs, suggesting that uncharacterised alternative pathways may mediate the biosynthesis of these hormones in these bacteria.

The concentrations of PGPHs produced varied between the different bacterial strains, with the Alphaproteobacterium *Phaeobacter* sp. 23 often producing the highest concentration of PGPHs. This strain produced the highest intracellular concentrations of IBA, ABA, TZ and BSN, and released the highest extracellular concentrations of IBA, ABA, GA and JA. Further genomic analysis of this strain's PGPH biosynthesis capacity also revealed that *Phaeobacter* sp. 23 harbours three different pathways to synthesise IAA (Indole-3 acetonitrile, Indole-3-

acetamide and Tryptamine), the majority of genes within the GA pathway and all genes necessary for TZ biosynthesis, a pathway of eukaryotic origin. The ability of *Phaeobacter* sp. 23 to produce large concentrations of PGPHs may contribute to the abundance of this genus in phytoplankton-associated bacterial communities, and its ability to modulate phytoplankton growth (Majzoub et al., 2019; Segev, Wyche, Hyun Kim, et al., 2016; Shibl et al., 2020).

Although the production of IAA and GA by phytoplankton-associated bacteria had been reported, none of the other five hormones were previously identified in phytoplankton-bacteria studies. However, some hormones, such as IBA, ABA, and JA, are known to enhance phytoplankton biomass in biotechnological settings (Czerpak et al., 2006; Jusoh et al., 2015; Kobayashi et al., 1997; Mansouri & Talebizadeh, 2017; Mc Gee et al., 2021; Piotrowska-Niczypruk et al., 2012). Indeed, only rhizobacteria within the Pseudomonadaceae family were previously known to produce both TZ and BSN, while only members of the Bacillus, and Enterobacteriaceae produced BSN (Koenig et al., 2002; Ryu et al., 2005). Furthermore, BSN intracellular concentrations in our marine bacteria were the highest among the seven PGPHs quantified here, while TZ concentrations surpassed those of more well-known PGPHs, such as GA. These results clearly demonstrate that BSN and TZ production is not limited to specific rhizobacteria clades, and may be widespread in phytoplankton-associated bacteria.

2.4.2 Effect of bacterial-produced PGPH on marine diatoms:

The concentrations of IAA exuded by the 14 bacterial strains were significantly and positively correlated with the ability of these strains to enhance *Actinocyclus* growth (Le Reun et al., 2023). This correlation suggests that IAA provision by the different bacterial isolates may be a key determinant of the *Actinocyclus* growth promotion previously reported (Le Reun et al., 2023). This finding was further confirmed when we examined *Actinocyclus* growth responses to direct PGPH additions. Indeed, only IAA and GA additions elicited a growth enhancing effect on *Actinocyclus* cells. The provision of IAA to *Actinocyclus* cells resulted in a nearly a two-fold increase in cell numbers. This is consistent with observations in other phytoplankton species, where IAA additions resulted in significant growth enhancement (Mazur et al., 2001; Peng et al., 2020). All three concentrations of IAA tested here elicited a significant growth promoting effect, but studies in other species have found that an inhibitory effect can occur at high concentrations (Chung et al., 2018; Palacios et al., 2016), suggesting that the concentration of hormones received by the phytoplankton is very important to induce a growth benefit. Importantly, the concentrations of IAA that caused a growth promoting effect on *Actinocyclus*

here are the same order of magnitude as the extracellular concentrations we quantified in our bacterial strains, further confirming that the exuded concentrations can affect the growth of phytoplankton.

In contrast, the addition of GA only impacted *Actinocyclus* growth at low (10^{-9} $\mu\text{g/mL}$) and high (10^{-7} $\mu\text{g/mL}$) concentrations, perhaps suggesting a narrower range of effective phytoplankton growth enhancement compared to IAA. Significant changes in growth of *Actinocyclus* were only noted beyond late exponential phase (6-11 d) (Repeated-measures ANOVA, $p\text{-value} < 0.05$; Figure 6, Supplementary Table S15). This suggests GA may only affect *Actinocyclus* cell proliferation after cells have reached late exponential stages of growth. It is indeed plausible that the growth-promoting effects of PGPHs may be influenced by a range of factors, including the concentration of the hormone and physiological state of the cells.

Despite the 14 bacteria producing quantifiable amounts of IBA, ABA, TZ, JA, and BSN, supplementation of *Actinocyclus* cultures with these PGPHs had negligible effects on the diatom's growth. This would mean *Actinocyclus* sp. may only respond to certain PGPHs (i.e., IAA and GA), even though the 14 bacteria also produce other PGPHs. This is in contrast to other studies that have shown that some of these hormones can have beneficial properties for phytoplankton. These include changes in cell growth in response to JA supplementation experiments (Czerpak et al., 2006; Jusoh et al., 2015; Piotrowska-Niczyporuk et al., 2012), the stimulation of heterocyst formation and chlorophyll *a* accumulation in response to IBA (Mansouri & Talebizadeh, 2017), or increases in carotenogenesis (algal defence system) when treated with ABA (Kobayashi et al., 1997). Given that most of these health-related phenotypes were not measured during our experiments and may be independent of cell density, it is possible that these five PGPHs may still positively affect *Actinocyclus* health. It is also possible that *Actinocyclus* sp. require a combination of PGPHs to elicit a growth response. Previous studies in terrestrial systems have demonstrated that a combination of IAA and Benzyl adenine enhanced morphological parameters (shoot length, leaves numbers and branching) (Elakbawy et al., 2022). Given that all isolates tested here exhibit a growth-promoting effect on *Actinocyclus* and, on average, produce 6 out of the 7 PGPHs, it is possible these PGPHs could affect phytoplankton growth, and remains an intriguing area for future study. The diverse and abundant microbiome of *Actinocyclus* (Le Reun et al., 2023) may therefore have a crucial role in enabling phytoplankton to access a suitable mixture of PGPHs.

2.5 Conclusion:

In planktonic systems, bacterial-produced metabolites play important roles in regulating the biological functions of phytoplankton (Koksharova & Safronov, 2022). Emerging evidence suggests that PGPHs could play a pivotal role as metabolites in mutualistic partnerships between phytoplankton and bacteria. However, there is limited knowledge regarding the range of PGPHs produced by marine bacteria and their precise impact on the growth of phytoplankton. Here, we provide evidence that production and exudation of PGPHs is widespread among marine bacteria and that some of these PGPHs enhance the growth of the marine diatom *Actinocyclus*. Strikingly, all 14 bacteria tested here produced a wide suite of PGPHs. We found that several bacteria have the capacity to simultaneously produce and extracellularly release significant quantities of a suite of PGPHs, pointing towards a potentially significant ecological importance of these chemicals. Our demonstration that some of these PGPHs, in particular IAA, enhance phytoplankton growth provide clear evidence for their role in bacteria-phytoplankton interactions. Yet, on the other hand, the limited impact of several of the bacterial-produced PGPHs on phytoplankton growth, indicates a more complex dynamic, whereby a suite of PGPHs may be required for phytoplankton growth promotion. Previously, the simultaneous biosynthesis of several PGPHs by bacteria was only believed to occur in plant root systems, but our observations have confirmed the presence of numerous PGPHs within a phytoplankton-bacteria association. Cumulatively, these observations deliver important new insights into the apparent ubiquity of a potentially significant chemical exchange at the base of the marine food web.

Authors' contributions: A.K., J.S., J-B.R., and A.B. designed all the experiments, wrote the main text and edited the supplementary material. N.R. isolated the 14 bacteria and completed preliminary experiments for the correlation analysis (Fig. 5). N.W. prepared Figs. 3 and 4 and A.B. isolated the diatom. A.K. performed all the experiments and processed all data. U.K aided in LC-MS/MS analysis and A.F analysed genome sequencing data. All authors edited the manuscript and agree to the final submitted version.

Production Note:
Justin Seymour: Signature removed prior to publication.

Production Note:
Jean-Baptiste Raina: Signature removed prior to publication.

Production Note:
Anna Bramucci: Signature removed prior to publication.

Production Note:
Amaranta Focardi: Signature removed prior to publication.

Production Note:
Nine Le Reun: Signature removed prior to publication.

Production Note:
Nathan L. R. Willams: Signature removed prior to publication.

Production Note:
Unnikrishnan Kuzhiumparambil: Signature removed prior to publication.

Chapter 3:

Quantifying the contribution of indole-3 acetic acid in phytoplankton-bacteria partnerships using a CRISPR-Cas9 mediated knockout approach

Abeeha Khalil¹, Jean-Baptiste Raina¹, Rashad Mahbub², Amaranta Focardi¹, Alen Faiz²,
Justin R. Seymour¹

¹Climate Change Cluster, University of Technology Sydney, Ultimo, 2007, NSW, Australia.

² Respiratory Bioinformatics and Molecular Biology, University of Technology Sydney, Ultimo, 2007, NSW, Australia.

In preparation for submission to *Frontiers in Microbiology*

3.1 Introduction:

Plant growth promoting hormones (PGPHs) are important metabolites that play pivotal roles in many aspects of plant growth and development (Desai, 2017; Gaskins et al., 1985; Ross et al., 2011; Jiang et al., 2017; Ross & Reid, 2010). Of these hormones, Indole-3 acetic acid (IAA) is the most widely distributed PGPH in terrestrial environments (Spaepen & Vanderleyden, 2011; Zhao, 2010b), where it is produced by bacteria inhabiting plants' rhizosphere and plays a critical role in governing plant growth, cell division, elongation, and differentiation (Ali et al., 2009; Spaepen et al., 2007; Spaepen & Vanderleyden, 2011; Zhao, 2010a). While most of the research on the ecological influence of IAA has focused on terrestrial systems, recent evidence indicates that this molecule could also play important roles in aquatic ecosystems by impacting phytoplankton growth (Amin et al., 2015; Elakbawy et al., 2022; Labeeuw et al., 2016; Matthews et al., 2023.; Segev et al., 2016). Although some phytoplankton can independently synthesize low levels of IAA (Labeeuw et al., 2016), the main producers and providers of these hormones are believed to be symbiotic heterotrophic bacteria (Amin et al., 2015; Matthews et al., 2023).

A growing body of research has revealed that Alpha- and Gammaproteobacteria can provide IAA to diverse phytoplankton species including the diatoms *Pseudo-nitzschia multiseries* (Amin et al., 2015), *Actinocyclus* sp. (Khalil et. al. 2024); the coccolithophore *Emiliania huxleyi* (Segev, Wyche, Kim, et al., 2016); and the dinoflagellates *Symbiodinium microadriaticum* and *Breviolum minutum* (Matthews et al., 2023). Additionally, IAA supplementation can lead to growth enhancements in phytoplankton, and in some instances increase in fatty acids, pigments, and polysaccharide production (Yu et al., 2024; Zhou et al., 2024). These effects have been reported across a wide range of phytoplankton species, including diatoms (Nikolayevich et al., 2023; Fierli et al., 2022; Khalil et. al. 2024) chlorophytes (Elakbawy et al., 2022; Mazur et al., 2001; Peng et al., 2020; Piotrowska-Niczyporuk & Bajguz, 2014; Yu et al., 2024; Zhou et al., 2024) euglenoids (J. Y. Kim et al., 2019); and cyanobacteria (Silveira et al., 2024). We recently demonstrated that several phytoplankton-associated bacteria significantly enhance the growth of the diatom *Actinocyclus* sp. (Le Reun et al., 2023) and that many of these bacteria synthesized multiple PGPHs, including IAA (Khalil et al. 2024). Furthermore, provision of IAA resulted in a two-fold increase in *Actinocyclus* sp. cell numbers over a single growth cycle (Khalil et al. 2024).

While the provision of IAA from phytoplankton-associated bacteria increasingly appears to represent a key component of these partnerships, these interactions are multifarious and often involve the simultaneous exchange of multiple metabolites (Durham et al., 2015, 2019; Mayali, 2018; Raina et al., 2023). Therefore, the relative importance of bacterial provision of IAA in phytoplankton growth promotion remains unquantified. To address this question, we knocked out the capacity for IAA synthesis in a phytoplankton-associated bacterium (*Alteromonas mediterranea*), which both synthesises high levels of IAA and has been demonstrated to enhance diatom growth (Khalil et al. 2024). We subsequently compared the capacity of the wildtype *A. mediterranea* and IAA-deficient mutant to enhance phytoplankton growth.

3.2 Methods:

3.2.1 Diatom and bacteria culturing:

Previously, we identified the growth-promoting benefits of a set of 14 phytoplankton-associated bacteria on the marine diatom *Actinocyclus* sp. (Le Reun et al., 2023). We confirmed that each of these bacteria synthesizes a suite of PGPHs, including IAA, indole-3-butyric acid, abscisic acid, gibberellic acid, jasmonic acid, trans-zeatin, and brassinolide (Khalil et. al. 2024). Among these 14 bacterial strains, we identified *A. mediterranea* as a suitable candidate for further examination because it (i) significantly enhanced the growth of *Actinocyclus* sp., (ii) synthesizes high levels of IAA and low levels of all other PGPHs, and (iii) harbours a relatively simple and well characterised pathway for IAA biosynthesis.

The *A. mediterranea* strain was previously isolated from a culture of the diatom *Actinocyclus* sp., which was itself isolated from seawater collected from an oceanographic reference station (Port Hacking – 34° 05.00 S, 151° 15.00 E) on the east coast of Australia (Brown et al., 2018; Le Reun et al., 2023). Xenic cultures of *Actinocyclus* sp. were grown under controlled light conditions of 55-65 µE, with a 12:12 day/night cycle, at 20-22 °C. The *A. mediterranea* strain were stored in 80% glycerol stocks and subsequently re-cultured by spreading a small aliquot of the frozen stock onto 100% Marine Agar (Difco) and incubating the plates at room temperature for 3–4 days. Single colonies were then selected and further grown in liquid 100% Marine Broth (Difco) for 12 h. These cultures were then utilised for experimentation.

3.2.2 CRISPR – Cas9 editing in *A. mediterranea*:

Genomic analyses suggest that *A. mediterranea* harbours two tryptophan-dependent IAA biosynthesis pathways (Khalil et. al. 2024), the indole-3-acetamide and tryptamine pathways (Figure 3.1a). However, genes comprising the indole-3-acetamide pathway had higher e-values than those from the tryptamine pathways (Figure 3.1b), suggesting that homologues of the indole-3-acetamide pathway may not be functional. Within the tryptamine pathway homologues, the indole-3-acetamide dehydrogenase (*IAAldD*) gene was of particular interest because it showed the highest similarity (94.937% amino acid similarity) to *IAAldD* from bacteria closely related to *A. mediterranea*. *IAAldD* was therefore chosen as a target for CRISPR-Cas 9 mediated knockout (Supplementary table S3.1).

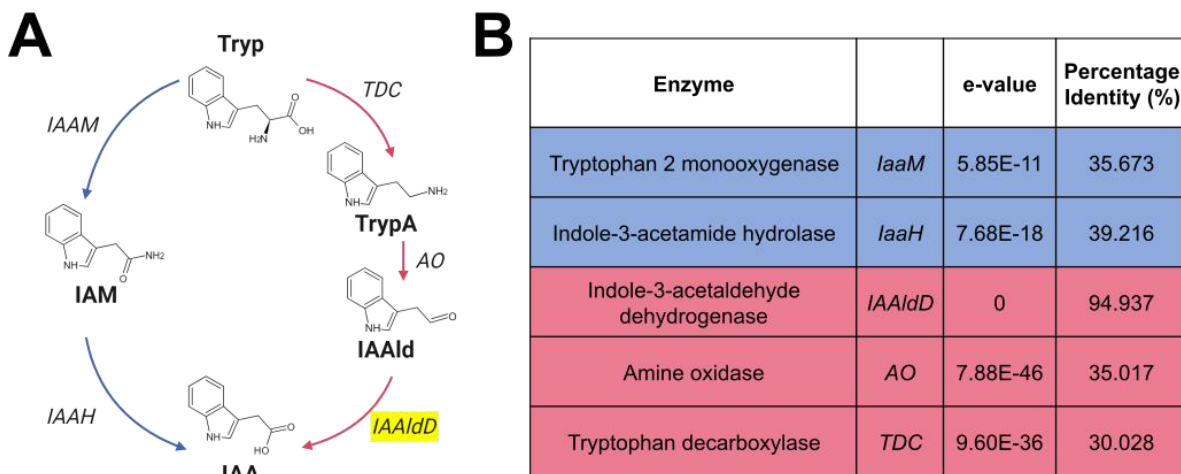


Figure 3.1: Tryptophan-dependent Indole-3 acetic acid biosynthesis pathway in *A. mediterranea*. **A)** Homologs of two IAA biosynthesis pathways, Indole-3-acetamide (blue) and Tryptamine (red) pathways were identified in the genome (query) of *A. mediterranea*. Intermediate molecules are depicted with black bold text and the targeted gene is highlighted. IAM, indole-3-acetamide; TrypA, Tryptamine; IAALd, indole-3-acetaldehyde (highlighted in yellow). Enzymes are depicted un-bold black text and lines. IaaM, Tryptophan-2-monooxygenase; IaaH, Indole-3-acetamide hydrolase; TDC, Tryptophan decarboxylase; AO, Amine oxidase; IAALdD, indole-3-acetaldehyde dehydrogenase. **B)** E-values and percentage similarity of *A. mediterranea* homologous proteins to closely related bacteria, using Blastp searches for bacterial homologs. BLASTp hits with an e-value $\geq 10^{-10}$ or less was used as a cut-off.

3.2.3 Vector Design:

To generate a plasmid vector for knocking out IAA biosynthesis, the plasmid backbone pST_140_LVL₊cam (Addgene) (Stukenberg et al., 2022) was used. Plasmids were purified from DH5 α *E. coli* using a Qiagen plasmid purification kit, resulting in a concentration of 100 ng/ μ L. Specific gRNA sequences (20 bp) targeting the indole-3-acetaldehyde dehydrogenase (*IAALdD*) gene and primers for confirming guide ligation were designed using Benchling and synthesized (Integrated DNA Technologies (IDT)) (Supplementary table S3.2). To fuse the gRNA fragments to the plasmid backbone, the guide region within the plasmid was identified, and the appropriate restriction enzyme was selected using Geneious Prime (Figure 3.2). The guide sequences were flanked with 5 bp on each side of the gRNA, which were complementary to the plasmid pST_LVL2₊cam (Addgene).

3.2.4 Expression Vector Construction:

For gRNA ligation into the CRISPR-Cas9 expression vector, oligonucleotides were annealed in a 0.2 mL PCR tube with 1 μ L each of forward and reverse primers, 1 μ L T4 ligation buffer, 6.5 μ L Milli-Q water, and 0.5 μ L T4 polynucleotide kinase (New England Biolabs). The phosphorylation and annealing were carried out in a thermocycler (Thermo Fisher) at 37 °C for 30 min (phosphorylation), followed by 95 °C for 5 min (annealing), and a ramp down to 25 °C at 5 °C per minute. The oligonucleotide mixture was then diluted 1:250. For the digestion-ligation reaction, 1 μ L of 100 ng/ μ L plasmid vector was combined with 2 μ L of the diluted annealed oligonucleotide, 2 μ L of 10X FastDigest buffer, 2 μ L of 10 mM DTT, 2 μ L of 10 mM ATP, 1 μ L FastDigest BsaI, and 0.5 μ L T7 DNA ligase (New England Biolabs). The ligation reaction was incubated in a thermocycler at 37 °C for 5 min, followed by 25 °C for 5 min for 6 cycles, and held at 4 °C until further use. The ligation product was treated with PlasmidSafe (New England Biolabs). To prevent unwanted recombination, 11 μ L of the ligation reaction was incubated with 1.5 μ L 10X PlasmidSafe buffer, 1.5 μ L 10 mM ATP, and 1 μ L PlasmidSafe exonuclease at 37 °C for 30 min (Figure 3.2).

3.2.5 Transformation and Screening:

The gRNA ligated into the expression vector (2 μ L) was transformed into 50 μ L of competent DH5 α *E. coli* cells, incubated on ice for 30 min, heat-shocked at 42 °C for 30 seconds, and returned to ice for 2 min. The cells were then incubated in 150 μ L LB broth while shaken at 230 rpm at 37 °C for 1 hr. The transformed cells were plated on chloramphenicol-positive (100 mg/mL) and negative plates, prior to being incubated at 37 °C overnight. After 12 h, plates were incubated 4 °C for 6 h. A single colony from each plate was selected for overnight culture in LB Broth (Difco) with 100 mg/mL chloramphenicol. Cultures were prepared for long-term storage by adding 200 μ L of the culture to 800 μ L sterile glycerol, before being frozen in liquid nitrogen and stored at -80 °C. The remaining culture was centrifuged and plasmid DNA was extracted using a Qiagen kit. The plasmid was sequenced to confirm successful guide ligation (Figure 3.2).

3.2.6 Gene Knockout:

Plasmids with successfully ligated *IAAldD* guide sequences were transfected into *A. mediterranea* cells. *A. mediterranea* cultures were grown on Marine Agar plates (Difco Marine Broth 2216) as previously described and incubated at room temperature for 3 days. A single

colony was inoculated into 5 mL of 0.22 μ m filter-sterilized Marine Broth and incubated with shaking at 160 rpm for 12 h. A 200 μ L aliquot of the culture was mixed with 2 μ L of the plasmid containing the *IAAldD* guide and transfected as previously done for DH5 α *E. coli*. Transfected cultures were plated on chloramphenicol-positive and negative plates (Figure 3.2). A total of 6 single colonies from positive plates were isolated and grown in 5 mL of sterile Marine Broth supplemented with chloramphenicol (50 μ g/mL), and then incubated at room temperature with shaking at 160 rpm for 12 h. Cultures were centrifuged and DNA was extracted using the PowerWater DNA extraction kit (Qiagen). PCR was performed using primers designed to amplify the *IAAldD* gene region in *A. mediterranea* under the following cycling conditions: 95 °C for 10 min, followed by 30 cycles of 95 °C for 30 seconds, 50 °C for 30 seconds, and 72 °C for 120 seconds, with a final extension at 72 °C for 10 min. PCR products were sequenced (Ramaciotti Centre for Genomics, UNSW). To confirm a knockout of the *IAAldD* gene, sanger sequencing results were input into TIDE (<https://tide.nki.nl/>), which identified and quantified deletions within the samples. A single *A. mediterranea* isolate that displayed mutations within the *IAAldD* gene region was considered for further experiments.

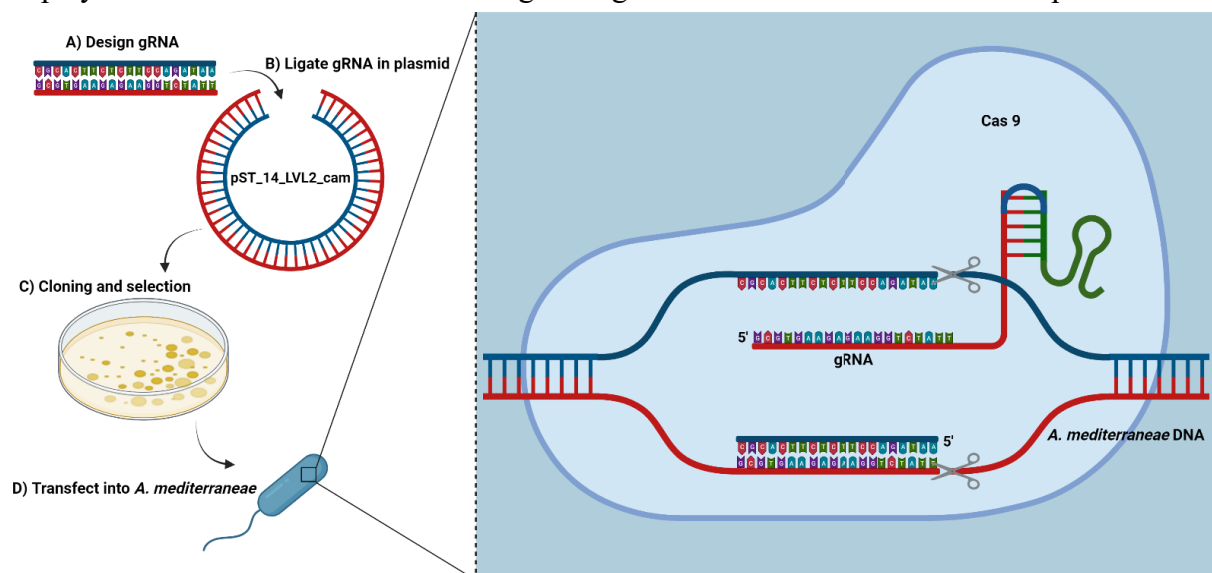


Figure 3.2: CRISPR-Cas9 knockout protocol. The left side depicts A) preparation of gRNA oligonucleotide sequences specific to *IAAldD* expression with flanking regions complementary to the pST_140_LVL2_cam plasmid, B) ligation of gRNA to pST_140_LVL2_cam plasmid backbone, C) clone and selection of plasmid with DH5 α *E. coli* colonies and D) transfection of purified plasmid with *IAAldD* gRNA into *A. mediterranea*. The right side shows the process of the Cas9 protein editing the *A. mediterranea* genome to knockout expression of *IAAldD*.

3.2.7 IAA characterisation using LC-MS/MS analysis:

To confirm the elimination of IAA production in mutated *A. mediterranea* strains, we quantified the concentration of IAA in both mutated and wildtype strains. IAA levels were also quantified in the diatoms *Actinocyclus* sp. and *P. tricornutum* and the marine green microalgae *N. oceanica*. IAA levels were measured during the cells' exponential growth phase. Specifically, 50 mL of each culture was grown to exponential phase in quadruplicate and enumerated (see below). Each replicate was then centrifuged at 2,000 rpm for 30 min, the medium was discarded and the pellet was flash frozen in liquid nitrogen and stored at -80 °C until IAA extraction.

Cells were enumerated using flow cytometry. A 200 μ L aliquot from each replicate was taken and fixed with 2% glutaraldehyde. For bacterial enumeration, samples were stained with SYBR-Green I (final concentration 1:10000; SYBR-Green I, Invitrogen) and incubated in the dark for 15 min. Flow cytometry was performed using a CytoFLEX LX (Beckman Coulter), with bacterial cells identified according to side scatter (SSC) and green fluorescence (SYBR-Green) (Marie et al., 1997). Phytoplankton were enumerated in unstained samples, with cells discriminated according to forward scatter (FSC), side scatter (SSC) and red fluorescence (chlorophyll).

For IAA quantification, we used the protocol described in Khalil et. al. (2024). Briefly, 2 mL of a 14:4:1 solution of 99% methanol (Sigma-Aldrich), ultrapure water, and 99% formic acid (Sigma-Aldrich) was added to each sample, which was then sonicated for 2 min to lyse the cells. The cellular debris was subsequently pelleted via centrifugation at 2000 rpm, and the extracted supernatant freeze-dried at -80 °C. The freeze-dried extracts were then reconstituted into 1 mL of 1 M formic acid, and further purified on Evolute express CX columns (Biotage) that had been pre-conditioned with methanol and 1 M formic acid. The samples were first eluted in 3 mL of 99% methanol, then 3 mL of 0.35 M ammonium hydroxide (Sigma-Aldrich), and finally 3 mL of 0.35 M in ammonium hydroxide in 60% methanol. All samples were then freeze dried at -80 °C and reconstituted with 99% ultrapure high-pressure liquid chromatography (UHPLC) grade methanol (Sigma-Aldrich) for LC-MS/MS analysis (Balcke et al., 2012; Van Bruggen et al., 2018).

IAA standards were used to calibrate the LC-MS/MS to mobile phase, run time and energy requirements for phytohormone fragmentation. A 10-point standard curve spanning: 50, 25,

12.5, 6.25, 3.12, 2.5, 1.25, 0.624, 0.312, and 0.03 ng/mL was prepared (this concentration range was based on Khalil et. al. 2024). Quantification of IAA was performed using a Shimadzu LCMS-8060 (Shimadzu, Kyoto, Japan) instrument with a dual ion source (DUIS) interfaced to Shimadzu Nexera X2 liquid chromatography system. The separation was performed on an Acquity UPLC HSS T3 column (1.8 μ m, 2.1 \times 150 mm) using a binary gradient of milliQ water (A) and methanol (B) for 15 min, at a flow rate of 0.18 mL/min. The linear gradient program was run at: 0–10 min, 20–95% B; 10–11 min, 95–20% B; 11–15 min, 20% B. Column temperature was maintained at 30 °C. Samples were analysed in the multiple reaction monitoring mode. The following transitions were monitored with a fragmentor voltage of 160 V and collision energy of -6 eV m/z 174 \rightarrow 130, d₅-IAA m/z 179 \rightarrow 135. The resulting peaks were then quantified using the 10-point calibration curves (Balcke et al., 2012). Statistical differences in hormone concentrations between the isolates were assessed using a one-way ANOVA.

3.2.8 Cogrowth experiments:

To assess the impact of *A. mediterranea* IAA synthesis on phytoplankton growth, we conducted co-culture experiments with both wildtype and *IAAldD*-deficient strains of *A. mediterranea* and the three different phytoplankton species: *Actinocyclus* sp., *Phaeodactylum tricornutum* and *Nannochloropsis oceanica*. Co-growth experiments followed the protocols described in Le Reun et al. (2023). Briefly, each co-culture was set up in a 70 mL tissue culture flask with a final volume of 50 mL (n = 4). For all experiments, bacteria were freshly plated from glycerol stock onto 100% Marine Agar plates 3–4 days prior to the start of the experiment and were grown from single colonies in Marine Broth. Bacteria were centrifuged at 1400 rpm for 6 min in 1.5 mL microcentrifuge snap-seal Eppendorf tubes. The bacterial pellet was then washed with sterile f/2 media twice, centrifuged (1,400 g for 6 min) and reconstituted in 1 mL of media. Bacteria and phytoplankton were then enumerated via flow cytometry as described above. Phytoplankton were inoculated from 7 d old cultures into fresh media (n = 4) to a density of 5,000 cells/mL and bacterial isolates were added to the axenic phytoplankton cultures at a density of 1,000 cells/mL to achieve a final ratio of 1:5 bacteria:phytoplankton. *Actinocyclus* sp. and *A. mediterranea* co-cultures were then incubated at 21 °C, at 60–70 μ E light intensity. Co-cultures of *N. oceanica* and *P. tricornutum* with *A. mediterranea* were incubated at 23 °C at 70–100 μ E light intensity. All cultures were gently shaken daily over a period of 20 days. Axenic phytoplankton cultures were maintained along-side the co-growth treatments and acted

as controls ($n = 5$ for *Actinocyclus sp.* and *P. tricornutum* and $n = 3$ for *N. oceanica*). Over the course of the co-culture experiments, 200 μL aliquots were sampled and fixed with glutaraldehyde (2% final concentration) every two days and both phytoplankton and bacterial cells were quantified using flow cytometry as described above. The axenic culture controls were checked for contamination throughout the course of the co-culture using flow cytometry (Le Reun et al., 2023). Using the difference in phytoplankton cell abundance between the wildtype and mutant co-cultures, we then calculated the percentage contribution of IAA to the growth enhancement caused by *A. mediterranea*.

All data was analysed using repeated-measures ANOVA to identify significant changes in growth between control and bacteria co-cultures. All data was assessed for normality and sphericity, and differences between treatments at each time point were assessed using pairwise comparisons between treatment groups (corrected using Bonferroni) (Quinn & Keough, 2002).

3.3 Results:

3.3.1 CRISPR-Cas9 mediated knockout of IAA in *A. mediterranea*:

Successful CRISPR-Cas9 mediated editing led to the knockout of the *IAA1dD* gene in one *A. mediterranea* mutant. Sanger sequencing of the *IAA1dD* gene followed by Indel (insertion and deletion) analysis revealed a deletion, as indicated by a dominant red peak at -1 deletion spectrum. This targeted editing resulted in 87.9% of the mutant sequence attributing a 1 base pair deletion. The goodness of fit was estimated using R^2 , and the statistical significance of the detection of each indel was calculated. An Aberrant Sequence Signal Plot highlighted base pair decomposition in *IAA1dD*-deficient *A. mediterranea* mutant beyond base pair 64 (Figure 3.3).

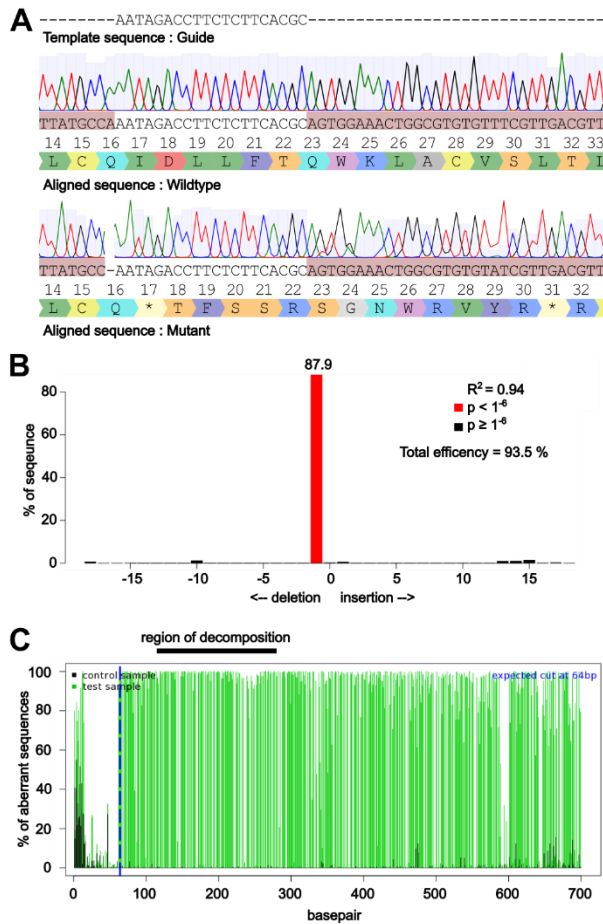


Figure 3.3: Confirmation of IAALdD gene knockout in *A. mediterranea*. **A)** Aligned IAALdD gene sequences for the wildtype and mutant *A. mediterranea*. The top sequence displays the gRNA, which corresponds to the first 20 base pairs of the IAALdD gene. The middle sequence shows the wildtype *A. mediterranea* strain, the bottom sequence represents the mutant *A. mediterranea*, and the dashed line indicates the point mutation. Amino acid translation (letters under the sequence) indicate a stop codon at the site of the knockout. **B)** Indel spectrum plot showing the types and frequencies of insertions and deletions introduced at the CRISPR-Cas9 target site in the mutant population. The x-axis denotes specific indel sizes; the red peak highlights a dominant single base-pair deletion, detected in 87.9% of reads, representing the most frequent editing outcome. Total knockout efficiency (all indels combined) is 93.5%, calculated as the proportion of reads containing any edit compared to the total read count. **C)** Aberrant sequence signal plot comparing the test (mutant) and control (wildtype) sequences. Each green bar represents sequence divergence from the wildtype at a given base pair. The pronounced peak near position 64 bp (blue dashed line) corresponds to the expected Cas9 cut site and reflects the high frequency of the editing event. Minor sequence noise seen at earlier

positions, including in the wildtype, is likely due to base calling variation or sequencing artefacts.

3.3.2 Quantification of IAA production by bacterial and phytoplankton isolates:

In-line with the evidence that the *IAAldD* gene had been successfully inactivated, IAA quantification revealed that the mutated strain of *A. mediterranea* was unable to synthesise any measurable levels of IAA, while the wildtype *A. mediterranea* produced high levels of IAA ($0.35 \pm 0.042 \mu\text{g IAA}/\mu\text{m}^3$ Figure 3.4). This result confirms that IAA production through the tryptamine pathway was prevented through the inactivation of *IAAldD*, while the second putative IAA biosynthesis route identified in the *A. mediterranea* genome, the indole-3-acetamide pathway, was likely not functional.

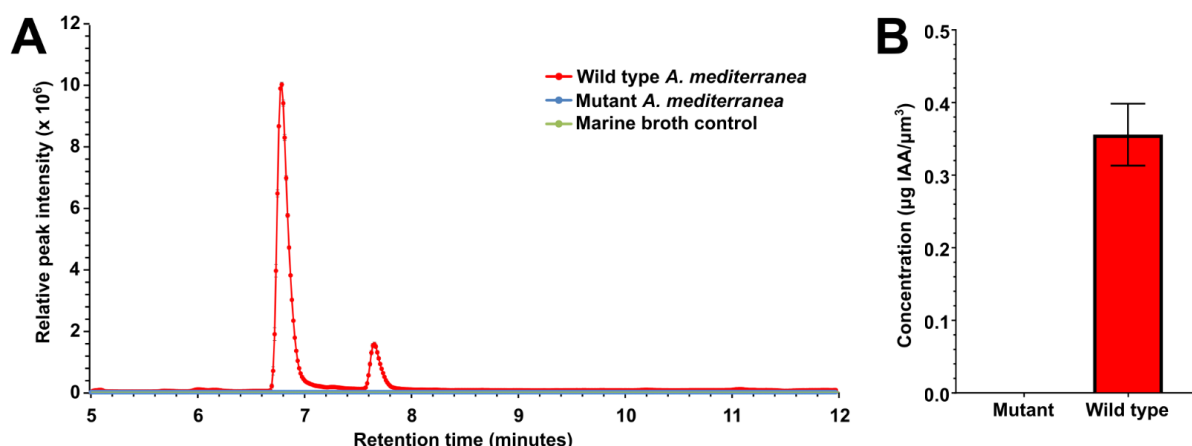


Figure 3.3: Quantification of IAA in *A. mediterranea*. **A)** LC-MS/MS chromatogram depicting peak intensity of wildtype *A. mediterranea* (red), mutant *A. mediterranea* (blue), and Marine Broth control (green). **B)** Biovolume concentration of IAA produced by mutant (blue) and wildtype (red) *A. mediterranea*. Error bars are standard error of the mean (SEM), $n = 4$.

All phytoplankton strains synthesised low concentrations of IAA, with *N. oceanica* and *P. tricornutum* producing on average 17271 times more than *Actinocyclus* sp. (One-way ANOVA $p < 0.05$, Table S3.4), followed by *P. tricornutum* and *Actinocyclus* sp., which produced the lowest (Figure 3.5). However, for comparison to bacterial IAA production, the IAA concentrations measured in the highest IAA producer, *N. oceanica*, were 508 times lower than those measured in the wildtype *A. mediterranea*.

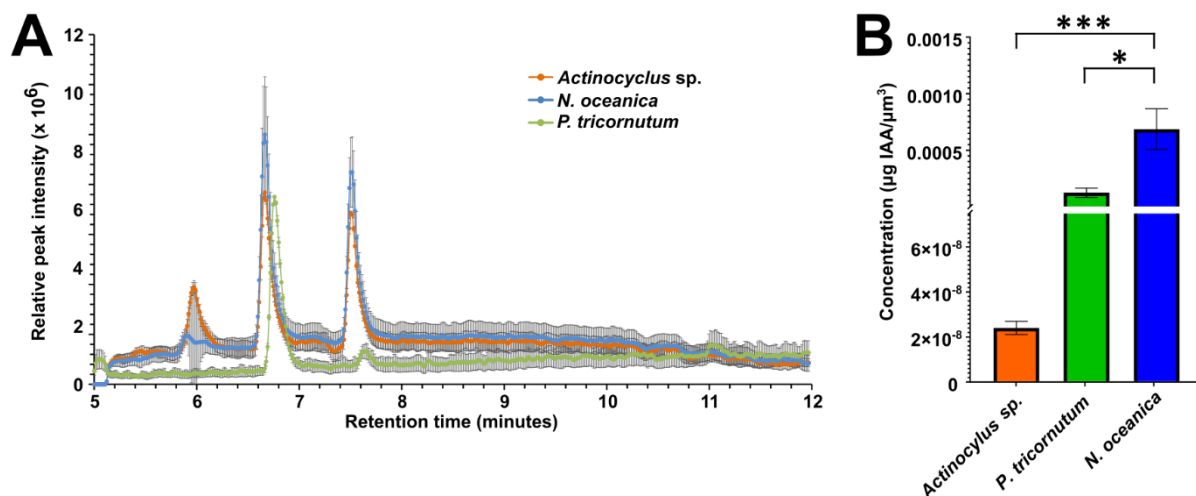


Figure 3.4: Quantification of IAA in three phytoplankton species. A) LC-MS/MS chromatogram depicting peak intensity of *Actinocyclus* sp. (orange), *N. oceanica* (blue) and *P. tricornutum* (green). Error bars are standard error of the mean (SEM), n = 4. **B)** Biovolume concentration of IAA produced by *Actinocyclus* sp. (orange), *N. oceanica* (blue) and *P. tricornutum* (green). Error bars are standard error of the mean (SEM), n = 4. Significant differences are depicted with asterisks (*; One-way ANOVA, p<0.05, Table S3.4).

3.3.3 Co-growth experiments:

To determine the degree of phytoplankton growth enhancement induced by IAA, we compared the outcomes of co-growth experiments involving mutated and wildtype *A. mediterranea* with their diatom host – *Actinocyclus*. The presence of the wildtype *A. mediterranea* caused a significant enhancement of *Actinocyclus* cell abundance after 10 days of co-culture and this effect was sustained until the end of the experiment (Pairwise comparisons, p<0,05; Figure 3.6A; Supplementary Table S3.3). The largest difference in cell abundance occurred on 20 d, with 2.2 times more diatom cells in the wildtype co-culture compared to the axenic control. Importantly, *Actinocyclus* cell abundances in co-culture with the *IAAldD*-deficient mutant were not significantly different from the axenic control at any timepoints. Using the difference in *Actinocyclus* cell abundance between the wildtype and mutant co-cultures, we calculated the contribution of IAA to the growth enhancement caused by *A. mediterranea*. Our estimate suggests that IAA contributed to 98.9 ± 13.1% of the observed *Actinocyclus* growth enhancement induced by *A. mediterranea*.

To determine if IAA production by *A. mediterranea* also affect the growth of other phytoplankton, we extended our co-cultures experiments to two other marine phytoplankton species, *N. oceanica* and *P. tricornutum*, which are not the native hosts of *A. mediterranea*. In

both co-cultures, the growth of the axenic phytoplankton was indistinguishable from the co-growth with *IAA1dD*-deficient mutant (Pairwise comparisons, $p>0,05$; Figure 3.6B-C; Supplementary Table S3.3). Growth enhancement of the wild type *A. mediterranea* occurred at only one timepoint (8 d) in co-culture *P. tricornutum*, and the positive effect was modest and not sustained through time (Pairwise comparisons, $p>0,05$; Figure 3.6B-C; Supplementary Table S3.3).

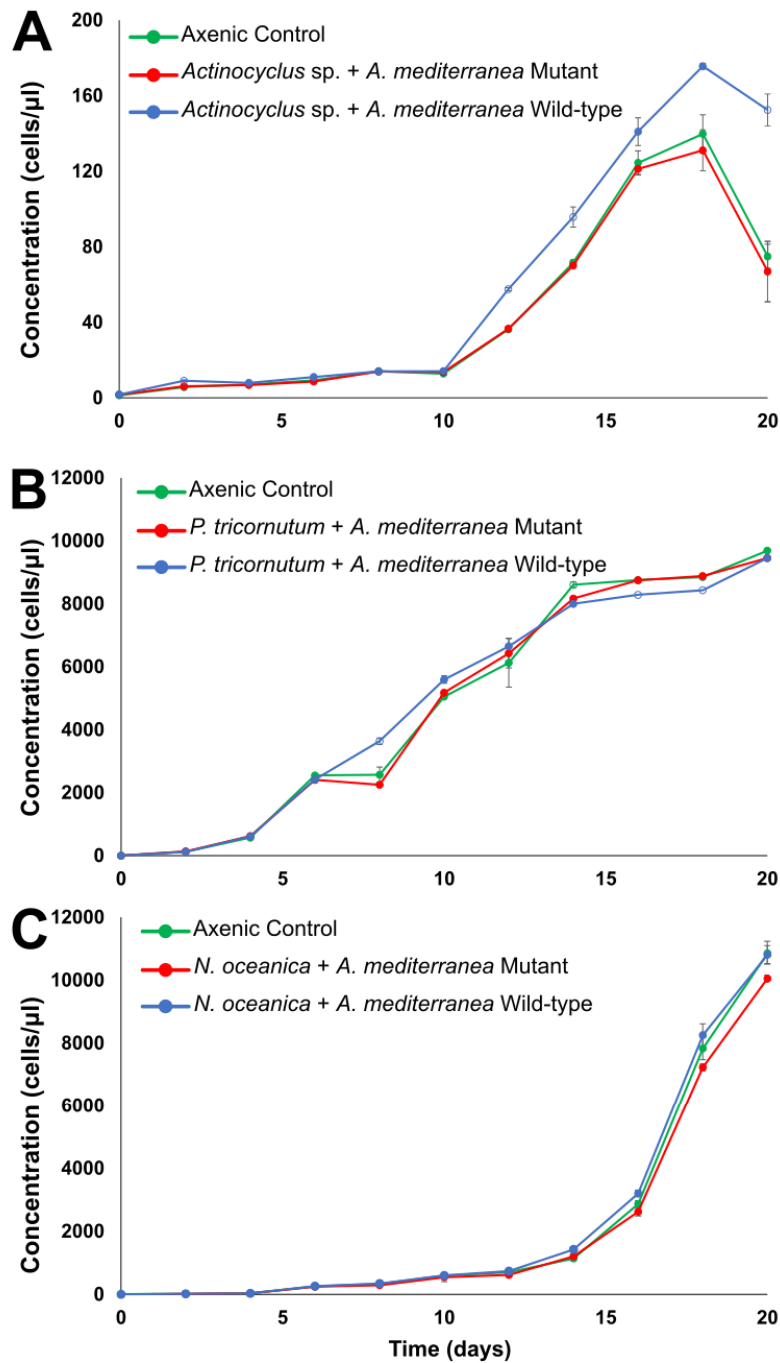


Figure 3.5: Growth of three phytoplankton species with wild-type and IAAldD-deficient *A. mediterranea* over the course of 20 days. Phytoplankton cell numbers per millilitre in co-culture with IAAldD-deficient mutant (red), and wild-type (blue) *A. mediterranea*, compared to the axenic controls (green). **A**) Growth dynamics of *Actinocyclus* sp. co-cultures (n = 5); **B**) *P. tricornutum* co-cultures (n = 5); and **C**) *N. oceanica* co-culture (n = 3). A significant difference between a given concentration and the control is depicted as an empty circle (Repeated-measures ANOVA, $p < 0.05$, *Supplementary table S3.3*). Error bars are standard error of the mean (SEM)."

3.4 Discussion:

Ecological interactions between phytoplankton and bacteria involve the exchange of diverse chemical currencies, which are critical for the health and survival of both taxa (Amin et al., 2015; Durham et al., 2015; Grossart, 1999; Le Reun et al., 2023; Martínez-Pérez et al., 2024; Mayali, 2018; Seymour et al., 2017). PGPHs such as IAA are potentially crucial regulators of phytoplankton growth (Amin et al., 2015; Matthews et al., 2023.; Segev, Wyche, Hyun Kim, et al., 2016), but the relative importance of these chemicals among the suite of molecules exchanged in phytoplankton-bacteria partnerships has yet to be quantified. Our goal was to quantify the impact of bacterial provision of IAA on phytoplankton growth by contrasting the effects of a known phytoplankton growth-promoter (*A. mediterranea*) with a mutant that was genetically modified to prevent IAA synthesis. This is the first attempt to genetically modify a marine bacterium to assess the effects of IAA provision in a symbiosis. We used a CRISPR-Cas9 knockout approach to successfully inactivate a key gene (*IAAldD*) involved in IAA biosynthesis, resulting in undetectable IAA production by the mutated strain. Using this system, we found variable importance of IAA provision on the growth of three different phytoplankton species, with evidence that in one diatom species (*Actinocyclus* sp.) bacterial provision of IAA contributed to ~98% of the observed growth enhancement.

3.4.1 Understanding single-metabolite interactions through genetic engineering:

Genetic engineering approaches allow for selective quantification of the specific role and impact of individual metabolites. Recent studies have started to adopt similar approaches to the one applied here. For instance, the development of genetically engineered whole-cell bioreporters has advanced our understanding of nutrient limitations in marine systems (Blanco-Ameijeiras et al., 2019), while the metabolic engineering of *Escherichia coli* for high-level terpenoid production has been used to characterise terpenoid biosynthesis pathways (Rinaldi et al., 2022). Similarly, efforts to engineer *Streptomyces coelicolor* have permitted the production of novel polyketides, shedding light on their biosynthesis (Gomez-Escribano et al., 2012). These examples underscore the effectiveness of using genetic engineering to elucidate the roles of individual metabolites within complex microbial ecosystems. However, the work presented in this chapter, is to my knowledge, the first attempt to use these approaches to precisely elucidate the roles of specific metabolites within the framework of phytoplankton-bacteria interactions.

3.4.2 The role of IAA in phytoplankton-bacteria interactions:

We have previously demonstrated that the marine bacterium *A. mediterranea* significantly enhances the growth of the diatom *Actinocyclus* sp. (Le Reun et al., 2023), and produces and exudes IAA (Khalil et. al. 2024), while *Actinocyclus* growth is enhanced by IAA additions (Khalil et. al. 2024). Previous studies have indicated that *Alteromonas* strains can synthesise a variety of metabolites that have the potential to enhance phytoplankton growth, including petrobactin (siderophore that mediates iron acquisition), sucrose phosphorylase (enzymes that aid sucrose production), and other potentially important contributors to diatom metabolism (Manck et al., 2022; Pereira-Garcia et al., 2024; Robertson et al., 2024). Therefore, I wished to determine the relative importance of IAA among this soup of metabolites that could be potentially beneficial to phytoplankton associates. Despite the many molecules potentially exuded by *Alteromonas*, here we show that IAA provision by *A. mediterranea* plays a central role in enhancing *Actinocyclus* sp. growth. Co-growth experiments involving *Actinocyclus* sp. and *A. mediterranea* revealed an inherent reliance on bacterial provision of IAA for growth enhancement. Indeed, *Actinocyclus* cell numbers in co-culture with the *IAAldD*-deficient mutant were comparable to those observed in axenic cultures. As the ability to synthesise IAA constituted the only difference between the *IAAldD*-deficient mutant and the wildtype *A. mediterranea*, this result suggests that no other molecules produced by *A. mediterranea* impacted the growth of *Actinocyclus*. Indeed, the growth enhancement measured could be almost fully ascribed to the production of IAA. This further demonstrates how specific metabolite exchanges can drive phytoplankton-bacteria interactions, offering new insights into the selective nature of these relationships in marine ecosystems.

3.4.3 Effects of IAA on other phytoplankton species:

In contrast to the response observed in *Actinocyclus* sp., no sustained differences were observed in the growth of *N. oceanica* and *P. tricornutum* when co-cultured with the wildtype or mutated *A. mediterranea*. The lack of response of *N. oceanica* and *P. tricornutum* can be due to several factors.

First, the *A. mediterranea* strain was originally isolated from the *Actinocyclus* sp. culture. It is well-established that bacteria within a phytoplankton's native microbiome often exhibit beneficial properties for their host and might have negligible effects on others (Bruhn et al., 2007; Grossart, 1999; H. Kim et al., 2022; J. Y. Kim et al., 2019; Le Reun et al., 2023;

Matthews et al., 2023). Studies have shown variable results in co-cultures involving native versus non-native bacterial species. For instance, research in plant systems has demonstrated that, out of a large consortium of non-native IAA-synthesizing bacteria tested, seedling growth stages of the flowering plant *Capsicum annuum* was only enhanced by two non-native bacteria (Matthews et al., 2024). Additionally, microbiome assemblages often exhibit strong host specificity (Baker et al., 2022). For example, when five eukaryotic algae (*Chlorella sorokiniana*, *Coelastrum microporum*, *Monoraphidium minutum*, *Scenedesmus acuminatus*, and *Selenastrum capricornutum*) were supplemented with the same consortium of heterotrophic bacteria, a subset of taxa was recruited by each alga over time, forming unique consortia that benefited and enhanced algal growth (Baker et al., 2022). This suggests that non-native bacteria like *A. mediterranea* may not be able to affect the growth all types of phytoplankton hosts.

This lack of growth enhancement in non-native hosts may be due to the inability of the wild type *A. mediterranea* to (i) share IAA with phytoplankton; or (ii) produce IAA. Additionally, bacterial cell counts performed during the co-culture experiments indicate that the lack of response in *N. oceanica* and *P. tricornutum* was not due to insufficient bacterial growth. Despite adequate bacterial proliferation, these microalgae did not exhibit a growth response. Indeed, cell attachment, or specific delivery mechanisms, may be required for *A. mediterranea* to share IAA. The bacterial strategies to share metabolites and maintain physical proximity with their phytoplankton hosts remain understudied, but bacterial attachment (Arandia-Gorostidi et al., 2016; Graff et al., 2011; Martínez-Pérez et al., 2024; Shibl et al., 2020), and the use of specific mechanisms to transfer metabolites between cells (Durham et al., 2017; Geng & Belas, 2010) have been previously reported. These mechanisms often involved recognition cascades (Durham et al., 2017) that are underpinned by co-evolutionary relationships (Langerhans, 2008). It is possible that *N. oceanica* and *P. tricornutum* may lack the necessary receptors or signalling pathways to recognize and respond to *A. mediterranea*. In addition, the production of IAA in bacteria is Tryptophan-dependent. In other phytoplankton-bacteria interactions, Tryptophan is provided by the phytoplankton host, resulting in IAA production by the bacterial symbionts (Amin et al., 2015; Labeeuw et al., 2016; Spaepen et al., 2007). A lack of Tryptophan provision by *N. oceanica* and *P. tricornutum* may also result in a lack of IAA production in the wild type *A. mediterranea*.

Lastly, another possibility is that the growth *N. oceanica* and *P. tricornutum* may not be impacted by IAA supplementation. Indeed, both phytoplankton species produced IAA concentrations that were over 17000 times larger than *Actinocyclus* cells. The intracellular concentrations of these two species are similar with those used to enhance phytoplankton growth. For instance, concentrations of 0.02-0.2 mg/L of IAA were utilised to enhance *P. tricornutum* growth (Fierli et al., 2022), IAA concentrations of 1×10^{-7} to 1×10^{-9} significantly enhanced the growth of *Actinocyclus* (Khalil et al. 2024), while higher concentrations of 50 mg/L enhanced *Chlorella sorokiniana* growth (Peng et al., 2020). This possibility could be tested by exposing axenic *N. oceanica* and *P. tricornutum* to exogenous IAA and monitor their cell abundance through time.

3.5 Conclusion:

While there is substantial evidence that a combination of bacterial metabolites can benefit phytoplankton growth, the wide variety of chemicals produced makes it difficult to quantify the relative importance of individual compounds. In this study, we examined the effects of eliminating production of the well-known bacterial metabolite IAA from *A. mediterranea* to quantify its impact on the growth of three phytoplankton species. Our results revealed that the growth-promoting abilities of *A. mediterranea* on the diatom *Actinocyclus* sp. are almost entirely due to its production of IAA. This effect was not, however, universal, as the treatments applied here did not lead to any measurable differences in the growth of two other phytoplankton species. These observations provide the first quantification of the relative contribution of bacterial derived PGPHs on growth enhancement in phytoplankton. Highlighting the important role that IAA plays in the metabolic exchanges between specific phytoplankton and bacteria and enhancing our understanding of these important organisms at the base of the food web.

Chapter 4:

Distribution of plant growth promoting hormone biosynthesis genes across the global ocean

Abeeha Khalil¹, Jean-Batiste Raina¹, Amaranta Focardi¹, Nahshon Siboni¹, Nathan Willams²,
Sidaswar Krishnan¹, Chris Somgsomboon¹, Justin R. Seymour¹

¹Climate Change Cluster, University of Technology Sydney, Ultimo, 2007, NSW, Australia.

² Department of Biological Sciences—Marine and Environmental Biology, University of
Southern California, Los Angeles, California, United States.

4.1 Introduction:

Ecological interactions between phytoplankton and bacteria fundamentally control the health and stability of the ocean (Amin et al., 2012; Field et al., 1998; Le Reun et al., 2023; Mitri & Richard Foster, 2013; Reun et al., 2022; Seymour et al., 2017). These interactions involve complex chemical exchanges that facilitate nutrient cycling (Arrigo, 2004), impact food webs (Trombetta et al., 2020), and influence global biogeochemical processes (Buchan et al., 2014). Among the chemical currencies exchanged in these interactions, recent evidence indicates that bacterial-production and provision of plant growth-promoting hormones (PGPHs) can enhance phytoplankton growth and are potentially pivotal chemicals within the relationships between phytoplankton and bacteria (Amin et al., 2015; G. Dao et al., 2020; G. H. Dao et al., 2018; Krug et al., 2020; Zhang et al., 2022). PGPHs are often produced by bacteria, but the biosynthesis pathways of only two of these molecules have been characterised in prokaryotes, indole-3-acetic acid (IAA) (Labeeuw et al., 2016) and gibberellic acid (GA) (Salazar-Cerezo et al., 2018). Based on previous literature IAA and GA have been shown to be the most prominent PGPHs in phytoplankton bacteria interactions (Khalil et al., 2024; G. Dao et al., 2020; G. H. Dao et al., 2018; Labeeuw et al., 2016; Salazar-Cerezo et al., 2018).

Recent studies have begun to explore the role of bacterial-produced IAA and GA in aquatic systems, particularly involving phytoplankton (Amin et al., 2015; Bashan & De-Bashan, 2010; Matthews et al., 2023; Zhang et al., 2022), and the potential impact of bacteria-derived PGPHs on phytoplankton growth, stress response, and community structure is beginning to emerge (Bashan & De-Bashan, 2010; Zhang et al., 2022). Indeed, recent studies have revealed that IAA produced the Alphaproteobacterium *Sulfitobacter* sp. enhanced the growth of the diatom *Pseudo-nitzschia multiseries* (Amin et al., 2012; Durham et al., 2022; Grossart, 1999b; Seymour et al., 2017). Similarly, the production of GA by bacteria symbiotically associated with the microalgae *Scenedesmus* sp. resulted in a 51% increase in algal biomass over 4 days (G. H. Dao et al., 2018). Both IAA and GA have also been shown to have a growth promoting effect on the diatom *Actinocyclus* sp. (Khalil et. al. 2024). However, most of the emerging evidence for the potential role of PGPHs in phytoplankton-bacteria interactions comes from studies conducted in laboratory settings. While these laboratory studies have delivered a first level of understanding of the role of PGPHs in specific phytoplankton-bacteria interactions, we still do not know how widespread the potential to synthesise IAA and GA is in the ocean.

In recent years, with the advent of global scale sampling campaigns (Acinas et al., 2021; Sunagawa et al., 2020) and high-resolution oceanographic time-series (Brown et al., 2018; Yeh & Fuhrman, 2022) the effects of a wide range of abiotic and biotic factors on the distribution and dynamics of marine microorganism communities have been investigated. For instance, physicochemical parameters such as temperature, pH, dissolved organic carbon (DOC) and nutrients directly affect and are affected by bacterial community composition and activities (Taoufik et al., 2017). Other studies have investigated the distribution of specific phytoplankton and bacteria species in oceanic regions, their genomic potential to produce specific metabolites and the effect of biotic and abiotic variables on their community dynamics (Kisand & Nõges, 2004; O'Brien et al., 2022; Reun et al., 2022; Rooney-Varga et al., 2005; Sadeghi et al., 2021; Yeh & Fuhrman, 2022). However, to date no research has focused on the distribution of PGPH-producing bacteria and the influence of inter-organism relationships and environmental variables on their abundance.

The *Tara* Oceans expedition, which has generated extensive metagenomic data across 210 stations spanning diverse oceanographic provinces (Sunagawa et al., 2020), presents a unique opportunity to characterise the diversity and distribution of PGPH-producing bacteria within marine systems. Here, we used the *Tara* Oceans dataset to examine the global geographical distribution of homologues of IAA and GA biosynthesis genes, and used the presence of bacterial PGPH synthesis genes to identify putative phytoplankton-bacteria associations within natural marine ecosystems.

4.2 Methods:

4.2.1 IAA and GA gene collation and *Tara Oceans* metagenomic data:

Bacterial and archaeal metagenome assembled genomes (MAGs) from 210 diverse oceanographic sites sampled by the *Tara Oceans* expedition were surveyed for the presence of genes involved in IAA and GA synthesis pathways. Genes involved in IAA and GA biosynthesis were collated from the literature (Labeeuw et al., 2016 and Salazar-Cerezo et al., 2018 ; Supplementary Table S2.2) and downloaded from NCBI. All sequences for the identified IAA and GA synthesis genes were compared against raw reads from the *Tara Oceans* Bacterial and Archaeal Genomes (BAC_ARC_MAGs) within the Ocean Gene Atlas ([Ocean Gene Atlas- Interlude \(osupytheas.fr\)](#)), using a threshold e-values $\leq 1 \times 10^{-10}$ determined in Labeeuw et al., 2016. For each site, abundance values were normalised by dividing the number of read homologues of IAA and GA biosynthesis genes by the total number of reads in the sample (i.e., percent of total reads). The average relative abundance of genes involved in IAA and GA biosynthesis at sea surface, mixed layer, mesopelagic, and deep chlorophyll max were then extracted from the dataset and relative abundances in the size fractions $> 0.8 \mu\text{m}$, $0.22-3 \mu\text{m}$, $0.8-5 \mu\text{m}$, $5-20 \mu\text{m}$, $20-180 \mu\text{m}$, and $180-2000 \mu\text{m}$ were summed for each. Only MAGs which possessed all pathway genes for IAA and GA biosynthesis were utilised for downstream analysis.

4.2.2 Bacteria-phytoplankton network analysis:

To explore co-occurrence patterns between the presence of bacteria harbouring IAA and GA genes and the relative abundance of phytoplankton groups, the *Tara Oceans* 18S rDNA eukaryotic ASV data (DADA2) was obtained from the Ocean Gene Atlas ([Ocean Gene Atlas- Interlude \(osupytheas.fr\)](#)) and filtered to contain only the ASVs from the phytoplankton groups “Dinoflagellata”, “Chlorophyta”, “Cryptophyta”, “Haptophyta”, and “Ochrophyta”. The abundance matrix was downloaded and used for network analysis using the Mictools package on Python (version 3.13.Orc2). Bacterial MAGs which harboured IAA and GA gene homologues obtained previously were correlated against the phytoplankton taxa (from the filtered ASVs) present in *Tara Oceans* samples and co-occurrence networks were constructed based on Spearman’s correlations (Spearman’s Rho > 0). Networks were visualised using igraph and ggraph on R.

4.2.3 Statistical analysis:

All statistical analysis were performed using R (version 4.2.1) and Python (version 3.13.Orc2). To identify the differences in the composition of bacterial communities that possess IAA biosynthesis genes between the five different IAA pathways, we performed a permutational multivariate analysis of variance (PERMANOVA; $p<0.05$). To determine the differences in IAA and GA gene relative abundances between different oceanographic regions (Mediterranean Sea, Red Sea, Indian Ocean, South Atlantic Ocean, Southern Ocean, South Pacific Ocean, North Pacific Ocean, North Atlantic Ocean and Arctic Ocean) Kruskal-Wallis and Pairwise Wilcoxon tests ($p<0.05$) were conducted. To investigate the statistical relationships between PGPH gene relative abundance and the measured environmental factors at each site, Spearman's correlation was conducted. The gene relative abundance matrixes were correlated against all environmental parameters measured in the *Tara* Oceans expedition. This analysis used the *spearmanr* function from the *scipy.stats* library in Python, allowing for the identification of potential associations between relative abundance of genes potentially involved in IAA and GA biosynthesis and the various environmental variables.

4.3 Results:

4.3.1 Taxonomy and relative abundance of bacteria harbouring IAA biosynthesis gene homologues in the ocean:

We identified gene homologues to four out of five IAA biosynthesis pathways in the global ocean, as no hits were recorded for the Tryptophan side chain oxidase pathway (Supplementary Figure S4.1). A total of 1060 unique bacterial MAGs from 103 orders possessed homologues of genes IAA biosynthesis genes (Figure 4.1; Supplementary Table S4.5). The taxonomic composition of the bacteria harbouring these genes was significantly different between the four IAA pathways (pairwise PERMANOVA, $p < 0.05$, Supplementary Table S4.3; Figure 4.4).

The Pseudomonadales order contributed 54% and 38% of the overall bacterial diversity harbouring Indole-3 acetonitrile and Indole-3-acetamide pathway genes, respectively (Figure 4.1), followed by the Enterobacterales order (15% and 11 % respectively), mostly including members of the Alteromonadaceae family (13% and 11 % respectively). Bacteria within the Flavobacteriales order harboured the most genes from the Indole-3-pyruvate and Tryptamine pathways, accounting for 42% and 33% of the total bacterial diversity.

Importantly, 19 MAGs out of 1060 (i.e., 1.7%) possessed homologues of all genes required to synthesise all four IAA pathways (Indole-3 acetonitrile, Indole-3-acetamide, Indole-3-pyruvate, and Tryptamine). The majority of these MAGs belonged to the Proteobacteria phylum (28%) including the bacteria *Thioclava* sp. (4%), *Thalassobius* sp. (7%), *Silicibacter* (1%) and *Leucothrix* (2%), followed by Eremiobacteria (17%) and Microtrichales (13%) including the bacteria Ilumatobacteracea (13%).

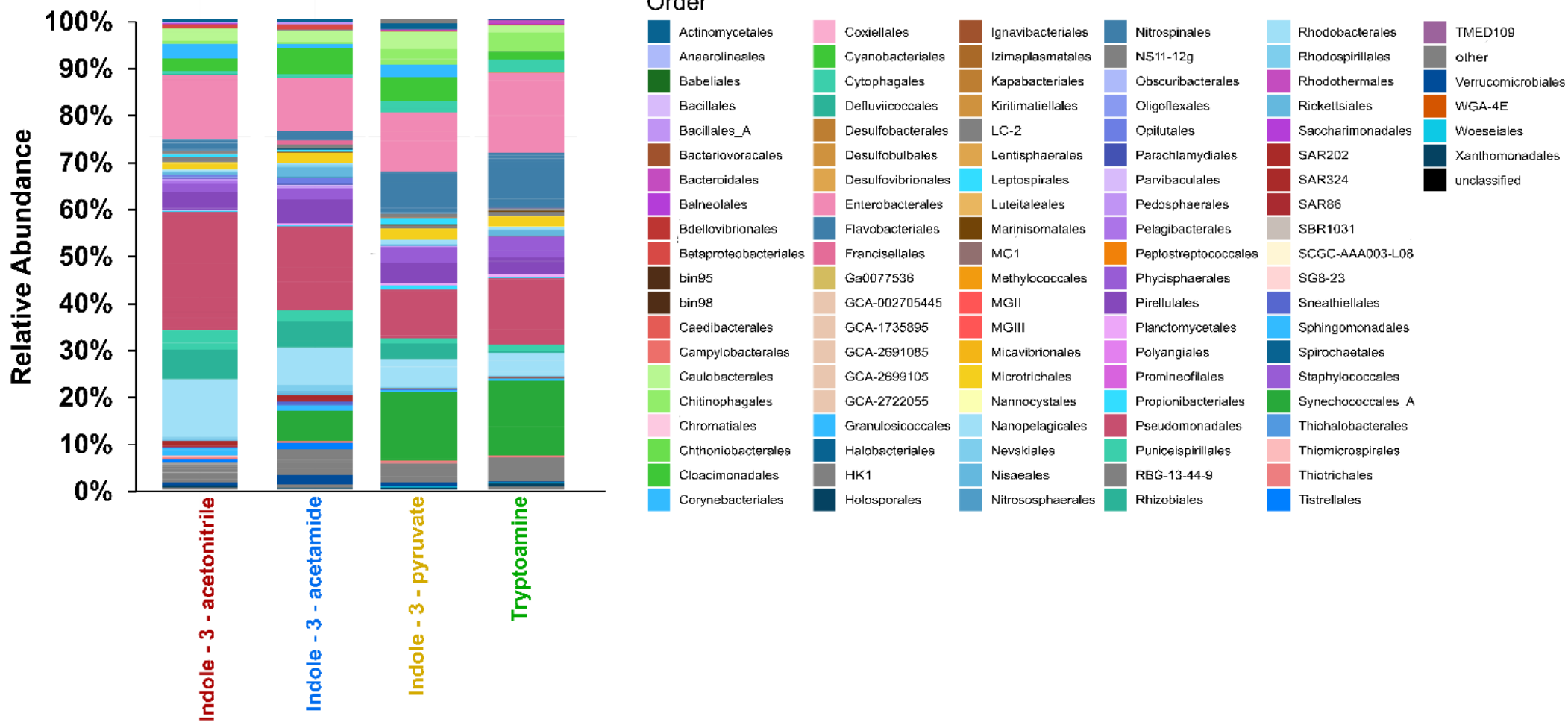


Figure 4.1: Relative abundance (%) of bacteria that harboured IAA biosynthesis gene homologues. Bacteria are coloured based on taxonomy (order), with similar colours associated to closely related bacteria.

4.3.2 Geographical abundance of bacterial-IAA genes:

4.3.2.1 Presence IAA genes in sea surface samples:

In sea surface samples, the presence of IAA biosynthesis genes within bacteria was found in 67% of all *Tara Oceans* sites tested. However, relative abundance levels differed greatly between regions (Kruskal-Wallis test; $p<0.05$; Supplementary table S4.1) (Figure 4.2A). Indeed, hotspots in the relative abundance of IAA synthesis genes occurred in the western Indian Ocean ($0.2\% \pm 0.03$), Red Sea ($0.16\% \pm 0.06$), and Mediterranean Sea ($0.08\% \pm 0.03$), where relative abundance levels were nearly twice as high as the global average. On average the relative abundance of IAA biosynthesis genes was significantly higher in the Indian Ocean compared to the South Pacific Ocean, and Arctic Ocean (Wilcoxon pairwise test; $p=0.0014$ and $p=0.0419$ respectively; Supplementary table S4.1), with the lowest relative abundance occurring in sites within the Arctic Ocean ($0.01\% \pm 0.0028$). Out of all the sites investigated, relative abundances of IAA biosynthesis genes recorded along the western coast of Madagascar were notably high at sites 58 (0.66%), 51 (0.64%) and, 53 (0.64%), all of which are within 200 km of each other. While the lowest relative abundances of bacterial-IAA biosynthesis genes were located in the South Pacific Ocean at site 125 ($6.8 \times 10^{-6}\%$), and North Pacific Ocean at site 133 ($8.5 \times 10^{-6}\%$) almost 100,000 times lower than the highest gene relative abundances noted at site 58.

4.3.2.2 Presence of IAA genes in deep chlorophyll maximum samples:

Bacteria samples at deep chlorophyll maximum followed a similar trend to those seen in surface samples, however, fewer sites (27%) contained genes for IAA biosynthesis (Kruskal-Wallis test; $p<0.05$) (figure 4.1B). The presence of IAA biosynthesis genes was again characterised by clear hotspots scattered throughout the world oceans, specifically within the Indian Ocean ($0.14\% \pm 0.049$), North Pacific Ocean ($0.13\% \pm 0.052$), and Mediterranean Sea ($0.12\% \pm 0.068$). Significantly higher relative abundances of IAA biosynthesis genes were observed in North Atlantic Ocean and South Pacific Ocean compared to the Arctic Ocean (Wilcoxon pairwise test; $p=0.0041$ and $p=0.0007$ respectively; Supplementary table S4.1), whereby the relative abundance of IAA biosynthesis genes in Arctic Ocean samples ($0.002\% \pm 0.00096$) were 35 times lower than the global average. Interestingly, both the highest and lowest relative abundance of bacterial-IAA biosynthesis genes were located within the Mediterranean Sea, with the highest relative abundance of IAA biosynthesis genes detected at

site 25 (0.89%) along the coast of Italy, which was over 4,000 times higher than the lowest relative abundance of IAA biosynthesis genes at site 9 (0.00022%). These two sites were only separated by 100 km.

Overall relative abundances for IAA biosynthesis genes decreased with depth, whereby their relative abundances were almost two times greater in surface samples than in the deep chlorophyll max (Supplementary Figure S4.3). Importantly, IAA genes were not detected in mixed layer and mesopelagic samples.

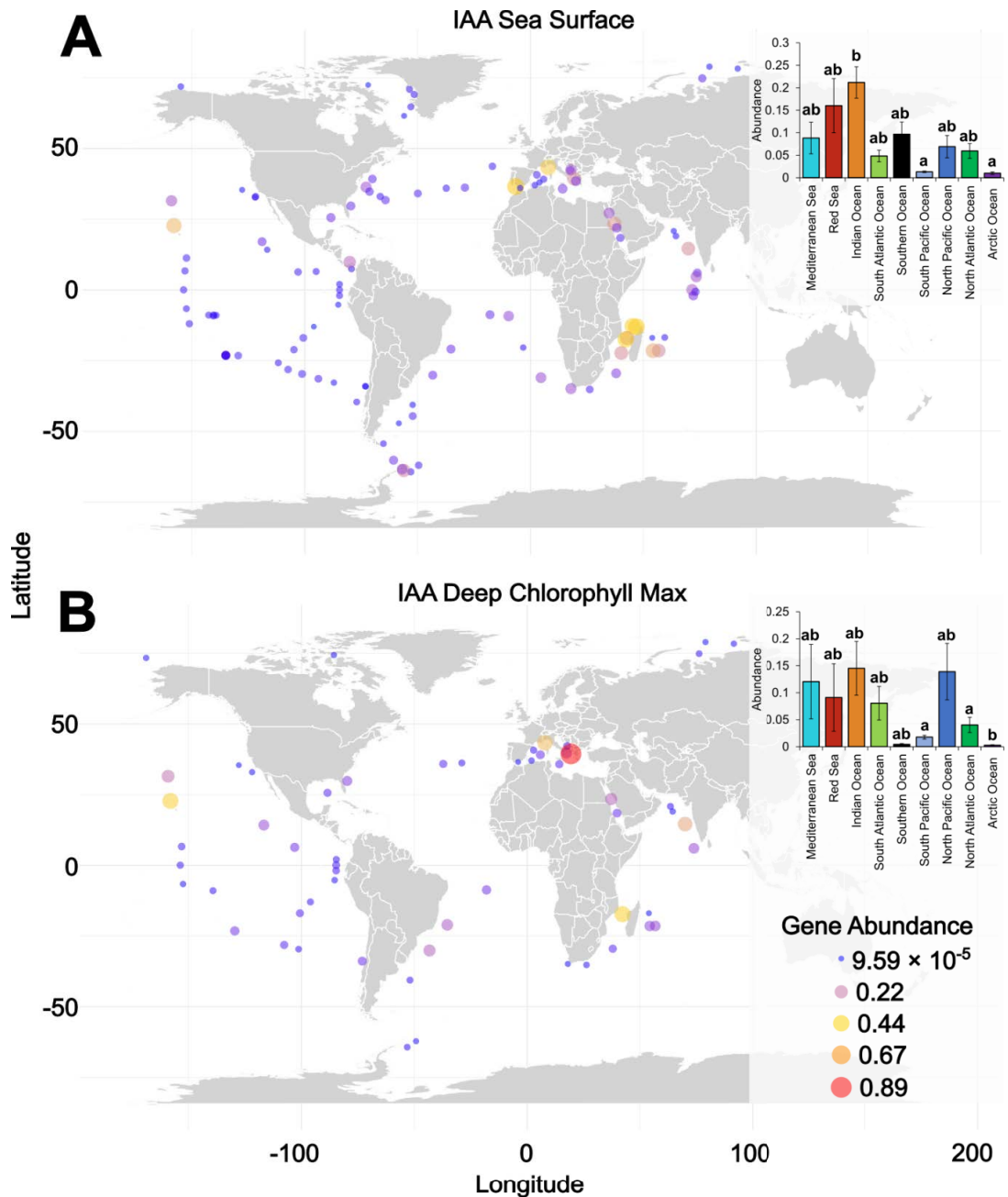


Figure 4.2: Distribution of indole-3-acetic acid (IAA) gene relative abundances across the Tara Oceans sites. A) IAA gene relative abundance at sea surface. B) IAA gene relative abundance at deep chlorophyll max. Colour-coded circles are representative of the varying abundance proportion of genes at each site. The bar chart on the left of the map illustrates the average abundance of IAA genes within nine different ocean regions (as defined in IHO General Sea Areas 1953), error bars are standard error of the mean (SEM) and significant differences are marked with letters (Wilcoxon pairwise test, $p < 0.05$, Supplementary Table S4.1).

4.3.3 Taxonomy and relative abundance of bacteria harbouring GA biosynthesis gene homologues in the ocean:

A total of 9 unique MAGs from 4 phyla possessed homologues required for GA biosynthesis (Figure 4.3; Supplementary Table S4.6). The majority of these MAGs (39%) belonged to the phylum Myxococcota, specifically to the UBA1671 order, represented by a single MAG (GCA_002453135.1). This was closely followed by the Bacteroidota phylum (38%), where four MAGs primarily from the Saprospiraceae (accounting for 97% of Bacteroidota MAGs) and Crocinitomicaceae (15%) families harboured GA biosynthesis gene homologues. Within the Proteobacteria (18%), one MAG was identified from the Rhodobacteraceae clade. Chloroflexota accounted for 6% of the GA-encoding MAGs, represented by two genomes (GCA_002699585.1 and GCA_002702065.1). Additionally, one MAG (5%) from the unclassified order SBR1031 also possessed GA biosynthesis gene homologues.

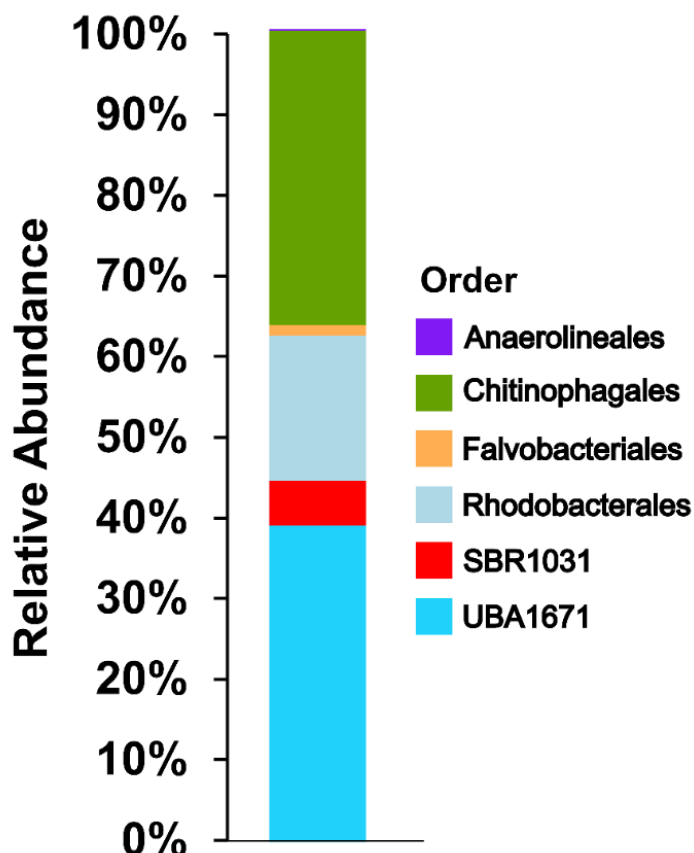


Figure 4.3: Relative abundance (%) of bacteria that harboured GA biosynthesis gene homologues. Bacteria are coloured based on taxonomy (order), with similar colours associated to closely related bacteria.

4.3.4 Geographical distribution of bacterial-GA genes:

4.3.4.1 Presence of GA genes in sea surface samples:

The presence of GA biosynthesis genes in sea surface samples was found in 49% of *Tara Oceans* sites, the relative abundance of these genes differed significantly between sites (Kruskal-Wallis test; $p < 0.05$; Figure 4.4A; Supplementary table S4.2). The majority of GA biosynthesis gene homologues were found in hotspots within the Southern Ocean ($0.26\% \pm 0.11$), North Pacific Ocean ($0.15\% \pm 0.058$), and in the Arctic Ocean ($0.09\% \pm 0.025$). On average, relative abundance levels in these three regions were twice as high as the global average. Lower relative abundances of GA biosynthesis gene homologues were found in samples collected from the Red Sea and Indian Ocean where the levels were 40 times smaller than the global average (Wilcoxon pairwise test; $p = 0.005$; Supplementary table S4.2). While sites within the North Pacific Ocean had significantly higher relative abundance of GA biosynthesis genes than within the South Pacific Ocean (Wilcoxon pairwise test; $p = 0.036$). Out of all of the sites investigated, the highest relative abundance of GA biosynthesis gene homologues was found in samples collected from site 138 in the North Pacific Ocean (0.51%), 128 in the South Pacific Ocean (0.26%), and 193 in the Arctic Ocean (0.20%), each site over 1000's of kilometres apart from one another. While the lowest relative abundance of GA biosynthesis gene homologues was located within the South Pacific Ocean at sites 94 ($9.59 \times 10^{-5}\%$), where gene relative abundance was almost 100,000 times lower than the relative abundance level recorded at site 138.

4.3.4.2 Presence of GA genes in deep chlorophyll maximum samples:

The average relative abundance of GA biosynthesis genes in deep chlorophyll maximum samples was half that observed in surface samples (Supplementary Figure S4.2). However, GA biosynthesis gene homologues were still recorded in 27% of the *Tara Oceans* sites (Figure 4.4B). Out of all of the ocean regions examined, the average relative abundance of GA biosynthesis genes was highest in the Arctic Ocean ($0.12\% \pm 0.057$), North Pacific Ocean ($0.057\% \pm 0.024$) and North Atlantic Ocean ($0.055\% \pm 0.028$). In addition, the relative abundance of GA genes in the Arctic Ocean and Mediterranean Sea samples were significantly higher (96 and 15 times higher, respectively) than within samples in the Indian Ocean (Wilcoxon pairwise test; $p = 0.018$ and $p = 0.0042$, respectively; Supplementary table S4.). No GA biosynthesis genes were found in the Red Sea and Southern Ocean sites. Out of the

investigated sites, relative abundance of GA biosynthesis gene homologues found at site 194 within the Arctic Ocean (0.32%) were over 3 orders of magnitude higher than the lowest relative abundance noted at site 41 (0.00024%) in the Indian Ocean.

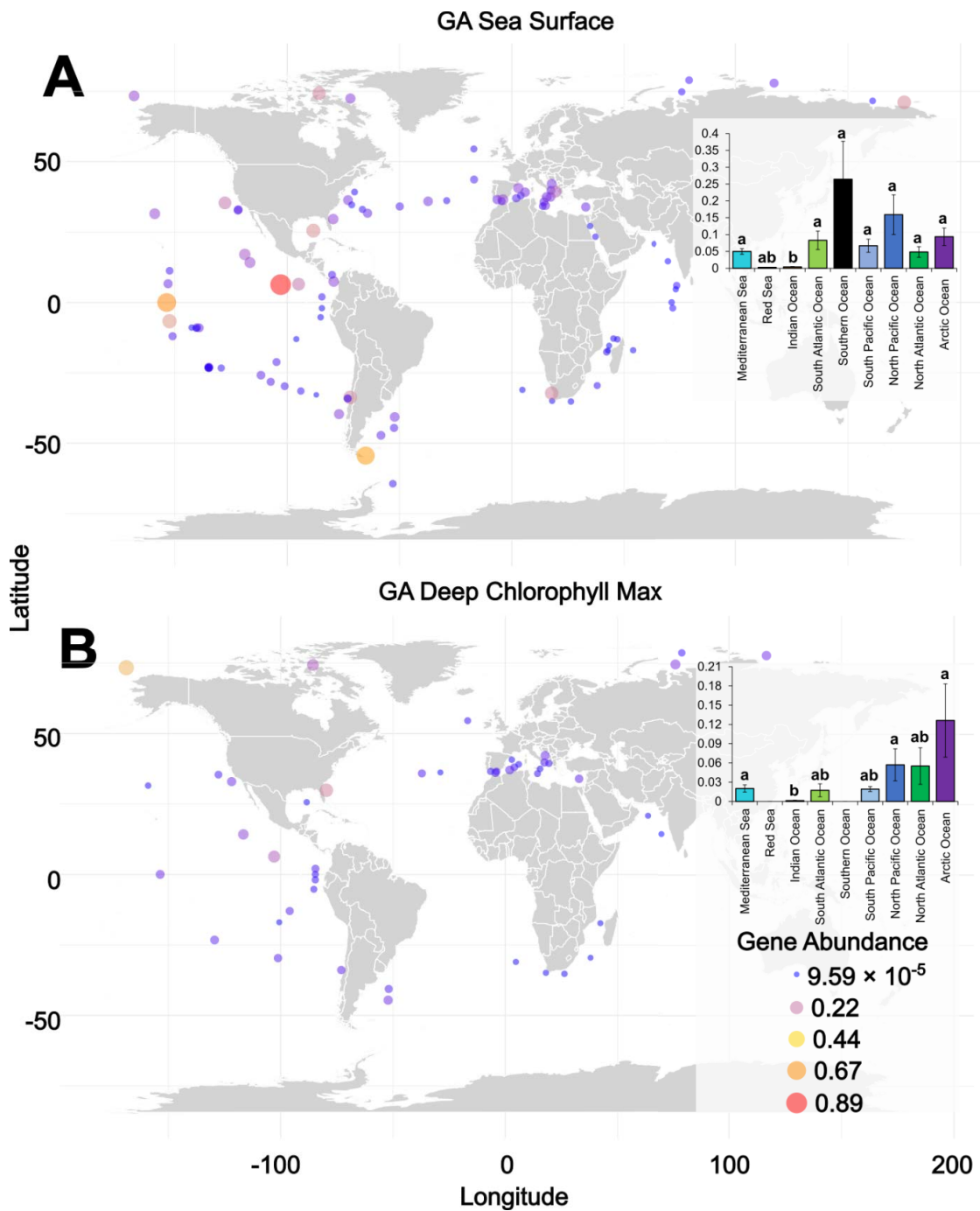


Figure 4.4: Distribution of gibberellic acid (GA) gene abundance across the *Tara Oceans* sites. A) Abundance of GA genes at sea surface. B) Abundance of GA genes at deep chlorophyll max depth. Colour-coded circles are representative of the varying abundance of genes at each site, illustrating special variability across different oceanic regions and depths. The bar chart on the left of the map illustrates the average abundance of GA genes within each ocean region, error bars are standard error of the mean (SEM) and significant differences are marked with letters (Wilcoxon pairwise test, $p < 0.05$, Supplementary Table S4.1).

4.3.5 Correlations between environmental variables and abundance of IAA and GA genes:

A total of 35 statistically supported correlations were identified between environmental variables and the relative abundance of IAA or GA biosynthesis gene homologues (Spearman's correlation; Supplementary Table S4.3, S4.7, S4.8). To limit the likelihood of false positives, we only focused on correlations that were consistent across depths. The abundance of IAA genes was negatively correlated to phosphate (PO_4 ; Spearman's correlation, $R = -0.1786757$ and -0.21386996) and bicarbonate (HCO_3 ; $R = -0.21114387$ and -0.114307694). The abundance of GA genes was positively correlated with chlorophyll a ($R = 0.32217252$ and 0.2684485) and nitrate ($R = 0.3496572$ and 0.26740423); and negatively correlated with temperature ($R = -0.29966834$ and -0.1781062) and salinity ($R = -0.5007697$ and -0.25022817).

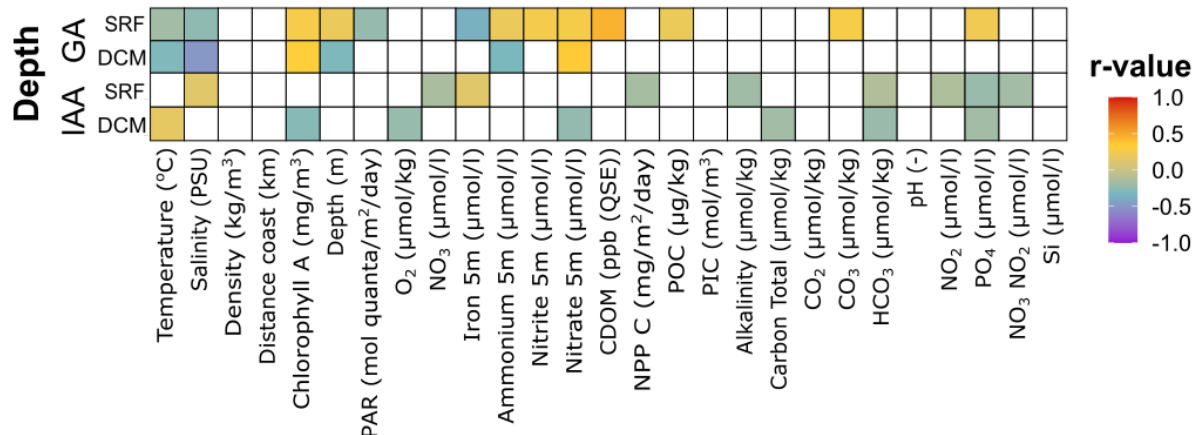


Figure 4.5: Correlations between environmental factors and abundance of IAA and GA gene homologues. Heatmap illustrating the correlation between the abundance of IAA (bottom) and GA (top) gene homologues and environmental variables. Statistically significant correlations are highlighted in colours (Spearman's correlation).

4.3.6 Bacteria-phytoplankton network analysis:

Six bacterial MAGs that possess homologues of IAA biosynthesis genes displayed strong positive correlations to 15 unique phytoplankton ASVs (Figure 4.6; Supplementary table S4.9). Specifically, a MAG belonging to the Planctomycetaceae was significantly and positively correlated with five different phytoplankton ASVs within the Ochrophyta, including *Chaetoceros elegans*, *Dictyocha* sp. and *Thalassiosira oceanica* (Spearman's Rho = 0.28). Other MAGs containing IAA biosynthesis gene homologues that were significantly correlated

to multiple phytoplankton ASVs included a member of the Microtrichales (four positive correlations with the diatoms *Thalassiosira* and *Chaetoceros*), a member of the Eremiobacterota (three positive correlations with diatoms, including *Thalassiosira oceanica* and *Pseudo-nitzschia*; Spearman's Rho = 0.47), a Rhodobacteraceae (positive correlation, including GCA-2732825-7), and a Cyanobacterium from the genus *Trichodesmium* (two positive correlations with diatoms belonging to *Chaetoceros* and *Minidiscus* genera). Notably, no positive correlations were detected between MAGs that possess GA biosynthesis gene homologues and any phytoplankton ASV within our analysis.

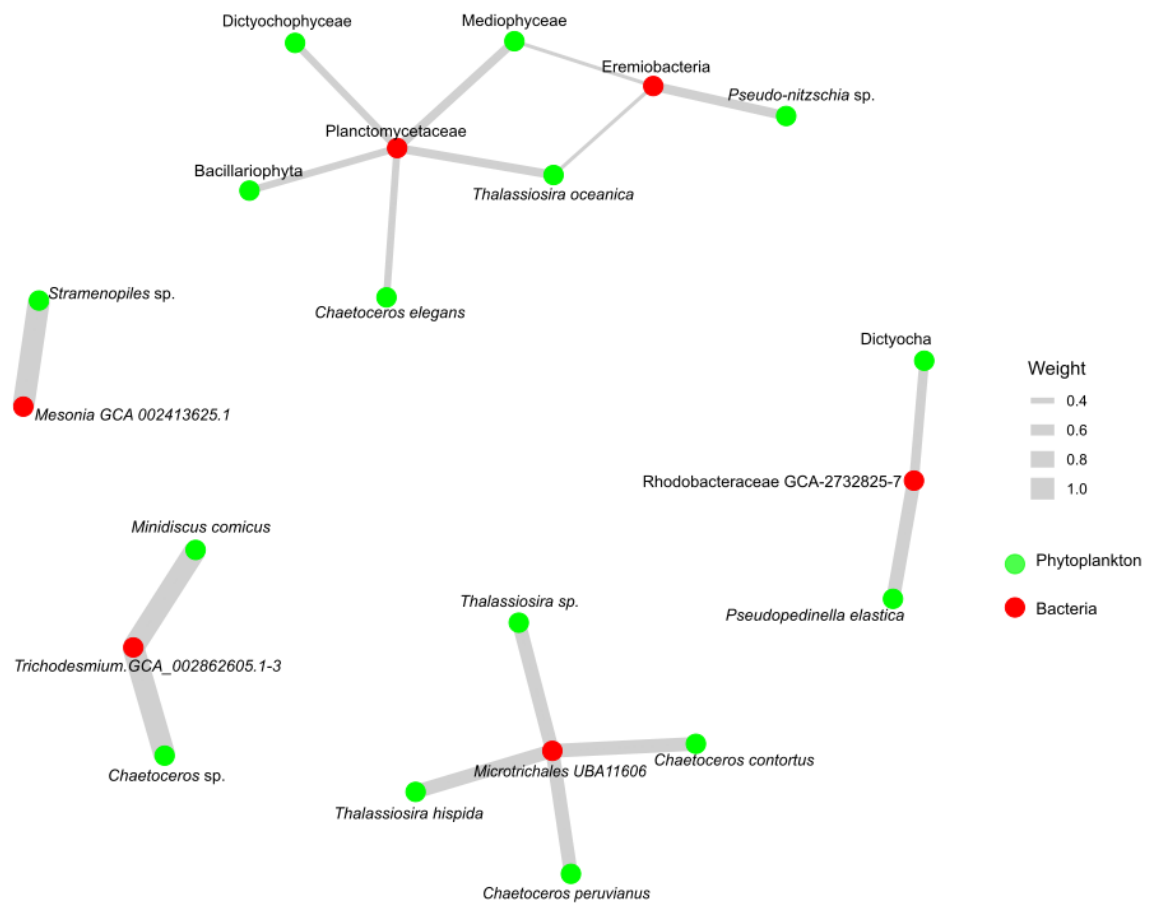


Figure 4.6: Correlative network of phytoplankton ASVs and bacterial MAGs that harbour IAA biosynthesis genes. All correlations are positive, nodes are edge weighted based on strength of Spearman's Rho, the stronger the correlation the thicker the line.

4.4 Discussion:

Interactions between phytoplankton and bacteria are integral to the functioning of marine ecosystems, particularly in relation to nutrient cycling and primary production (Azam & Malfatti, 2007; Buchan et al., 2014). There is emerging evidence that PGPHs such as IAA and GA may be key chemical currencies regulating these important interactions (Amin et al., 2015; G. Dao et al., 2020; Matthews et al., 2023.; Segev et al., 2016). Here we used the *Tara Oceans* metagenomic dataset to : i) characterise the taxonomy of prokaryotes harbouring homologues of genes involved IAA and GA biosynthesis, ii) identify where these genes are found in the global ocean, iii) determine which biotic and abiotic variables are correlated with these genes in ocean ecosystems and iv) link the abundance of specific MAGs that possess IAA and GA genes to phytoplankton species. By mining the *Tara Oceans* data, we determined that a wide array of bacteria harbour homologues of genes involved in the biosynthesis of IAA and GA, and these homologues were found throughout the global ocean. However, the abundance of these bacteria differed greatly between sites. We identified environmental variables, such as chlorophyll a and nitrate, that were positively correlated with the abundance of these genes, as well as specific positive correlations with a range of phytoplankton, suggesting IAA-synthesising bacteria may form tight associations with specific phytoplankton in the ocean.

4.4.1 Bacterial groups that possess IAA and GA biosynthesis genes:

We identified homologues of IAA biosynthesis genes in 1060 different bacterial MAGs belonging to 103 orders. This result greatly expands the taxonomic range of bacteria that have the genomic potential to produce this molecule. Indeed, prior to this analysis, the Indole-3-acetamide pathway genes had mostly been reported in Alphaproteobacteria (Rhizobiales; including *Agrobacterium tumefaciens*, *Rhizobium* and *Bradyrhizobium*) and Gammaproteobacteria (including *Pseudomonas syringae* and *Pantoea agglomerans*) (Foo et al., 2019; Glickmann et al., 2007; Sekine et al., 1989; Theunis et al., 2007). In comparison, our results reveal that homologues of these genes are also found in 58 other bacterial classes. Similarly, the Indole-3-pyruvate pathway had been previously described in Alphaproteobacteria (including *Bradyrhizobium* and *Azospirillum*, *Rhizobium*) and Gammaproteobacteria (including Enterobacterales) (Brandl & Lindow, 1996; Costacurta et al., 1994; Koga et al., 1991; Patten & Glick, 2002). Our results identified homologues of this pathway in 56 other bacterial classes. The Tryptamine pathway has been identified in *Bacillus cereus* (Perley & Stowe, 1966), 41 more classes were identified in our results and, Indole-3-

acetonitrile pathway genes are present in *Alcaligenes faecalis* and *Rhizobium* spp. (Kobayashi et al., 1995), our results indicate 58 more classes possess Indole-3-acetonitrile biosynthesis genes. Overall, over 47 different classes and 153 families of bacteria possess IAA biosynthesis genes in the *Tara Oceans* metagenomic dataset, suggesting that IAA producers may be much more diverse and widespread across the global ocean than previously thought.

Additionally, the capacity of bacteria to produce GA also surpasses what was observed in previous literature. Here, we identify bacteria that possess GA biosynthesis genes are found within the 6 unique class including Betaproteobacteria, Thermodesulfobacteria, Chitinophagia, Flavobacteria, Bacteroidia and Alphaproteobacteria. Previous studies have highlighted GA can be synthesised by Alpha (Khalil et al., 2024) and Gammaproteobacteria (G. Dao et al., 2020; Khalil et al., 2024). Overall our findings identify new bacteria class that have the capacity to produce GA adding to the previous repertoire of PGPH producing bacteria.

4.4.2 Widespread presence of IAA and GA genes in the global ocean:

The presence of IAA genes was widespread across all nine oceanographic regions. However, sites throughout the Indian Ocean, Red Sea, and Mediterranean Sea displayed distinct hotspots where significantly higher abundances of IAA biosynthesis genes were observed than all other sites. Interestingly, high abundances of IAA biosynthesis genes within the Indian Ocean, close to the coast of India and near to Madagascar correspond with high productivity regions.

Indeed, the productivity of the coastal regions south of Madagascar is significantly enhanced by coastal upwelling, which contributes greatly to biological productivity in this area. These coastal upwellings increase nutrient availability by bringing nutrient-rich waters from the deep ocean, promoting phytoplankton growth. This not only benefits phytoplankton but also supports the heterotrophic bacteria that thrive in these nutrient-rich environments (Lutjeharms & Machu, 2000; Ramanantsoa et al., 2018). Additionally, regular phytoplankton blooms occur on the west coast of India following the onset of the monsoon season (Sreekumaran Nair et al., 1992). Increased biogeochemical activities, such as carbon, nitrogen, and sulfur cycling, have also been observed along the Agulhas Current, where many of the high-abundance sites are located, leading to increased microbial and phytoplankton activity (Olson & Evans, 1986; Phoma et al., 2018). This may indicate that the presence of IAA-synthesizing bacteria is more abundant in areas of high productivity and phytoplankton bloom formations.

A stark contrast was apparent between the global distribution of bacterial IAA and GA biosynthesis gene homologues. Hotspots of GA biosynthesis gene homologues were mostly located within the Southern Ocean, North Pacific Ocean, and Arctic Ocean, with high abundances near the polar regions. This distribution does not overlap with the hotspots recorded for IAA gene homologues, suggesting a strong spatial partitioning in the bacterial potential to produce these two important PGPHs. Additionally, the abundance of GA gene homologues strongly and positively correlated with chlorophyll a and nitrate, suggesting that bacteria with the genomic potential to produce GA co-occur with phytoplankton and thrive in high nutrient environments.

4.4.3 Associations between phytoplankton and PGPH-synthesising bacteria:

The IAA biosynthesis pathways were identified in many bacteria that are known to have beneficial associations with phytoplankton. Generally, all four IAA pathway genes were found within various species of Pseudomonadales, Alteromonadales, Flavobacteriales, and Cyanobacteriales orders. For example, members of the Pseudomonadales were identified in previous research as among the most abundant microbes during phytoplankton blooms and possess receptors required for vitamin B₁₂ production (Isaac et al., 2021). Meanwhile, bacteria within the Alteromonadales, have previously shown associations with diatoms (such as *Actinocyclus* sp. and *Thalassiosira pseudonana*) (Le Reun et al., 2023; Khalil et. al. 2024), Cyanobacteria (*Prochlorococcus*) (Hennon et al., 2018), and green algae (*Dunaliella* sp.) (Le Chevanton et al., 2016), and have been identified as key producers of vitamins B₁ and B₁₂ (Joglar et al., 2021), which are required for phytoplankton growth.

Additionally, the specific bacteria *Thalassobius*, and *Ruegeria* identified here also possessed IAA biosynthesis genes and are also known for the beneficial associations they form with phytoplankton. *Thalassobius* isolates enhanced the growth of to the diatom *Actinocyclus* (Le Reun et al., 2023), while *Roseobacters* form association with numerous phytoplankton species including *Pfiesteria piscicida*, *Emiliania huxleyi* and *Rhodomonas* (Geng & Belas, 2010). Observed associations between *Ruegeria* and diatoms have shown *Ruegeria* possess genes to utilise phytoplankton produced compounds including dimethylsulphoniopropionate (DMSP) and glycine betaine (Moran et al., 2004).

Correlative network analysis identified potential associations between bacteria that harbour IAA biosynthesis gene homologues and specific phytoplankton species. Half of the interactions

identified involved diatoms belonging to the *Thalassiosira* and *Chaetoceros* genera. Previous research has highlighted that *Thalassiosira* species benefit from IAA-synthesising bacteria within the Flavobacteriales and Rhodobacteraceae (Tran et al., 2023), bacteria have shown to enhance the growth and nutrient acquisition of *Chaetoceros* by assimilating carbon and nitrogen from the diatom's exudates (Nelson et al., 1995; Stenow et al., 2023) and finally, *Pseudo-nitzschia*, which was strongly correlated with an Eremiobacteria in the ocean, is also known to benefit from IAA-producing *Sulfitobacter* sp. under laboratory conditions (Amin et al., 2015). These results suggest that bacteria that possess homologues of IAA biosynthesis genes have the capability to form beneficial associations with phytoplankton in the ocean. Conversely, GA genes were predominantly found within the family Saprospiraceae, which includes species that have previously been identified during *Gymnodinium* and diatom blooms (Shao et al., 2020). However, our analysis revealed no associations between bacteria with the potential to synthesise GA and specific phytoplankton species.

4.5 Conclusion:

Here, we demonstrate the bacteria harbouring the genomic potential to synthesise PGPHs that have previously been shown to enhance the growth of phytoplankton are widely distributed across the global ocean. This study has significantly advanced our understanding of the taxonomy, abundance and distribution of bacteria with the genomic potential to synthesise two important PGPHs, IAA and GA across the global ocean. Our analysis vastly expands the taxonomic range of bacteria that may produce IAA and GA, to incorporate 47 and 6 new bacterial classes, respectively. In addition, IAA and GA gene homologues were present across almost all *Tara* Oceans sites, but gene abundances differ greatly between oceanographic regions. Bacteria that harboured genes for IAA synthesis were largely restricted to sunlit regions of the water column and were correlated with specific phytoplankton, including *Thalassiosira oceanica* and *Chaetoceros*. These results reveal the wide geographical distribution of IAA genes and identify some strong correlation between bacterial producers and phytoplankton species *in situ* for the first time. This suggests that the capacity of PGPH-synthesising bacteria to enhance phytoplankton growth via hormone production may be very widespread across the ocean, and therefore play a significant role in shaping marine ecosystem dynamics.

Chapter 5: General Discussion

The research presented in my thesis delivers fundamental new knowledge on the chemical ecology involved in phytoplankton-bacteria interactions by yielding a deeper understanding of the role of PGPHs within these interactions. Cumulatively, my PhD research has answered crucial questions by defining: (i) the identity of PGPHs produced by phytoplankton-associated bacteria; (ii) the diversity of bacteria that produce PGPHs; (iii) the role of PGPHs in phytoplankton growth promotion, and iv) the distribution of bacteria harbouring the genomic potential to synthesise key PGPHs in the global ocean. To address these questions, my research has spanned across scales from the intimate inter-cellular metabolite interactions occurring at the microscale to the global ocean scale. In this final chapter, I will synthesise the results presented in my thesis (**Chapters 2 to 4**), highlight the broader implications of my research, and how it contributes to our current and future understanding of marine microbial interactions (Figure 5.1).

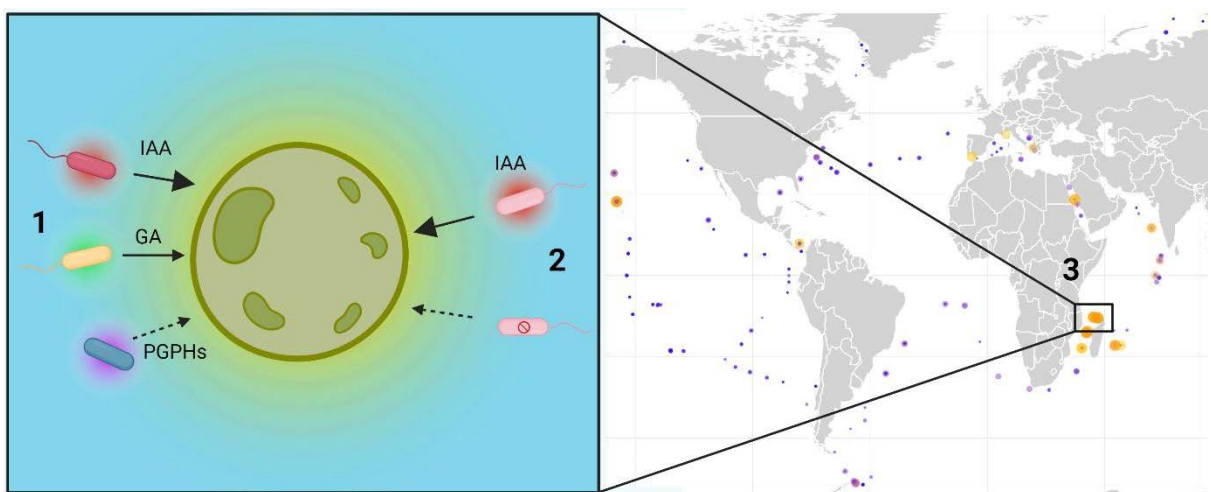


Figure 5.1: Schematic summary of the contributions of my research, spanning the microscale to global ocean scale. **1)** Interactions between *Actinocyclus* sp. (green diatom) and heterotrophic bacteria (red, blue, yellow cells) producing IAA (red halo), GA (green halo), and other PGPHs (purple halo) were examined, revealing that IAA had the largest effect on *Actinocyclus* growth (large arrow), followed by GA (smaller arrow), while other PGPHs had no measurable effects (dashed arrow). **2)** A bacterial mutant unable to synthesize IAA (pink bacteria with a cross) had no effects on *Actinocyclus* growth, indicating that bacterial-synthesized IAA was responsible for nearly all the growth enhancement measured. **3)** Global distributions of bacterial IAA and GA biosynthesis gene homologues demonstrating that PGPH-synthesizing bacteria are ubiquitous across the global ocean.

5.1 Phytoplankton-associated bacteria produce many PGPHs:

Prior to my PhD research, the only PGPHs reported to be produced by phytoplankton-associated bacteria were IAA and GA (Amin et al., 2015; G. Dao et al., 2020; G. H. Dao et al., 2018; Labeeuw et al., 2016; Matthews et al., 2023.; Salazar-Cerezo et al., 2018). The results presented in **Chapter 2** highlight the remarkable diversity of PGPHs produced by phytoplankton-associated bacteria, far surpassing what was previously known in planktonic systems. Fourteen strains of heterotrophic bacteria, which enhance the growth of the marine diatom *Actinocyclus* (Le Reun et al., 2023), harboured homologues of genes involved in the biosynthesis of multiple PGPHs, and produced seven unique PGPHs, including indole-3 acetic acid, indole-3 butyric acid, abscisic acid, gibberellic acid, jasmonic acid, trans-zeatin and brassinolide. Several of these PGPHs had never been reported in marine bacteria. While previous studies on plant systems have explored the capacity of rhizosphere bacteria to produce many PGPHs (Costacurta et al., 1994; Desai, 2017; Hakim et al., 2021; Maheshwari et al., 2015), this is the first study to highlight the presence of such a large variety of PGPHs in marine bacteria. By revealing the capacity of phytoplankton-associated bacteria to produce seven unique PGPHs, the findings of **Chapter 2** extend the diversity of growth-affecting molecules shared by marine bacteria and the potential ecological importance of PGPHs in phytoplankton-bacteria interactions.

5.2 PGPH-producing bacteria are taxonomically divers:

Before my PhD research, only six different bacterial genera were known to produce IAA and GA in association with phytoplankton (G. Dao et al., 2020; G. H. Dao et al., 2018). My PhD research has significantly expanded upon this diversity by showing that a large diversity of bacteria can synthesise PGPHs. **Chapter 2** highlights that the production of PGPHs was ubiquitous across all 14 bacteria strains tested, which included bacteria spanning 8 genera from both the Alpha and Gammaproteobacteria classes, a level of diversity that has only been rivalled in terrestrial plant-bacteria studies (Costacurta et al., 1994; Desai, 2017). In addition, **Chapter 4** highlighted the genomic potential of bacteria within the *Tara Oceans* dataset to produce IAA and GA, revealing that over 1,000 bacterial MAGs, spanning 45 additional classes, possessed homologues of IAA biosynthesis genes (Foo et al., 2019; Glickmann et al., 2007; Sekine et al., 1989; Theunis et al., 2007). Similarly, previous research identified 6 bacterial genera all within the Gammaproteobacteria class were able to synthesise GA in marine environments (G. Dao et al., 2020). I further identified 8 genera able to synthesise this compound (**Chapter 2**), and bacteria that harboured homologues of GA biosynthesis genes

were identified in 9 more belonging to 6 bacterial classes in the global ocean (**Chapter 4**). By emphasising the extensive diversity of marine bacteria that harbour PGPH biosynthesis genes, and further confirming their production in 14 different strains, these findings reveal the capacity of bacteria to produce PGPHs is far larger than previously believed.

5.3 PGPHs have an impact on phytoplankton growth:

Recent research has begun to demonstrate that IAA and GA produced by marine bacteria positively influence the growth of specific phytoplankton (Amin et al., 2015; Labeeuw et al., 2016; Salazar-Cerezo et al., 2018), but our understanding of the effect of a broader range of PGPHs on phytoplankton growth remains limited. In **Chapter 2**, I added each of the 7 hormones produced by members of the *Actinocyclus* microbiome to axenic *Actinocyclus* sp. cells. This experiment revealed that even though multiple members of the *Actinocyclus* microbiome produced several other PGPHs, only IAA and GA enhanced growth of the diatom. This enhancement of *Actinocyclus* sp. growth after IAA provision, provides clear support to previous observations (Amin et al., 2015, Elakbawy et al., 2022; Fierli et al., 2022; Nikolayevich et al., 2023; Peng et al., 2020; Piotrowska-Niczyporuk & Bajguz, 2014) of its key role as a chemical currency in phytoplankton-bacteria interactions. **Chapter 2** indicated that IAA and GA are the only PGPHs that had an effect of *Actinocyclus* growth, therefore I delved deeper into bacterial-synthesised IAA and confirmed its importance in **Chapter 3**.

Bacteria engaged in reciprocal chemical exchanges often produce a wide variety of metabolites that can potentially enhance the growth of their phytoplankton partner (Amin et al., 2012; Durham et al., 2022; Grossart, 1999; Seymour et al., 2017) which makes it challenging to decipher the relative importance of specific metabolites. In **Chapter 3**, I developed a novel approach to determine the relative importance of IAA in enhancing phytoplankton growth. Using CRISPR-Cas9 gene knockout approaches, I eliminated the production of IAA in the marine bacterium *A. mediterranea*, which had previously been isolated from the *Actinocyclus* microbiome and was shown to significantly enhance the growth of this diatom. The IAA-deficient mutant was then inoculated into cultures of *Actinocyclus*. By comparing the growth of wild-type *A. mediterranea* with an IAA-deficient mutant, I found that IAA synthesized by *A. mediterranea* accounted for over 98% of the observed growth enhancement. Conversely, the growth of *P. tricornutum* and *N. oceanica* was minimally affected by both wild-type and mutant *A. mediterranea*, indicating that the growth promoting effects of bacteria are not universal across all phytoplankton species. Within the framework of phytoplankton-bacteria

interactions this is the first study to use novel gene editing tools to explore the role of specific metabolite production by bacteria. Collectively, **Chapters 2** and **3** confirm the growth-enhancing effects of bacterial-derived IAA for some phytoplankton.

5.4 Genomic potential for PGPHs production is widespread in the ocean:

Many previous studies have explored the genomic potential of specific phytoplankton and bacteria species to produce particular metabolites, their distribution across oceanic regions, and the influence of biotic and abiotic factors on their community dynamics (Kisand & Nõges, 2004; O'Brien et al., 2022; Reun et al., 2022; Rooney-Varga et al., 2005; Sadeghi et al., 2021; Yeh & Fuhrman, 2022). However, the potential for marine bacteria to produce PGPHs at larger scales remain unknown. Therefore, after elucidating the importance of bacterial-derived IAA and GA for phytoplankton in **Chapters 2** and **3**, I examined the natural occurrence of the bacteria capable of producing these hormones across the global ocean. By exploring global patterns of IAA and GA gene abundances in the *Tara Oceans* metagenomic dataset (**Chapter 4**), I identified that bacteria harbouring homologues of genes required for both IAA and GA biosynthesis were present across most *Tara Oceans* sites. However, the relative abundances of these genes differed greatly between oceanographic regions, and the genes were also only present in the photic zone. This analysis revealed that heterotrophic bacteria with the genomic potential to synthesise IAA and GA are common in the marine environment.

5.5 PGPH-synthesising bacteria form putative associations with phytoplankton in the marine environment:

Using a network analysis approach, I also showed that bacteria with the capacity to synthesis IAA co-occur with specific phytoplankton such as members of the genera *Thalassiosira*, *Pseudo-nitzschia*, and *Chaetoceros*. Previous examinations of phytoplankton and bacterial community dynamics in oceanographic time-series have revealed co-occurrences between diatoms and specific bacterial families (e.g., Rhodobacteraceae, Flavobacteriaceae, and Alteromonadaceae) (Le Reun et al., 2022). Further explorations of phytoplankton-bacteria interactions in laboratory settings have revealed *Thalassiosira oceanica*, *Pseudo-nitzschia*, and *Chaetoceros* benefit from associations with heterotrophic bacteria (Amin et al., 2015; Nelson et al., 1995; Stenow et al., 2023; Tran et al., 2023). The correlation identified here suggests that associations observed in laboratory settings may also occur in the natural environment.

5.6 Future directions:

Not all the PGPHs tested affected phytoplankton growth when tested individually (**Chapter 2**). Indeed, out of the seven PGPHs tested, only IAA and GA enhanced *Actinocyclus* growth. Similarly, the ability of a bacterium to produce IAA only affected the growth of the IAA-sensitive *Actinocyclus* (**Chapter 3**). These results suggest that different PGPHs may affect the growth of different phytoplankton, and the ability of individual phytoplankton associates to produce several of these molecules suggests that some of these bacteria may be generalists and associate with multiple phytoplankton species. Future work should therefore examine the sensitivity of different phytoplankton to the range of PGPHs produced by marine bacteria.

Chapter 3 used a novel gene knockout approach to examine the impact of bacterial-IAA biosynthesis on the growth of phytoplankton, and this type of approach has the potential to be extended to study the impact of other PGPHs, and even other groups of metabolites, produced by phytoplankton-associated bacteria. The interactions between phytoplankton and bacteria remain a complex web of chemical exchanges that warrant further investigation to fully understand their ecological implications and I believe that some of the approaches used in this thesis will have utility in further deciphering these interactions.

Although the *Tara Oceans* dataset utilised in **Chapter 4** provides a good overview of the plankton community in the world's oceans, many geographical areas are missing. Alongside the *Tara Oceans* expedition, many other voyages have sampled the world's oceans, which has led to a higher resolution of results. For instance, the Pacific Ocean transect, the Australian microbiome project, COPEPOD (Coastal and Oceanic Plankton Ecology Production and Observation Database), SPOTS (Synthetic Product for Ocean Time Series) and IMOS (Integrated Marine Observation System) have all contributed valuable data. Integrating all these datasets will provide us with a more robust overview of the distributions of PGPHs biosynthesis genes and may help us understand the ecological impacts of these molecules on a global scale.

Conclusion:

My PhD thesis has significantly enhanced our understanding of the role of PGPHs in phytoplankton-bacteria interactions. Cumulatively, my thesis presents the first evidence of such a large diversity of PGPHs produced by a variety of heterotrophic bacteria, from the small scale of the phycosphere to the larger context of global oceans. In addition to providing new

insights into the potential of bacteria to produce PGPHs, my thesis has also demonstrated the capacity of IAA and GA to enhance phytoplankton growth, highlighting the integral impact that bacteria-synthesized PGPHs have on phytoplankton health. By illustrating that IAA was almost entirely responsible for bacterial growth promotion observed in a diatom, this thesis also suggests that despite the complex range of molecules exuded by both phytoplankton and bacteria, phenotypic effects (such as growth promotion), may be fully ascribed to a restricted range of compounds. Using analytical chemistry, genetic engineering and phenotypic assessments, this thesis has quantified the effect of one of these key chemical currencies, IAA. Ultimately, the approaches used here have the potential to quantify the relative importance of specific molecules, not only in phytoplankton-bacteria interactions, but more broadly across other marine and terrestrial symbioses.

Appendix:

Supplementary figures:

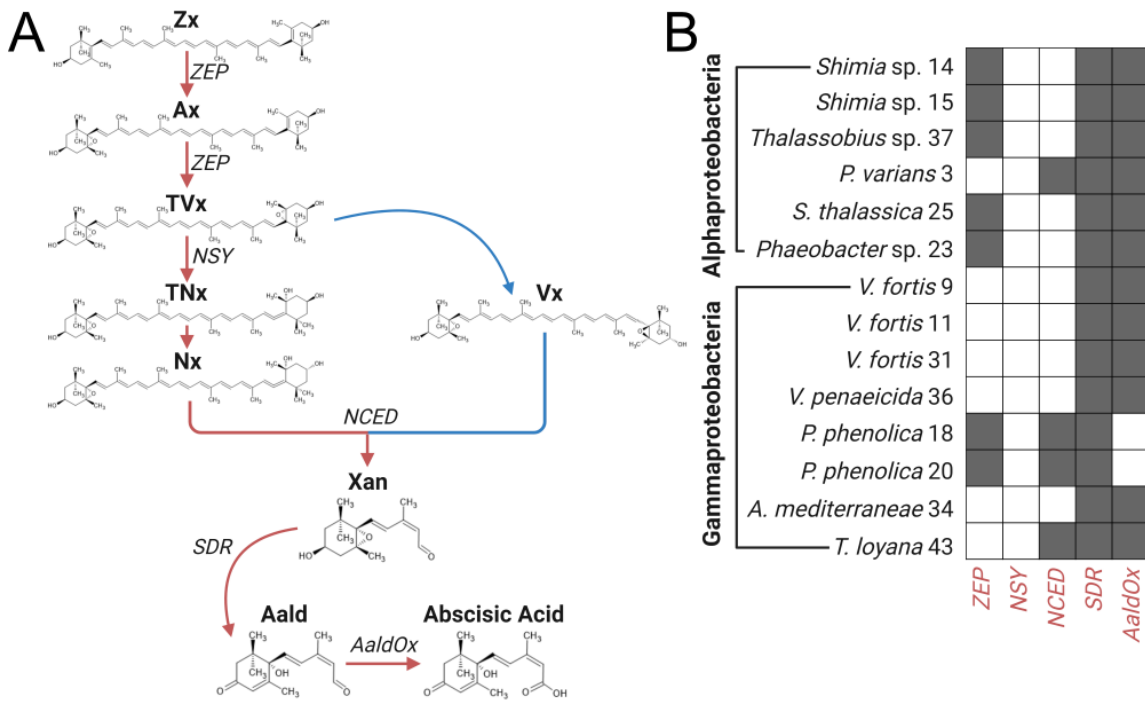


Figure S2.1: Abscisic acid biosynthesis pathway and production potential in the 14 bacteria isolates. A: ABA pathways in eukaryotes (plants). ABA biosynthesis pathway intermediate molecules are depicted with black bold text. Zx, Zeaxanthin; Ax, Antheraxanthin; TVx, Trans-violaxanthin; TNx, Trans-neoxanthin; Nx, 9-cis- neoxanthin; Vx, 9-cis-violaxanthin; Xan Xanthoxin; Aald, Abscisic aldehyde. Genes and enzymes are depicted with italic black text. ZEP, Zeaxanthin epoxidase; NSY, Neoxanthin synthase; NCED, 9-cis-epoxycarotenoid dioxygenase; SDR, Short chain dehydrogenase/reductase; AaldOx, Abscisic aldehyde oxidase. The two biosynthesis routes are depicted with red and blue coloured arrows. **B:** The presence of orthologues of ABA biosynthesis genes in *Actinocyclosporin* associated bacteria. Grey squares depict the detection of orthologues of ABA synthesis genes (bottom) in the bacteria (left), as indicated by a BLASTp search (e -value $< 10^{-10}$, *Supplementary Table S3*).

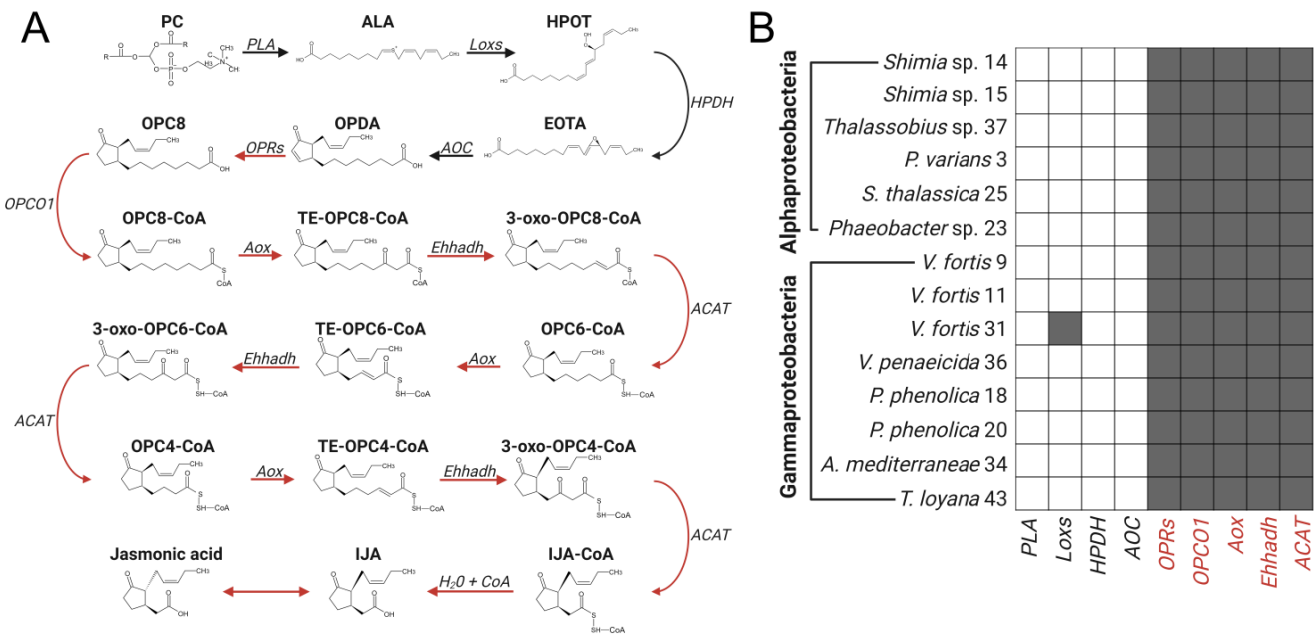


Figure S2.2: Jasmonic acid biosynthesis pathway and production potential in the 14 bacteria isolates. A: JA pathways in eukaryotes (plants). JA biosynthesis pathway molecules are depicted with black bold text. PC, Phosphatidylcholine; ALA, Alpha-Linolenic acid; HPOT, (9Z,11E,15Z)-(13S)-Hydroperoxyoctadeca-9,11,15-trienoate; EOTA, (9Z,15Z)-(13S)-12,13-Epoxyoctadeca-9,11,15-trienoic acid; OPDA, (15Z)-12-Oxophytodienoic acid; OPC8, 8-[(1S,2S)-3-Oxo-2-{(Z)-pent-2-enyl}cyclopentyl]octanoate; OPC8-CoA, TE-OPC8-CoA, 3-oxo-OPC8-CoA, OPC6-CoA, TE-OPC6-CoA, 3-oxo-OPC6-CoA, OPC4-CoA, TE-OPC4-CoA, 3-oxo-OPC4-CoA, IJA-CoA, IJA. Enzymes are depicted in italic black text. phospholipase (PLA) lipoxygenase (Loxs) hydroperoxide dehydratase (HPDH) allene oxide synthase (AOC) Allene oxide cyclase (AOC) 12-oxophytodienoic acid reductase (OPRS) CoA ligase (OPCO1) acyl-CoA oxidase (Aox) enoyl-CoA hydratase/3-hydroxyacyl-CoA dehydrogenase (Ehhadh), acetyl-CoA acyltransferase (ACAT). The biosynthesis pathway is split into black (genes from eukaryotes) and red (genes with known bacterial origin) coloured arrows. **B:** The presence of orthologues of JA biosynthesis genes in *Actinocyclus* associated bacteria. Grey squares depict the detection of orthologues of JA synthesis genes (bottom) in the bacteria (left), as indicated by a BLASTp search (e-value < 10⁻¹⁰, *Supplementary Table S5*).

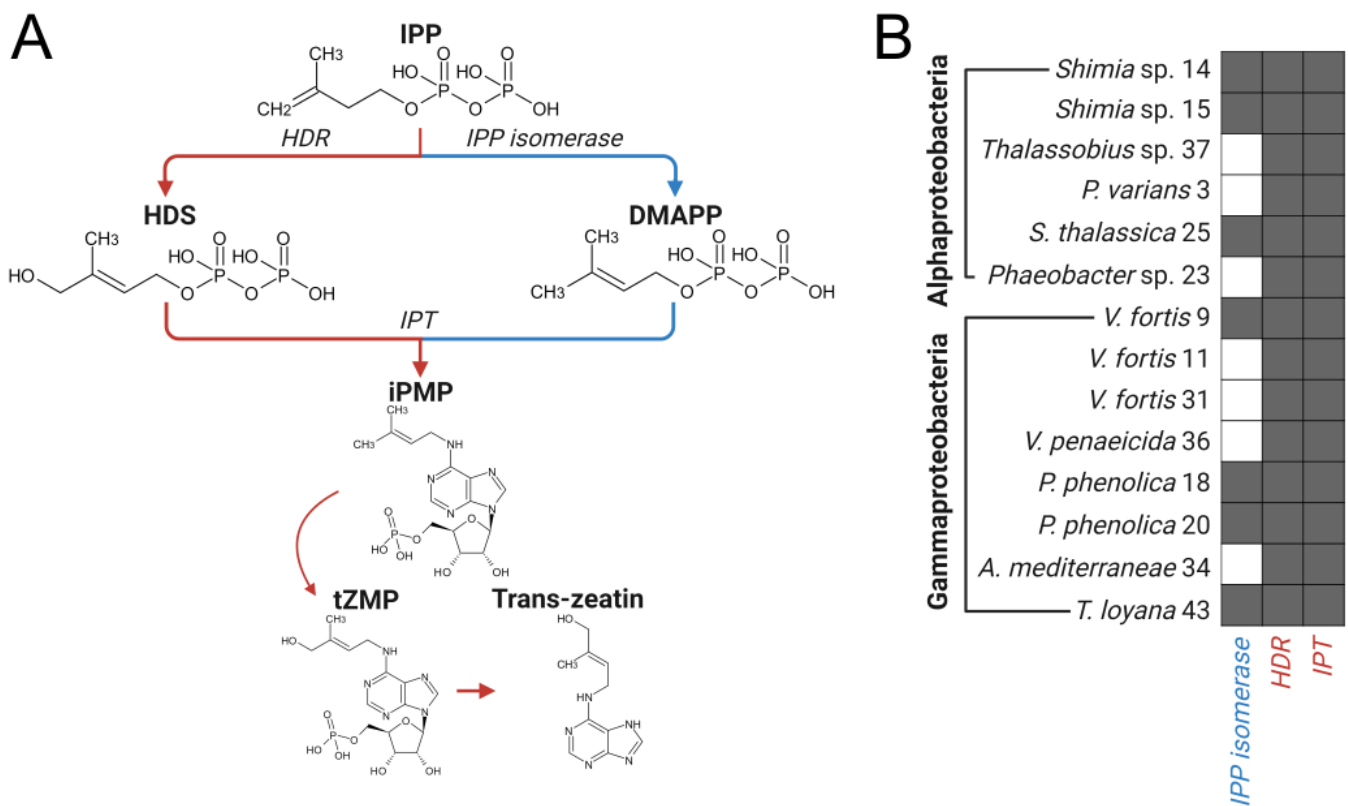


Figure S2.3: Trans-zeatin biosynthesis pathway and production potential in the 14 bacteria isolates. A: TZ pathways in bacteria. TZ biosynthesis pathway intermediate molecules are depicted with black bold text. IPP, Isopentenyl pyrophosphate; HDS, Hydroxymethylbutenyl diphosphate; iPMP, Isopentenyladenosine 5'-monophosphate; tZMP, Trans-zeatin riboside 5'-monophosphate, DMAPP, Dimethylallyl diphosphate. Genes and enzymes are depicted with un-bold italic black text. HDR, 4-hydroxy-3-methylbut-2-enyl diphosphate reductase; IPT, Isopentenyl transferase; IPP isomerase, Isopentenyl-diphosphate delta-isomerase. The two biosynthesis routes are depicted in red (most abundant in *Actinocyclosporin A isolated bacteria*) and blue coloured arrows. **B:** The presence of orthologues of TZ biosynthesis genes in *Actinocyclosporin A* associated bacteria. Grey squares depict the detection of orthologues of TZ synthesis genes (bottom) in the bacteria (left), as indicated by a BLASTp search (e-value < 10⁻¹⁰, *Supplementary Table S6*).

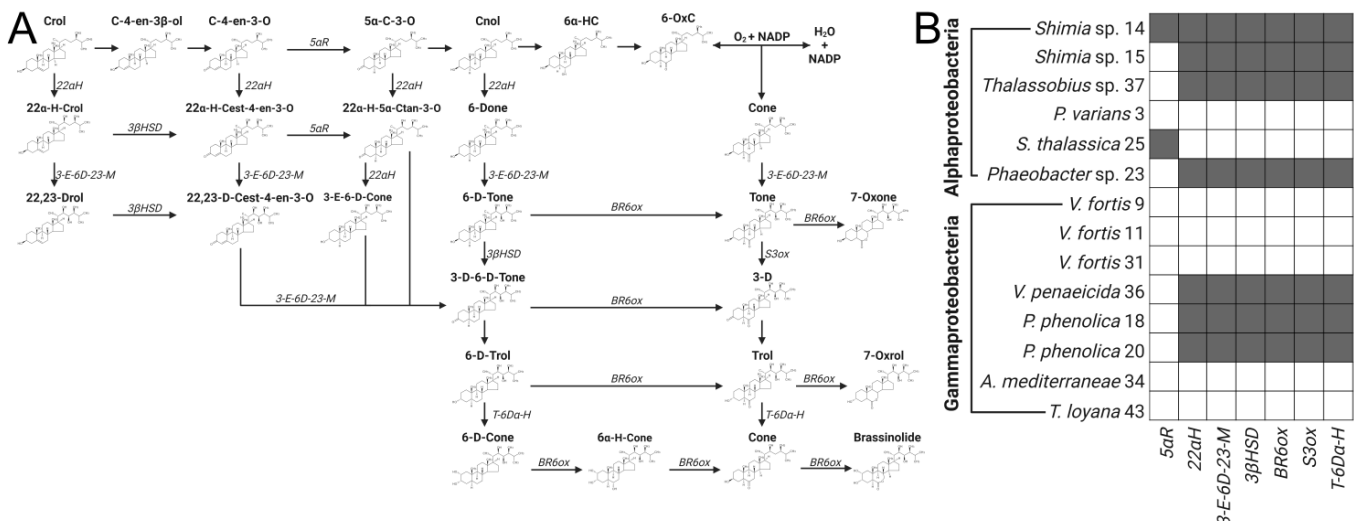


Figure S2.4: Brassinolide biosynthesis pathway and production potential in the 14 bacteria isolates. **A:** BSN pathways in eukaryotes (plants). BSN biosynthesis pathway intermediate molecules are depicted with black bold text. Crol, Campesterol; C-4-en-3 β -ol, Campester-4-en-3beta-ol; C-4-en-O, Campester-4-en-3-one; 5 α -C-3-O, 5alpha-Campestan-3-one; Cnol, Campestanol; 6 α -HC, 6alpha-Hydroxy campestanol; 6-OxC, 6-Oxocampestanol; 22 α -H-Crol, 22alpha-Hydroxy-campesterol; 22,23-Drol, 22,23-Dihydroxycampesterol; 22 α -H-Cest-4-en-3-O, 22alpha-Hydroxy-campester-4-en-3-one; 22,23-D-Cest-4-en-3-O, 22,23-Dihydroxy-campester-4-en-3-one; 22 α -H-5 α -Ctan-3-O, 22alpha-Hydroxy-5alpha-campestan-3-one; 3-E-6-D-Cone, 3-epi-6-deoxo-cathasterone; 6-Done, 6-Deoxocathasterone; 6-D-Tone, 6-Deoxo-teasterone; 3-D-6-D-Tone, 3-Dehydro-6-deoxo-teasterone; 6-D-Trol, 6-Deoxo-typhasterol; 6-D-Cone, 6-Deoxo-castasterone; 6 α -H-Cone, 6alpha-hydroxy-castasterone; Cone, Castasterone; Tone, Teasterone; 3-D, 3-Dehydroteasterone; Trol, Typhasterol; 7-oxone, 7-oxatesterone; 7-oxrol, 7-oxatypasterol. Genes and enzymes are depicted with un-bold italic black text. 5 α R, Steroid 5-alpha-reductase; 22 α H, steroid 22-alpha-hydroxylase; 3-E-6D-23-M, 3-epi-6-deoxocathasterone 23-monooxygenase; 3 β HSD, 3beta,22alpha-dihydroxysteroid 3-dehydrogenase; BR6ox, Brassinosteroid-6-oxidase; S3ox, Steroid 3-oxidase; T-6Da-H, Typhasterol/6-deoxotyphasterolalpha-hydroxylase. The biosynthesis routes are depicted in black arrows. **B:** The presence of orthologues of BSN biosynthesis genes in *Actinocyclus* associated bacteria. Grey squares depict the detection of orthologues of BSN synthesis genes (bottom) in the bacteria (left), as indicated by a BLASTp search (e-value < 10⁻¹⁰, *Supplementary Table S7*).

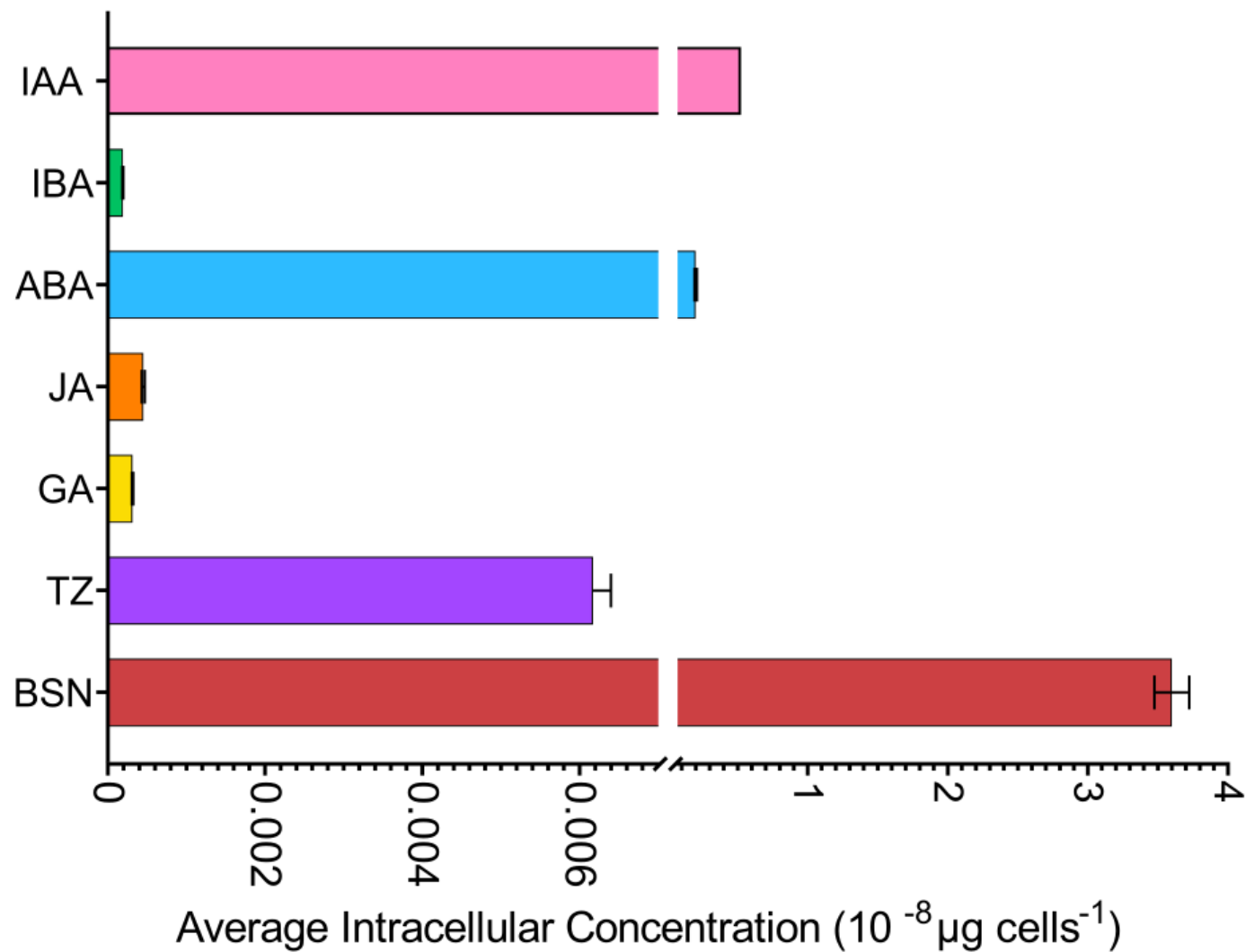


Figure S2.5: Average intracellular plant growth promoting hormone concentration in (μg/cell) the 14 bacteria tested. (± SEM; n = 56).

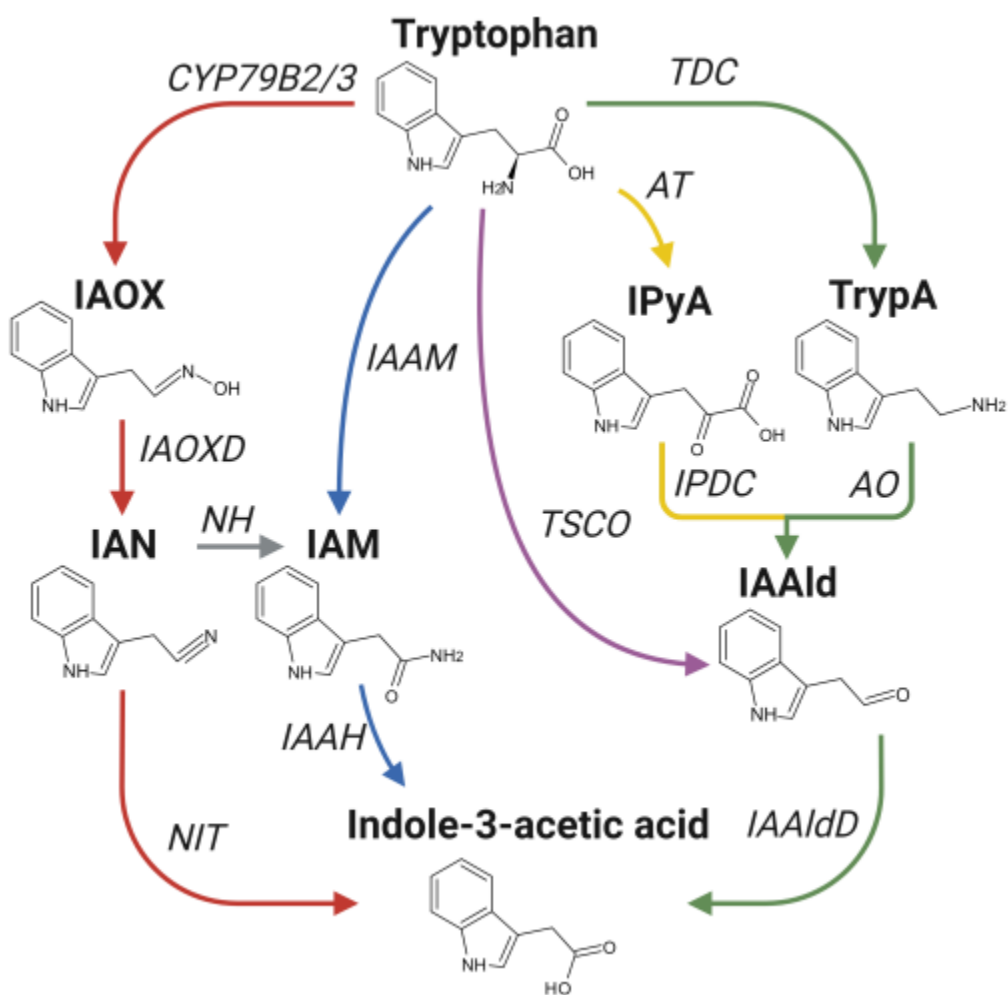


Figure S4.1: Tryptophan dependent IAA pathways in bacteria. Five main IAA biosynthesis pathways, including the Indole-3 acetonitrile (red), Indole-3-acetamide (blue), Tryptophan side chain oxidase (purple), Indole-3-pyruvate (yellow), and Tryptamine (green) pathways are depicted. Intermediate molecules are depicted with black bold text. IAOx, Indole-3-acetaldoxime; IAN, Indole-3-acetonitrile; IAM, indole-3-acetamide; IPyA, Indole-3-pyruvate; TrypA, Tryptamine; IAald, indole-3-acetaldehyde. Enzymes are depicted un-bold black text and lines. CYP79B2/3, cytochrome P450; IAOxD, Indole-acetaldoxime dehydratase; NIT, Nitrilase; NH, Nitrile hydrolase; IaaM, Tryptophan-2-monooxygenase; IaaH, Indole-3-acetamide hydrolase; TSO, Tryptophan side-chain oxidase; TDC, Tryptophan decarboxylase; IPDC, Indole-3-pyruvate decarboxylase; AO, Amine oxidase; AT, Amino transferase; IAaldD, indole-3-acetaldehyde dehydrogenase.

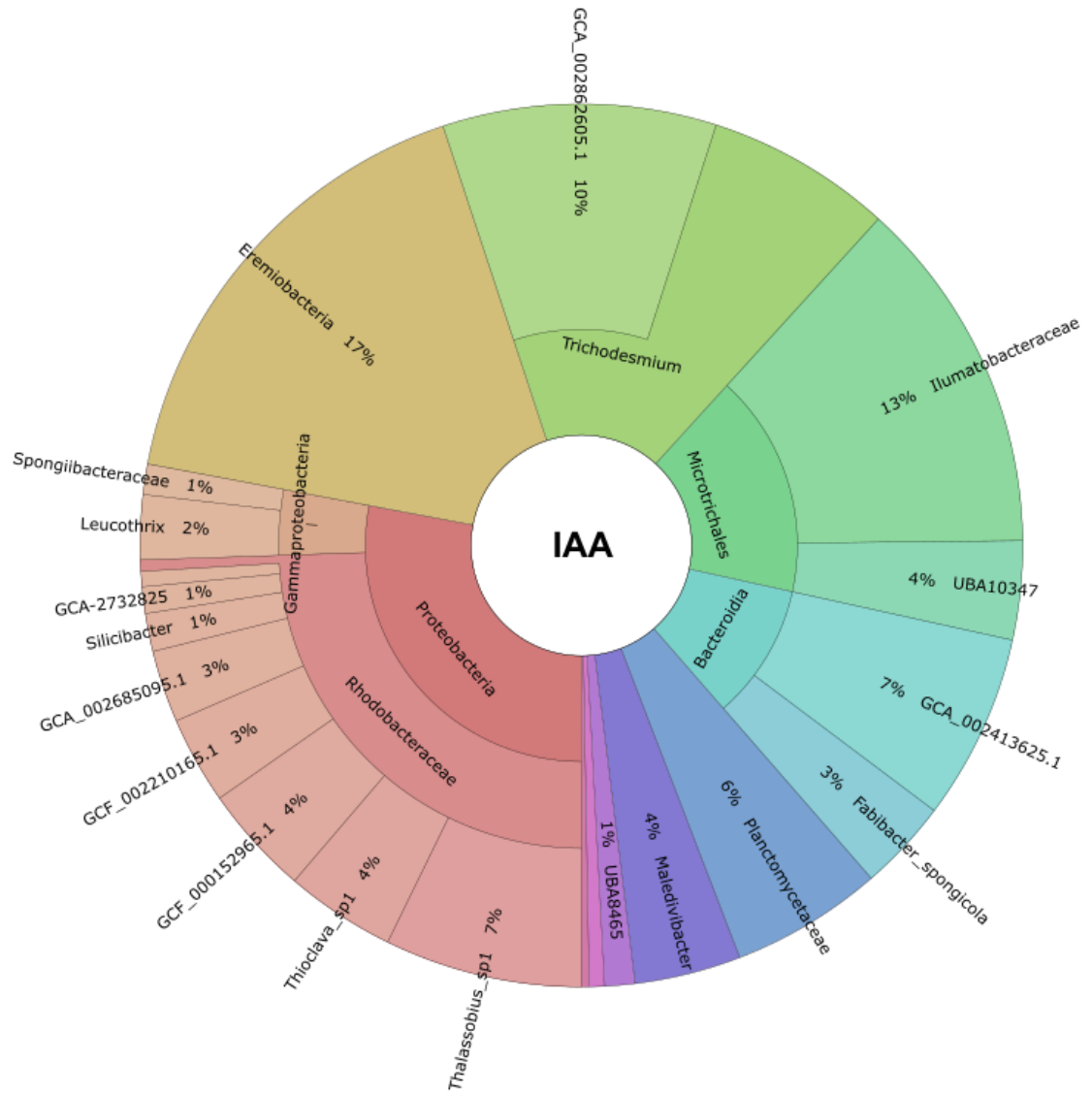


Figure S4.25: A) Multi-layered pie charts (Krona charts) displaying *Tara Oceans* bacteria that A) possess IAA genes and, B) possess GA genes. Each segment represents distinct bacterial taxa, with its size indicating the proportion of total hormone gene abundance attributed to that group.

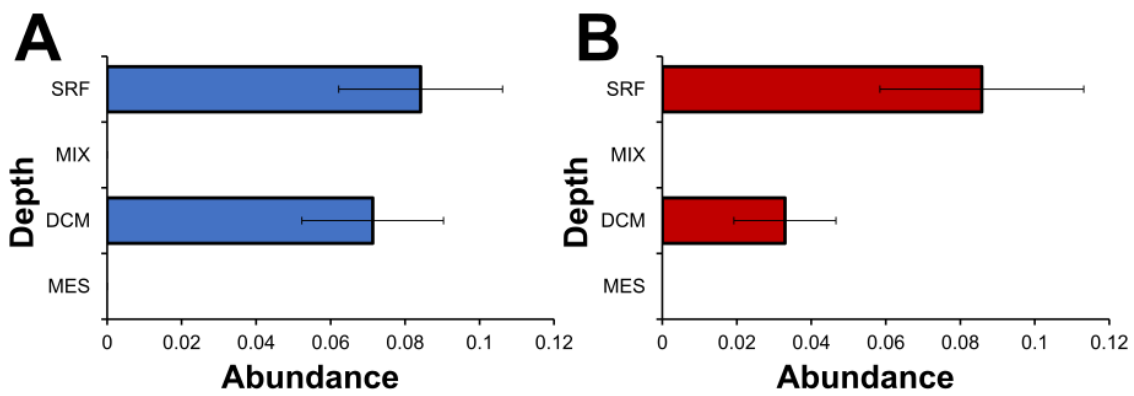


Figure S4.3: Average abundance of bacterial-IAA genes across all *Tara* oceans sites at sea surface, mixed layer, mesopelagic, and deep chlorophyll max oceanographic depths. A) Average IAA gene abundance across all *Tara* oceans sites at 4 depths. **B)** Average IAA gene abundance across all *Tara* oceans sites at 4 depths. Error bars are standard error of the mean (SEM). Significant differences are depicted with asterisks (*; One-way ANOVA, $p < 0.05$, Table X).

Supplementary Tables:

All supplementary tables can be found in Excel file “Supplementary tables PhD thesis Abeeha Khalil 12584355”.

Table S2.1: Bacterial taxonomic identification for the 14 bacteria isolates tested. The table is available as a separate Supplementary File.

Table S2.2: Orthologous genes for the Indole-3-acetic acid pathway found in the 14 bacteria isolates (Figure 1B). The table is available as a separate Supplementary File.

Table S2.3: Orthologous genes for the Abscisic acid pathway found in the 14 bacteria isolates (Figure S1B). The table is available as a separate Supplementary File.

Table S2.4: Orthologous genes for the Gibberellic acid pathway found in the 14 bacteria isolates (Figure 2B). The table is available as a separate Supplementary File.

Table S2.5: Orthologous genes for the Jasmonic acid pathway found in the 14 bacteria isolates (Figure S3B). The table is available as a separate Supplementary File.

Table S2.6: Orthologous genes for the Trans-zeatin pathway found in the 14 bacteria isolates (Figure S4B). The table is available as a separate Supplementary File.

Table S2.7: Orthologous genes for the Brassinolide pathway found in the 14 bacteria isolates (Figure S5B). The table is available as a separate Supplementary File.

Table S2.8: One-way ANOVA and post-hoc (Turkey's test) comparing the Indole 3-acetic acid concentrations between the 14 bacteria tested (Figure S6A). The table is available as a separate Supplementary File.

Table S2.9: One-way ANOVA and post-hoc (Turkey's test) comparing the Indole 3-butyric acid concentrations between the 14 bacteria tested (Figure S6A). The table is available as a separate Supplementary File.

Table S2.10: One-way ANOVA and post-hoc (Turkey's test) comparing the Abscisic acid concentrations between the 14 bacteria tested (Figure S6A). The table is available as a separate Supplementary File.

Table S2.11: One-way ANOVA and post-hoc (Turkey's test) comparing the Gibberellic acid concentrations between the 14 bacteria tested (Figure S6A). The table is available as a separate Supplementary File.

Table S2.12: One-way ANOVA and post-hoc (Turkey's test) comparing the Jasmonic acid concentrations between the 14 bacteria tested (Figure S6A). The table is available as a separate Supplementary File.

Table S2.13: One-way ANOVA and post-hoc (Turkey's test) comparing the Trans-zeatin concentrations between the 14 bacteria tested (Figure S6A). The table is available as a separate Supplementary File.

Table S2.14: One-way ANOVA and post-hoc (Turkey's test) comparing the Brassinolide concentrations between the 14 bacteria tested (Figure S6A). The table is available as a separate Supplementary File.

Table S2.15: Univariate Simple Main Effect test between PGPH treated (three concentrations) *Actinocyclus* and axenic *Actinocyclus* controls for each sampling day (Figure 6 (A to F)). The table is available as a separate Supplementary File.

Table S3.1: Orthologous genes for the Indole-3-acetic acid pathway found in *Alteromonas mediterranea* (Figure 3.1).

Table S3.2: Oligonucleotides used to assemble gRNA sequences. All sequences written as 5' - > 3'.

Table S3.3: ANOVA test and post hoc Univariate Simple pairwise comparison between axenic phytoplankton control and wildtype vs. mutant *A. mediterranea* treated *Actinocyclus* sp., *N. oceanica* and *P. tricornutum* for each sampling day (Figure 3.6)

Table S3.4: One-way ANOVA and post-hoc (Turkey's test) comparing IAA concentration between wildtype and mutant *A. mediterranea* and IAA concentrations between the phytoplankton species *Actinocyclus* sp., *N. oceanica* and *P. tricornutum*.

Table S3.5: Biovolume calculation of IAA concentration in wildtype and mutant *A. mediterranea*, *Actinocyclus* sp., *N. oceanica* and *P. tricornutum*.

Table S4.1: One-way ANOVA and post-hoc (Tukey's test, adjusted Bonferroni) comparing the abundance of bacterial-IAA genes in sea surface and deep chlorophyll max samples between various oceanographic regions (North Atlantic Ocean, Mediterranean Sea, Red Sea, Indian Ocean, South Atlantic Ocean, Southern Ocean, South Pacific Ocean, North Pacific Ocean and Arctic Ocean).

Table S4.2: One-way ANOVA and post-hoc (Turkey's test, adjusted Bonferroni) comparing the abundance of bacterial-GA genes in sea surface and deep chlorophyll max samples between various oceanographic regions (North Atlantic Ocean, Mediterranean Sea, Red Sea, Indian Ocean, South Atlantic Ocean, Southern Ocean, South Pacific Ocean, North Pacific Ocean and Arctic Ocean).

Table S4.3 Correlations (Spearman's) between abundance of IAA or GA genes in bacteria to environmental factors observed in the *Tara* Oceans expedition (r-value <0)

Table S4.4 PERMANOVA pairwise comparison of bacterial community between IAA pathways.

Table S4.5: Bacteria within the *Tara* Oceans sites that possess genes for IAA biosynthesis via the Indole-3-acetonitrile, Indole-3-acetamide, Indole-3-pyruvate and Tryptamine pathway.

Table S4.6: Bacteria within the *Tara* Oceans sites that possess genes for GA biosynthesis.

Table S4.7: Environmental variables at each *Tara* Oceans site for bacteria that possess IAA genes.

Table S4.8: Environmental variables at each *Tara* Oceans site for bacteria that possess GA genes.

Table S4.9 Positive correlations between bacteria that possess IAA genes and *Tara* Oceans phytoplankton.

References:

Acinas, S. G., Sánchez, P., Salazar, G., Cornejo-Castillo, F. M., Sebastián, M., Logares, R., Royo-Llonch, M., Paoli, L., Sunagawa, S., Hingamp, P., Ogata, H., Lima-Mendez, G., Roux, S., González, J. M., Arrieta, J. M., Alam, I. S., Kamau, A., Bowler, C., Raes, J., ... Gasol, J. M. (2021). Deep ocean metagenomes provide insight into the metabolic architecture of bathypelagic microbial communities. *Nature Communications*, 12(1), 1-15. <https://doi.org/10.1038/s42003-021-02112-2>

Ali, B., Sabri, A. N., Ljung, K., & Hasnain, S. (2009). Auxin production by plant associated bacteria: Impact on endogenous IAA content and growth of *Triticum aestivum L.* *Letters in Applied Microbiology*, 48(5), 542–547. <https://doi.org/10.1111/J.1472-765X.2009.02565.X>

Amin, S. A., Hmelo, L. R., Van Tol, H. M., Durham, B. P., Carlson, L. T., Heal, K. R., Morales, R. L., Berthiaume, C. T., Parker, M. S., Djunaedi, B., Ingalls, A. E., Parsek, M. R., Moran, M. A., & Armbrust, E. V. (2015). Interaction and signalling between a cosmopolitan phytoplankton and associated bacteria. *Nature*, 522(7554), 98–101. <https://doi.org/10.1038/nature14488>

Amin, S. A., Parker, M. S., & Armbrust, E. V. (2012). Interactions between diatoms and bacteria. *Microbiology and Molecular Biology Reviews*, 76(3), 667–684. <https://doi.org/10.1128/mmbr.00007-12>

Anam, G. B., Guda, D. R., & Ahn, Y. H. (2021). Hormones induce the metabolic growth and cytotoxin production of *Microcystis aeruginosa* under terpinolene stress. *Science of The Total Environment*, 769, 145083. <https://doi.org/10.1016/J.SCITOTENV.2021.145083>

Añorga, M., Pintado, A., Ramos, C., De Diego, N., Ugena, L., Novák, O., & Murillo, J. (2020). Genes ptz and idi, Coding for Cytokinin Biosynthesis Enzymes, Are Essential for Tumorigenesis and In Planta Growth by *P. syringae* pv. savastanoi NCPPB 3335. *Frontiers in Plant Science*, 11, 1294. <https://doi.org/10.3389/FPLS.2020.01294/BIBTEX>

Arandia-Gorostidi, N., Weber, P. K., Alonso-Sáez, L., Morán, X. A. G., & Mayali, X. (2016). Elevated temperature increases carbon and nitrogen fluxes between phytoplankton and heterotrophic bacteria through physical attachment. *The ISME Journal*, 11(3), 641–650. <https://doi.org/10.1038/ismej.2016.156>

Arrigo, K. R. (2004). Marine microorganisms and global nutrient cycles. *Nature*, 437(7057), 349–355. <https://doi.org/10.1038/nature04159>

Attar, N. (2015). Marine microbiology: An interkingdom partnership. *Nature Reviews Microbiology*, 13(7), 400. <https://doi.org/10.1038/nrmicro3515>

Azam, F., & Malfatti, F. (2007). Microbial structuring of marine ecosystems. *Nature Reviews Microbiology*, 5(10), 782–791. <https://doi.org/10.1038/nrmicro1747>

Baker, D., Lauer, J., Ortega, A., Jackrel, S. L., & Denef, V. J. (2022). Effects of phycosphere bacteria on their algal host are host species-specific and not phylogenetically conserved. *Microorganisms*, 11(1). <https://doi.org/10.3390/MICROORGANISMS11010062>

Balcke, G. U., Handrick, V., Bergau, N., Fichtner, M., Henning, A., Stellmach, H., Tissier, A., Hause, B., & Frolov, A. (2012). An UPLC-MS/MS method for highly sensitive high-throughput analysis of phytohormones in plant tissues. *Plant Methods*, 8(1), 1–11. <https://doi.org/10.1186/1746-4811-8-47/FIGURES/4>

Bankevich, A., Nurk, S., Antipov, D., Gurevich, A. A., Dvorkin, M., Kulikov, A. S., Lesin, V. M., Nikolenko, S. I., Pham, S., Prjibelski, A. D., Pyshkin, A. V., Sirotkin, A. V., Vyahhi, N., Tesler, G., Alekseyev, M. A., & Pevzner, P. A. (2012). SPAdes: A new genome assembly algorithm and its applications to single-cell sequencing. *Genome Research*, 22(3), 455–477. <https://doi.org/10.1089/CMB.2012.0021>

Barak-Gavish, N., Dassa, B., Kuhlisch, C., Nussbaum, I., Brandis, A., Rosenberg, G., Avraham, R., & Vardi, A. (2023). Bacterial lifestyle switch in response to algal metabolites. *eLife*, 12. <https://doi.org/10.7554/eLife>

Bashan, Y., & De-Bashan, L. E. (2010). How the plant growth-promoting bacterium *Azospirillum* promotes plant growth—A critical assessment. *Advances in Agronomy*, 108, 77–136. [https://doi.org/10.1016/S0065-2113\(10\)08002-8](https://doi.org/10.1016/S0065-2113(10)08002-8)

Bell, W., & Mitchell, R. (1972). Chemotactic and growth responses of marine bacteria to algal extracellular products. *The Biological Bulletin*, 143(2), 265–277. <https://doi.org/10.2307/1540052>

Blanco-Ameijeiras, S., Cabanes, D. J. E., & Hassler, C. S. (2019). Towards the development of a new generation of whole-cell bioreporters to sense iron bioavailability in oceanic systems—Learning from the case of *Synechococcus* sp. PCC7002 iron bioreporter. *Journal of Applied Microbiology*, 127(5), 1291–1304. <https://doi.org/10.1111/JAM.14277>

Bolger, A. M., Lohse, M., & Usadel, B. (2014). Trimmomatic: A flexible trimmer for Illumina sequence data. *Bioinformatics*, 30(15), 2114–2120. <https://doi.org/10.1093/BIOINFORMATICS/BTU170>

Bramucci, A. R., Focardi, A., Rinke, C., Hugenholtz, P., Tyson, G. W., Seymour, J. R., & Raina, J.-B. (2021). Microvolume DNA extraction methods for microscale amplicon and metagenomic studies. *ISME Communications*, 1(1), 1–5. <https://doi.org/10.1038/s43705-021-00079-z>

Brandl, M. T., & Lindow, S. E. (1996). Cloning and characterization of a locus encoding an indolepyruvate decarboxylase involved in indole-3-acetic acid synthesis in *Erwinia herbicola*. *Applied and Environmental Microbiology*, 62(11), 4121–4128. <https://doi.org/10.1128/AEM.62.11.4121-4128.1996>

Brown, M. V., Van De Kamp, J., Ostrowski, M., Seymour, J. R., Ingleton, T., Messer, L. F., Jeffries, T., Siboni, N., Laverock, B., Bibiloni-Isaksson, J., Nelson, T. M., Coman, F., Davies, C. H., Frampton, D., Rayner, M., Goossen, K., Robert, S., Holmes, B., Abell, G. C. J., & Bodrossy, L. (2018). Systematic, continental scale temporal monitoring of marine pelagic microbiota by the Australian Marine Microbial Biodiversity Initiative. *Scientific Data*, 5(1), 1–10. <https://doi.org/10.1038/sdata.2018.130>

Bruhn, J. B., Gram, L., & Belas, R. (2007). Production of antibacterial compounds and biofilm formation by *Roseobacter* species are influenced by culture conditions. *Applied and Environmental Microbiology*, 73(2), 442. <https://doi.org/10.1128/AEM.02238-06>

Buchan, A., LeCleir, G. R., Gulvik, C. A., & González, J. M. (2014). Master recyclers: Features and functions of bacteria associated with phytoplankton blooms. *Nature Reviews Microbiology*, 12(10), 686–698. <https://doi.org/10.1038/nrmicro3326>

Chklovski, A., Parks, D. H., Woodcroft, B. J., & Tyson, G. W. (2023). CheckM2: A rapid, scalable and accurate tool for assessing microbial genome quality using machine learning. *Nature Communications*, 14(1), 1–14. <https://doi.org/10.1038/s41467-022-33129-5>

Chung, T. Y., Kuo, C. Y., Lin, W. J., Wang, W. L., & Chou, J. Y. (2018). Indole-3-acetic-acid-induced phenotypic plasticity in *Desmodesmus* algae. *Scientific Reports*, 8(1), 1–13. <https://doi.org/10.1038/s41598-018-28627-z>

Cirri, E., & Pohnert, G. (2019). Algae–bacteria interactions that balance the planktonic microbiome. *New Phytologist*, 223(1), 100–106. <https://doi.org/10.1111/nph.15765>

Cole, J. J. (1982). Interactions between bacteria and algae in aquatic ecosystems. *Annual Review of Ecology, Evolution, and Systematics*, 34, 291–314. <https://doi.org/10.1146/annurev.es.34.110182.001451>

Cooper, M. B., & Smith, A. G. (2015). Exploring mutualistic interactions between microalgae and bacteria in the omics age. *Current Opinion in Plant Biology*, 26, 147–153. <https://doi.org/10.1016/j.pbi.2015.07.003>

Costacurta, A., Keijers, V., & Vanderleyden, J. (1994). Molecular cloning and sequence analysis of an *Azospirillum brasilense* indole-3-pyruvate decarboxylase gene. *MGG Molecular & General Genetics*, 243(4), 463–472. <https://doi.org/10.1007/BF00280477/METRICS>

Croft, M. T., Lawrence, A. D., Raux-Deery, E., Warren, M. J., & Smith, A. G. (2005). Algae acquire vitamin B12 through a symbiotic relationship with bacteria. *Nature*, 438(7064), 90–93. <https://doi.org/10.1038/nature04056>

Curl, E. A., & Truelove, B. (1986). Microbial interactions. In *Microbial Interactions* (pp. 140–166). Springer. https://doi.org/10.1007/978-3-642-70722-3_5

Czerpak, R., Piotrowska, A., & Szulecka, K. (2006). Jasmonic acid affects changes in the growth and some component content in the alga *Chlorella vulgaris*. *Acta Physiologiae Plantarum*, 28(3), 195–203. <https://doi.org/10.1007/BF02706531>

Dao, G. H., Wu, G. X., Wang, X. X., Zhang, T. Y., Zhan, X. M., & Hu, H. Y. (2018). Enhanced microalgae growth through stimulated secretion of indole acetic acid by symbiotic bacteria. *Algal Research*, 33, 345–351. <https://doi.org/10.1016/J.AL GAL.2018.06.006>

Dao, G., Wang, S., Wang, X., Chen, Z., Wu, Y., Wu, G., Lu, Y., Liu, S., & Hu, H. (2020). Enhanced *Scenedesmus* sp. growth in response to gibberellin secretion by symbiotic bacteria. *Science of The Total Environment*, 740, 140099. <https://doi.org/10.1016/J.SCITOTENV.2020.140099>

Desai, S. A. (2017). Isolation and characterization of gibberellic acid (GA3) producing rhizobacteria from sugarcane roots. *Bioscience Discovery*, 8(3), 488–494. <http://biosciencediscovery.com>

Durham, B. P., Boysen, A. K., Carlson, L. T., Groussman, R. D., Heal, K. R., Cain, K. R., Morales, R. L., Coesel, S. N., Morris, R. M., Ingalls, A. E., & Armbrust, E. V. (2019). Sulfonate-based networks between eukaryotic phytoplankton and heterotrophic bacteria in the surface ocean. *Nature Microbiology*, 4(10), 1706–1715. <https://doi.org/10.1038/s41564-019-0507-5>

Durham, B. P., Boysen, A. K., Heal, K. R., Carlson, L. T., Boccamazzo, R., Deodato, C. R., Qin, W., Cattolico, R. A., Armbrust, E. V., & Ingalls, A. E. (2022). Chemotaxonomic patterns in intracellular metabolites of marine microbial plankton. *Frontiers in Marine Science*, 9, 864796. <https://doi.org/10.3389/FMARS.2022.864796/XML/NLM>

Durham, B. P., Dearth, S. P., Sharma, S., Amin, S. A., Smith, C. B., Campagna, S. R., Armbrust, E. V., & Moran, M. A. (2017). Recognition cascade and metabolite transfer in a marine bacteria-phytoplankton model system. *Environmental Microbiology*, 19(9), 3500–3513. <https://doi.org/10.1111/1462-2920.13834>

Durham, B. P., Sharma, S., Luo, H., Smith, C. B., Amin, S. A., Bender, S. J., Dearth, S. P., Van Mooy, B. A. S., Campagna, S. R., Kujawinski, E. B., Armbrust, E. V., & Moran, M. A. (2015). Cryptic carbon and sulfur cycling between surface ocean plankton. *Proceedings of the National Academy of Sciences*, 112(2), 453–457. <https://doi.org/10.1073/pnas.1413137112>

Elakbawy, W. M., Shanab, S. M. M., & Shalaby, E. A. (2022). Enhancement of plant growth regulators production from microalgae cultivated in treated sewage wastewater (TSW). *BMC Plant Biology*, 22(1), 1–14. <https://doi.org/10.1186/S12870-022-03764-W/FIGURES/3>

Eng, F., Zienkiewicz, K., Gutiérrez-Rojas, M., Favela-Torres, E., & Feussner, I. (2018). Jasmonic acid biosynthesis by microorganisms: Derivatives, first evidences on biochemical pathways, and culture conditions for production. *PeerJ Preprints*, 6, e26655. <https://doi.org/10.7287/PEERJ.PREPRINTS.26655V1>

Falkowski, P., & Knoll, A. H. (2007). Evolution of primary producers in the sea. In *Evolution of Primary Producers in the Sea* (pp. 1–14). Elsevier Inc. <https://doi.org/10.1016/B978-0-12-370518-1.X5000-0>

Fidler, J., Zdunek-Zastocka, E., & Bielawski, W. (2015). Regulation of abscisic acid metabolism in relation to the dormancy and germination of cereal grains. *Acta Societatis Botanicorum Poloniae*, 84(1), 3–12. <https://doi.org/10.5586/asbp.2015.001>

Field, C. B., Behrenfeld, M. J., Randerson, J. T., & Falkowski, P. (1998). Primary production of the biosphere: Integrating terrestrial and oceanic components. *Science*, 281(5374), 237–240. <https://doi.org/10.1126/science.281.5374.237>

Fierli, D., Aranyos, A., Barone, M. E., Parkes, R., & Touzet, N. (2022). Influence of exogenous phytohormone supplementation on the pigment and fatty acid content of three

marine diatoms. *Applied Microbiology and Biotechnology*, 106(18), 6195–6207. <https://doi.org/10.1007/S00253-022-12140-5/FIGURES/6>

Foo, E., Plett, J. M., Lopez-Raez, J. A., & Reid, D. (2019). Editorial: The role of plant hormones in plant-microbe symbioses. *Frontiers in Plant Science*, 10, 1391. <https://doi.org/10.3389/FPLS.2019.01391/BIBTEX>

Gaskins, M. H., Albrecht, S. L., & Hubbell, D. H. (1985). Rhizosphere bacteria and their use to increase plant productivity: A review. *Agriculture, Ecosystems and Environment*, 12(2), 99–116. [https://doi.org/10.1016/0167-8809\(85\)90071-4](https://doi.org/10.1016/0167-8809(85)90071-4)

Geng, H., & Belas, R. (2010). Molecular mechanisms underlying *Roseobacter*–phytoplankton symbioses. *Current Opinion in Biotechnology*, 21(3), 332–338. <https://doi.org/10.1016/J.COPBIO.2010.03.013>

Glickmann, E., Gardan, L., Jacquet, S., Hussain, S., Elasri, M., Petit, A., & Dessaix, Y. (2007). Auxin production is a common feature of most pathovars of *Pseudomonas syringae*. *Molecular Plant-Microbe Interactions*, 11(2), 156–162. <https://doi.org/10.1094/MPMI.1998.11.2.156>

Gomez-Escribano, J. P., Song, L., Fox, D. J., Yeo, V., Bibb, M. J., & Challis, G. L. (2012). Structure and biosynthesis of the unusual polyketide alkaloid coelimycin P1, a metabolic product of the cpk gene cluster of *Streptomyces coelicolor* M145. *Chemical Science*, 3(9), 2716–2720. <https://doi.org/10.1039/C2SC20410J>

Graff, J. R., Rines, J. E. B., & Donaghay, P. L. (2011). Bacterial attachment to phytoplankton in the pelagic marine environment. *Marine Ecology Progress Series*, 441, 15–24. <https://doi.org/10.3354/MEPS09353>

Grossart, H.-P. (1999). Interactions between marine bacteria and axenic diatoms (*Cylindrotheca fusiformis*, *Nitzschia laevis*, and *Thalassiosira weissflogii*) incubated under various conditions in the lab. *FEMS Microbiology Ecology*, 19(11), 29. <https://doi.org/10.1111/j.1574-6941.1999.tb00695.x>

Guo, J. (2015). Impact of pharmaceuticals on algal species. *PhD Thesis, University of York*.

Hughes, D. J., Varkey, D., Doblin, M. A., Ingleton, T., McInnes, A., Ralph, P. J., van Dongen-Vogels, V., & Suggett, D. J. (2018). Impact of nitrogen availability upon the electron requirement for carbon fixation in Australian coastal phytoplankton communities. *Limnology and Oceanography*, 63(5), 1891–1910. <https://doi.org/10.1002/lno.10814>

Hyatt, D., Chen, G. L., LoCascio, P. F., Land, M. L., Larimer, F. W., & Hauser, L. J. (2010). Prodigal: Prokaryotic gene recognition and translation initiation site identification. *BMC Bioinformatics*, 11(1), 119. <https://doi.org/10.1186/1471-2105-11-119>

Isaac, A., Francis, B., Amann, R. I., & Amin, S. A. (2021). Tight adherence (Tad) pilus genes indicate putative niche differentiation in phytoplankton bloom associated *Rhodobacterales*. *Frontiers in Microbiology*, 12, 718297. <https://doi.org/10.3389/FMICB.2021.718297/BIBTEX>

Jiang, Z., Li, J., & Qu, L.-J. (2017). Hormone metabolism and signaling in plants. In *Hormone Metabolism and Signaling in Plants* (pp. 1–16). Academic Press. <https://doi.org/10.1016/B978-0-12-811562-6.00002-5>

Joglar, V., Pontiller, B., Martínez-García, S., Fuentes-Lema, A., Pérez-Lorenzo, M., Lundin, D., Pinhassi, J., Fernández, E., & Teira, E. (2021). Microbial plankton community structure and function responses to vitamin B12 and B1 amendments in an upwelling system. *Applied and Environmental Microbiology*, 87(22). <https://doi.org/10.1128/AEM.01525-21>

Jusoh, M., Loh, S. H., Chuah, T. S., Aziz, A., & Cha, T. S. (2015). Elucidating the role of jasmonic acid in oil accumulation, fatty acid composition and gene expression in *Chlorella vulgaris* (Trebouxiophyceae) during early stationary growth phase. *Algal Research*, 9, 14–20. <https://doi.org/10.1016/J.ALGAL.2015.02.020>

Kang, D. D., Li, F., Kirton, E., Thomas, A., Egan, R., An, H., & Wang, Z. (2019). MetaBAT 2: An adaptive binning algorithm for robust and efficient genome reconstruction from metagenome assemblies. *PeerJ*, 7, e7359. <https://doi.org/10.7717/PEERJ.7359>

Kaur, M., Khem, S., Saini, C., Ojah, H., Sahoo, R., Kriti Gupta, K., Kumar, A., & Felix Bast, F. (2023). Abiotic stress in algae: Response, signaling and transgenic approaches. *Journal of Applied Phycology*, 1, 3. <https://doi.org/10.1007/s10811-022-02746-7>

KEGG GENES Database. KEGG GENES database.
<https://www.genome.jp/kegg/genes.html>

Khalil, A., Bramucci, A. R., Focardi, A., Le Reun, N., Willams, N. L. R., Kuzhiumparambil, U., Raina, J. B., & Seymour, J. R. (2024). Widespread production of plant growth-promoting hormones among marine bacteria and their impacts on the growth of a marine diatom. *Microbiome*, 12(1), 1–14. <https://doi.org/10.1186/S40168-024-01899-6/FIGURES/6>

Kim, H., Kimbrel, J. A., Vaiana, C. A., Wollard, J. R., Mayali, X., & Buie, C. R. (2021). Bacterial response to spatial gradients of algal-derived nutrients in a porous microplate. *Environmental Microbiology*, 23(1), 134–144. <https://doi.org/10.1111/1462-2920.15510>

Kim, J. Y., Oh, J. J., Jeon, M. S., Kim, G. H., & Choi, Y. E. (2019). Improvement of *Euglena gracilis* paramylon production through a cocultivation strategy with the indole-3-acetic acid-producing bacterium *Vibrio natriegens*. *Applied and Environmental Microbiology*, 85(19). https://doi.org/10.1128/AEM.01548-19/SUPPL_FILE/AEM.01548-19-S0001.PDF

Kisand, V., & Nõges, T. (2004). Abiotic and biotic factors regulating dynamics of bacterioplankton in a large shallow lake. *FEMS Microbiology Ecology*, 50(1), 51–62. <https://doi.org/10.1016/J.FEMSEC.2004.05.009>

Kobayashi, M., Hirai, N., Kurimura, Y., Ohigashi, H., & Tsuji, Y. (1997). Abscisic acid-dependent algal morphogenesis in the unicellular green alga *Haematococcus pluvialis*. *Plant Growth Regulation*, 22, 79–85. <https://doi.org/10.1007/BF00024378>

Kobayashi, M., Suzuki, T., Fujita, T., Masuda, M., & Shimizu, S. (1995). Occurrence of enzymes involved in biosynthesis of indole-3-acetic acid from indole-3-acetonitrile in

plant-associated bacteria, *Agrobacterium* and *Rhizobium*. *Proceedings of the National Academy of Sciences*, 92(3), 714–718. <https://doi.org/10.1073/PNAS.92.3.714>

Koenig, R. L., Morris, R. O., & Polacco, J. C. (2002). tRNA is the source of low-level trans-zeatin production in *Methylobacterium* spp. *Journal of Bacteriology*, 184(7), 1832–1842. <https://doi.org/10.1128/JB.184.7.1832-1842.2002>

Koga, J., Adachi, T., & Hidaka, H. (1991). Molecular cloning of the gene for indolepyruvate decarboxylase from *Enterobacter cloacae*. *MGG Molecular & General Genetics*, 226(1–2), 10–16. <https://doi.org/10.1007/BF00273581/METRICS>

Koizumi, I., Shiga, K., Irino, T., & Ikebara, M. (2003). Diatom record of the late Holocene in the Okhotsk Sea. *Marine Micropaleontology*, 49(1–2), 139–156. [https://doi.org/10.1016/S0377-8398\(03\)00033-1](https://doi.org/10.1016/S0377-8398(03)00033-1)

Koksharova, O. A., & Safronov, N. A. (2022). The effects of secondary bacterial metabolites on photosynthesis in microalgae cells. *Biophysical Reviews*, 14(4), 843–853. <https://doi.org/10.1007/S12551-022-00981-3>

Krug, L., Morauf, C., Donat, C., Müller, H., Cernava, T., & Berg, G. (2020). Plant growth-promoting *Methylobacteria* selectively increase the biomass of biotechnologically relevant microalgae. *Frontiers in Microbiology*, 11, 427. <https://doi.org/10.3389/fmicb.2020.00427>

Kumar, D. S., & Perumal, S. (2021). Gibberellic acids promote growth and exopolysaccharides production in *Tetraselmis suecica* under reciprocal nitrogen concentration: An assessment on antioxidant properties and nutrients removal efficacy of immobilized iron-magnetic nanoparticles. *BMC Plant Biology*, 21(1), 1–20. <https://doi.org/10.1186/s12870-021-03151-4>

Labeeuw, L., Khey, J., Bramucci, A. R., Atwal, H., De La Mata, A. P., Harynuk, J., & Case, R. J. (2016). Indole-3-acetic acid is produced by *Emiliania huxleyi* coccolith-bearing cells and triggers a physiological response in bald cells. *Frontiers in Microbiology*, 7, 828. <https://doi.org/10.3389/fmicb.2016.00828>

Langerhans, R. B. (2008). Coevolution. In *Encyclopedia of Ecology* (Vol. 5, pp. 644–648). Elsevier. <https://doi.org/10.1016/B978-008045405-4.00471-7>

Le Chevanton, M., Garnier, M., Lukomska, E., Schreiber, N., Cadoret, J. P., Saint-Jean, B., & Bougaran, G. (2016). Effects of nitrogen limitation on *Dunaliella* sp.–*Alteromonas* sp. interactions: From mutualistic to competitive relationships. *Frontiers in Marine Science*, 3, 123. <https://doi.org/10.3389/FMARS.2016.00123>

Le Reun, N., Bramucci, A., Ajani, P., Khalil, A., Raina, J. B., & Seymour, J. R. (2023). Temporal variability in the growth-enhancing effects of different bacteria within the microbiome of the diatom *Actinocyclus* sp. *Frontiers in Microbiology*, 14, 1230349. <https://doi.org/10.3389/FMICB.2023.1230349/BIBTEX>

Lutjeharms, J. R. E., & Machu, E. (2000). An upwelling cell inshore of the East Madagascar Current. *Deep Sea Research Part I: Oceanographic Research Papers*, 47(12), 2405–2411. [https://doi.org/10.1016/S0967-0637\(00\)00026-1](https://doi.org/10.1016/S0967-0637(00)00026-1)

Majzoub, M. E., Beyersmann, P. G., Simon, M., Thomas, T., Brinkhoff, T., & Egan, S. (2019). *Phaeobacter inhibens* controls bacterial community assembly on a marine diatom. *FEMS Microbiology Ecology*, 95(1), fiz060. <https://doi.org/10.1093/femsec/fiz060>

Manck, L. E., Park, J., Tully, B. J., Poire, A. M., Bundy, R. M., Dupont, C. L., & Barbeau, K. A. (2022). Petrobactin, a siderophore produced by *Alteromonas*, mediates community iron acquisition in the global ocean. *The ISME Journal*, 16(2), 358–371. <https://doi.org/10.1038/S41396-021-01065-Y>

Mandava, N. B. (2003). Plant growth-promoting brassinosteroids. *Annual Review of Plant Biology*, 39(1), 23–52. <https://doi.org/10.1146/ANNUREV.PP.39.060188.000323>

Mansouri, H., & Talebizadeh, R. (2017). Effects of indole-3-butyric acid on growth, pigments and UV-screening compounds in *Nostoc linckia*. *Phycological Research*, 65(3), 212–216. <https://doi.org/10.1111/PRE.12177>

Marie, D., Partensky, F., Jacquet, S., & Vaulot, D. (1997). Enumeration and cell cycle analysis of natural populations of marine picoplankton by flow cytometry using the nucleic acid stain SYBR Green I. *Applied and Environmental Microbiology*, 63(1), 186–193. <https://doi.org/10.1128/AEM.63.1.186-193.1997>

Martínez-Pérez, C., Zweifel, S. T., Pioli, R., & Stocker, R. (2024). Space, the final frontier: The spatial component of phytoplankton–bacterial interactions. *Molecular Microbiology*. <https://doi.org/10.1111/MMI.15293>

Matthews, J. L., Khalil, A., Siboni, N., Bougoure, J., Guagliardo, P., Kuzhiumparambil, U., Demaere, M., Le Reun, N. M., Seymour, J. R., Suggett, D. J., & Raina, J.-B. (2023). Coral endosymbiont growth is enhanced by metabolic interactions with bacteria. *Nature Communications*, 14, 1232. <https://doi.org/10.1038/s41467-023-42663-y>

Matthews, S., Siddiqui, Y., Supramaniam, C. V., & Ali, A. (2024). Boosting *Capsicum annuum* growth through a non-native endophytic bacterial consortium. *Journal of Plant Growth Regulation*, 43(8), 2739–2760. <https://doi.org/10.1007/S00344-024-11302-1/FIGURES/9>

Mayali, X. (2018). Editorial: Metabolic interactions between bacteria and phytoplankton. *Frontiers in Microbiology*, 9, 727. <https://doi.org/10.3389/FMICB.2018.00727> BIBTEX

Mazur, H., Konop, A., & Synak, R. (2001). Indole-3-acetic acid in the culture medium of two axenic green microalgae. *Journal of Applied Phycology*, 13, 35–42. <https://doi.org/10.1023/A:1017503028383>

McGee, D., Archer, L., Parkes, R., Fleming, G. T. A., Santos, H. M., & Touzet, N. (2021). The role of methyl jasmonate in enhancing biomass yields and bioactive metabolites in *Stauroneis* sp. (Bacillariophyceae) revealed by proteome and biochemical profiling. *Journal of Proteomics*, 249, 104381. <https://doi.org/10.1016/J.JPROT.2021.104381>

Mitri, S., & Foster, K. R. (2013). The genotypic view of social interactions in microbial communities. *Annual Review of Genetics*, 47, 247–273. <https://doi.org/10.1146/ANNUREV-GENET-111212-133307>

Moran, M. A., Buchan, A., González, J. M., Heidelberg, J. F., Whitman, W. B., Klene, R. P., Henriksen, J. R., King, G. M., Belas, R., Fuqua, C., Brinkac, L., Lewis, M., Johri, S., Weaver, B., Pai, G., Elsen, J. A., Rahe, E., Sheldon, W. M., Ye, W., ... Ward, N. (2004). Genome sequence of *Silicibacter pomeroyi* reveals adaptations to the marine environment. *Nature*, 432(7019), 910–913. <https://doi.org/10.1038/nature03170>

Moubayidin, L., Di Mambro, R., & Sabatini, S. (2009). Cytokinin-auxin crosstalk. *Trends in Plant Science*, 14(10), 557–562. <https://doi.org/10.1016/j.tplants.2009.06.010>

Muharram, M., Satria Bayu, A., & Rahardjo, P. (2019). Gibberellin and IAA production by rhizobacteria from various private forests. *IOP Conference Series: Earth and Environmental Science*, 270, 012018. <https://doi.org/10.1088/1755-1315/270/1/012018>

Nelson, D. M., Tréguer, P., Brzezinski, M. A., Leynaert, A., & Quéguiner, B. (1995). Production and dissolution of biogenic silica in the ocean: Revised global estimates, comparison with regional data and relationship to biogenic sedimentation. *Global Biogeochemical Cycles*, 9(3), 359–372. <https://doi.org/10.1029/95GB01070>

Nikolayevich, K. N., Evgenyevna, L. S., & Valerevich, M. E. (2023). Effect of auxin plant hormones on growth and biochemical composition of microalgae *Phaeodactylum tricornutum* Bohlin, 1897. *Vestnik of Astrakhan State Technical University. Series: Fishing Industry*, 2023(3), 97–105. <https://doi.org/10.24143/2073-5529-2023-3-97-105>

O'Brien, J., McParland, E. L., Bramucci, A. R., Siboni, N., Ostrowski, M., Kahlke, T., Levine, N. M., Brown, M. V., Van de Kamp, J., Bodrossy, L., Messer, L. F., Petrou, K., & Seymour, J. R. (2022). Biogeographical and seasonal dynamics of the marine Roseobacter community and ecological links to DMSP-producing phytoplankton. *ISME Communications*, 2(1), 1–13. <https://doi.org/10.1038/s43705-022-00099-3>

Olson, D. B., & Evans, R. H. (1986). Rings of the Agulhas current. *Deep Sea Research Part A. Oceanographic Research Papers*, 33(1), 27–42. [https://doi.org/10.1016/0198-0149\(86\)90106-8](https://doi.org/10.1016/0198-0149(86)90106-8)

Paerl, H. W., Justić, D., & Paerl, H. (2011). Primary producers: Phytoplankton ecology and trophic dynamics in coastal waters. In *Global Ecology and Biogeography* (pp. 1-32). Elsevier. <https://doi.org/10.1016/B978-0-12-374711-2.00603-3>

Palacios, O. A., Gomez-Anduro, G., Bashan, Y., & de-Bashan, L. E. (2016). Tryptophan, thiamine and indole-3-acetic acid exchange between *Chlorella sorokiniana* and the plant growth-promoting bacterium *Azospirillum brasiliense*. *FEMS Microbiology Ecology*, 92(6), 1–11. <https://doi.org/10.1093/FEMSEC/FIW077>

Patten, C. L., & Glick, B. R. (2002). Role of *Pseudomonas putida* indoleacetic acid in development of the host plant root system. *Applied and Environmental Microbiology*, 68(8), 3795–3801. <https://doi.org/10.1128/AEM.68.8.3795-3801.2002/ASSET/A25B82B9-3425-4F76-9838-7FAD1812F5FA/ASSETS/GRAFIC/AM0822027001.JPG>

Peng, H., de-Bashan, L. E., Bashan, Y., & Higgins, B. T. (2020). Indole-3-acetic acid from *Azospirillum brasiliense* promotes growth in green algae at the expense of energy storage products. *Algal Research*, 47, 101845. <https://doi.org/10.1016/J.AL GAL.2020.101845>

Pereira-Garcia, C., Sanz-Sáez, I., Sánchez, P., Coutinho, F. H., Bravo, A. G., Sánchez, O., & Acinas, S. G. (2024). Genomic and transcriptomic characterization of methylmercury detoxification in a deep ocean *Alteromonas mediterranea* ISS312. *Environmental Pollution*, 347, 123725. <https://doi.org/10.1016/J.ENVPOL.2024.123725>

Perley, J. E., & Stowe, B. B. (1966). On the ability of *Taphrina deformans* to produce indoleacetic acid from tryptophan by way of tryptamine. *Plant Physiology*, 41(2), 234–237. <https://doi.org/10.1104/PP.41.2.234>

Phoma, S., Vikram, S., Jansson, J. K., Ansorge, I. J., Cowan, D. A., Van De Peer, Y., & Makhalaanyane, T. P. (2018). Agulhas Current properties shape microbial community diversity and potential functionality. *Scientific Reports*, 8(1), 1–12. <https://doi.org/10.1038/s41598-018-28939-0>

Piotrowska-Niczypruk, A., & Bajguz, A. (2014). The effect of natural and synthetic auxins on the growth, metabolite content and antioxidant response of green alga *Chlorella vulgaris* (Trebouxiophyceae). *Plant Growth Regulation*, 73(1), 57–66. <https://doi.org/10.1007/S10725-013-9867-7/FIGURES/5>

Piotrowska-Niczypruk, A., Bajguz, A., Zambrzycka, E., & Godlewska-Żyłkiewicz, B. (2012). Phytohormones as regulators of heavy metal biosorption and toxicity in green alga *Chlorella vulgaris* (Chlorophyceae). *Plant Physiology and Biochemistry*, 52, 52–65. <https://doi.org/10.1016/J.PLAPHY.2011.11.009>

Quinn, G. P., & Keough, M. J. (2002). *Experimental Design and Data Analysis for Biologists*. Cambridge University Press. <https://doi.org/10.1017/CBO9780511806384>

Raina, J.-B., Giardina, M., Brumley, D. R., Clode, P. L., Pernice, M., Guagliardo, P., Bougoure, J., Mendis, H., Smriga, S., Sonnenschein, E. C., Ullrich, M. S., Stocker, R., & Seymour, J. R. (2023). Chemotaxis increases metabolic exchanges between marine picophytoplankton and heterotrophic bacteria. *Nature Microbiology*, 8(4), 510–521. <https://doi.org/10.1038/s41564-023-01327-9>

Ramanantsoa, J. D., Krug, M., Penven, P., Rouault, M., & Gula, J. (2018). Coastal upwelling south of Madagascar: Temporal and spatial variability. *Journal of Marine Systems*, 178, 29–37. <https://doi.org/10.1016/J.JMARSYS.2017.10.005>

Reun, N. L., Bramucci, A., O'Brien, J., Ostrowski, M., Brown, M. V., Van de Kamp, J., Bodrossy, L., Raina, J. B., Ajani, P., & Seymour, J. (2022). Diatom biogeography, temporal dynamics, and links to bacterioplankton across seven oceanographic time-series sites spanning the Australian continent. *Microorganisms*, 10(2), 338. <https://doi.org/10.3390/MICROORGANISMS10020338/S1>

Reynolds, C. S. (2006). The ecology of phytoplankton. In *The Ecology of Phytoplankton* (Vol. 31). Cambridge University Press. <https://doi.org/10.1017/CBO9780511542145>

Rinaldi, M. A., Ferraz, C. A., & Scrutton, N. S. (2022). Alternative metabolic pathways and strategies to high-titre terpenoid production in *Escherichia coli*. *Natural Product Reports*, 39(1), 90–118. <https://doi.org/10.1039/D1NP00025J>

Robertson, J. M., Garza, E. A., Stubbensch, A. K. M., Dupont, C. L., Hwa, T., & Held, N. A. (2024). Marine bacteria *Alteromonas* spp. require UDP-glucose-4-epimerase for

aggregation and production of sticky exopolymer. *mBio*, 15(1). https://doi.org/10.1128/MBIO.00038-24/SUPPL_FILE/MBIO.00038-24-S0001.PDF

Rooney-Varga, J. N., Giewat, M. W., Savin, M. C., Sood, S., Legresley, M., & Martin, J. L. (2005). Links between phytoplankton and bacterial community dynamics in a coastal marine environment. *Microbial Ecology*, 49(1), 163–175. <https://doi.org/10.1007/S00248-003-1057-0/FIGURES/7>

Ross, J. J., & Reid, J. B. (2010). Evolution of growth-promoting plant hormones. *Functional Plant Biology*, 37(9), 795. <https://doi.org/10.1071/FP10063>

Ross, J. J., Weston, D. E., Davidson, S. E., & Reid, J. B. (2011). Plant hormone interactions: How complex are they? *Physiologia Plantarum*, 141(4), 299–309. <https://doi.org/10.1111/j.1399-3054.2011.01444.x>

Ryther, J. H., & Guillard, R. R. L. (1962). Studies of marine planktonic diatoms: II. Use of *Cyclotella nana* Hustedt for assays of vitamin B12 in sea water. *Canadian Journal of Microbiology*, 8(4), 437–445. <https://doi.org/10.1139/m62-057>

Ryu, C. M., Hu, C. H., Locy, R. D., & Kloepper, J. W. (2005). Study of mechanisms for plant growth promotion elicited by rhizobacteria in *Arabidopsis thaliana*. *Plant and Soil*, 268(1), 285–292. <https://doi.org/10.1007/S11104-004-0301-9/METRICS>

Sadeghi, J., Chaganti, S. R., Shahraki, A. H., & Heath, D. D. (2021). Microbial community and abiotic effects on aquatic bacterial communities in north temperate lakes. *Science of The Total Environment*, 781, 146771. <https://doi.org/10.1016/J.SCITOTENV.2021.146771>

Salazar-Cerezo, S., Martínez-Montiel, N., García-Sánchez, J., Pérez-Y-Terrón, R., & Martínez-Contreras, R. D. (2018). Gibberellin biosynthesis and metabolism: A convergent route for plants, fungi, and bacteria. *Microbiological Research*, 208, 85–98. <https://doi.org/10.1016/J.MICRES.2018.01.010>

Segev, E., Wyche, T. P., Kim, K. H., Petersen, J., Ellebrandt, C., Vlamakis, H., Barteneva, N., Paulson, J. N., Chai, L., Clardy, J., & Kolter, R. (2016). Dynamic metabolic exchange governs a marine algal-bacterial interaction. *eLife*, 5. <https://doi.org/10.7554/eLife.17473>

Sekine, M., Watanabe, K., & Syono, K. (1989). Molecular cloning of a gene for indole-3-acetamide hydrolase from *Bradyrhizobium japonicum*. *Journal of Bacteriology*, 171(3), 1718–1724. <https://doi.org/10.1128/JB.171.3.1718-1724.1989>

Seymour, J. R., Amin, S. A., Raina, J. B., & Stocker, R. (2017). Zooming in on the phycosphere: The ecological interface for phytoplankton-bacteria relationships. *Nature Microbiology*, 2(7), 1–12. <https://doi.org/10.1038/nmicrobiol.2017.65>

Shao, Q., Lin, Z., Zhou, C., Zhu, P., & Yan, X. (2020). Succession of bacterioplankton communities over complete *Gymnodinium*-diatom bloom cycles. *Science of The Total Environment*, 709, 135951. <https://doi.org/10.1016/J.SCITOTENV.2019.135951>

Shibl, A. A., Isaac, A., Ochsenkühn, M. A., Cárdenas, A., Fei, C., Behringer, G., Arnoux, M., Drou, N., Santos, M. P., Gunsalus, K. C., Voolstra, C. R., & Amin, S. A. (2020). Diatom modulation of select bacteria through the use of two unique secondary metabolites.

Proceedings of the National Academy of Sciences, 117(44), 27445–27455. https://doi.org/10.1073/PNAS.2012088117/SUPPL_FILE/PNAS.2012088117.SD04.TXT

Shurin, J. B., Abbott, R. L., Deal, M. S., Kwan, G. T., Litchman, E., McBride, R. C., Mandal, S., & Smith, V. H. (2013). Industrial-strength ecology: Trade-offs and opportunities in algal biofuel production. *Ecology Letters*, 16(11), 1393–1404. <https://doi.org/10.1111/ele.12176>

Silveira, J. T. da, Rosa, A. P. C. da, Morais, M. G. de, & Costa, J. A. V. (2024). Indole-3-acetic acid action in outdoor and indoor cultures of *Spirulina* in open raceway reactors. *Applied Sciences*, 14(9), 3715. <https://doi.org/10.3390/APP14093715/S1>

Smirnova, M. A., Kazarina, G. K., Matul, A. G., & Max, L. (2015). Diatom evidence for paleoclimate changes in the northwestern Pacific during the last 20000 years. *Oceanology*, 55(3), 383–389. <https://doi.org/10.1134/S0001437015030157>

Smith, S. M., Li, C., & Li, J. (2017). Hormone function in plants. *Hormone Metabolism and Signaling in Plants*, 1–38. <https://doi.org/10.1016/B978-0-12-811562-6.00001-3>

Smith, V. H., & McBride, R. C. (2015). Key ecological challenges in sustainable algal biofuels production. *Journal of Plankton Research*, 37(4), 671–682. <https://doi.org/10.1093/plankt/fbv053>

Smriga, S., Fernandez, V. I., Mitchell, J. G., & Stocker, R. (2016). Chemotaxis toward phytoplankton drives organic matter partitioning among marine bacteria. *Proceedings of the National Academy of Sciences*, 113(6), 1576–1581. <https://doi.org/10.1073/pnas.1512307113>

Spaepen, S. (2015). Plant hormones produced by microbes. In *Principles of Plant-Microbe Interactions: Microbes for Sustainable Agriculture* (pp. 247–256). Springer. https://doi.org/10.1007/978-3-319-08575-3_26

Spaepen, S., & Vanderleyden, J. (2011). Auxin and plant-microbe interactions. *Cold Spring Harbor Perspectives in Biology*, 3(4), 1–13. <https://doi.org/10.1101/CSHPERSPECT.A001438>

Spaepen, S., Vanderleyden, J., & Remans, R. (2007). Indole-3-acetic acid in microbial and microorganism-plant signaling. *FEMS Microbiology Reviews*, 31(4), 425–448. <https://doi.org/10.1111/j.1574-6976.2007.00072.x>

Sreekumaran Nair, S. R., Devassy, V. P., & Madhypratap, M. (1992). Blooms of phytoplankton along the west coast of India associated with nutrient enrichment and the response of zooplankton. *Science of the Total Environment*, SUPPL., 819–828. <https://doi.org/10.1016/B978-0-444-89990-3.50071-7>

Stenow, R., Robertson, E. K., Whitehouse, M. J., & Ploug, H. (2023). Single cell dynamics and nitrogen transformations in the chain-forming diatom *Chaetoceros affinis*. *The ISME Journal*, 17(11), 2070–2078. <https://doi.org/10.1038/s41396-023-01511-z>

Stocker, R. (2015). The 100 µm length scale in the microbial ocean. *Aquatic Microbial Ecology*, 76(3), 189–194. <https://doi.org/10.3354/ame01777>

Stukenberg, D., Hoff, J., Faber, A., & Becker, A. (2022). NT-CRISPR, combining natural transformation and CRISPR-Cas9 counterselection for markerless and scarless genome editing in *Vibrio natriegens*. *Nature Communications*, 13(1), 1-13. <https://doi.org/10.1038/s42003-022-03150-0>

Sunagawa, S., Acinas, S. G., Bork, P., Bowler, C., Babin, M., Boss, E., Cochrane, G., de Vargas, C., Follows, M., Gorsky, G., Grimsley, N., Guidi, L., Hingamp, P., Iudicone, D., Jaillon, O., Kandels, S., Karp-Boss, L., Karsenti, E., Lescot, M., ... Lombard, F. (2020). Tara Oceans: Towards global ocean ecosystems biology. *Nature Reviews Microbiology*, 18(8), 428–445. <https://doi.org/10.1038/s41579-020-0364-5>

Suttle, C. A. (2007). Marine viruses—Major players in the global ecosystem. *Nature Reviews Microbiology*, 5(10), 801–812. <https://doi.org/10.1038/nrmicro1750>

Taoufik, G., Khouni, I., & Ghrabi, A. (2017). Assessment of physico-chemical and microbiological surface water quality using multivariate statistical techniques: A case study of the Wadi El-Bey River, Tunisia. *Arabian Journal of Geosciences*, 10(7), 1–19. <https://doi.org/10.1007/S12517-017-2898-Z/FIGURES/5>

Theunis, M., Kobayashi, H., Broughton, W. J., & Prinsen, E. (2007). Flavonoids, NodD1, NodD2, and Nod-Box NB15 modulate expression of the y4wEFG locus that is required for indole-3-acetic acid synthesis in *Rhizobium* sp. strain NGR234. *Molecular Plant-Microbe Interactions*, 17(10), 1153–1161. <https://doi.org/10.1094/MPMI.2004.17.10.1153>

Tran, D. Q., Milke, F., Niggemann, J., & Simon, M. (2023). The diatom *Thalassiosira rotula* induces distinct growth responses and colonization patterns of Roseobacteraceae, Flavobacteria, and Gammaproteobacteria. *Environmental Microbiology*, 25(12), 3536–3555. <https://doi.org/10.1111/1462-2920.16506>

Trombetta, T., Vidussi, F., Roques, C., Scotti, M., & Mostajir, B. (2020). Marine microbial food web networks during phytoplankton bloom and non-bloom periods: Warming favors smaller organism interactions and intensifies trophic cascade. *Frontiers in Microbiology*, 11, 502336. <https://doi.org/10.3389/FMICB.2020.502336/BIBTEX>

Udayan, A., & Arumugam, M. (2017). Selective enrichment of eicosapentaenoic acid (20:5n-3) in *Nannochloropsis oceanica* CASA CC201 by natural auxin supplementation. *Bioresource Technology*, 242, 329–333. <https://doi.org/10.1016/J.BIOTECH.2017.03.149>

Van Bruggen, A. H. C., Mathesius, U., Cox, C. E., Brandl, M. T., De Moraes, M. H., Gunasekera, S., & Teplitski, M. (2018). Production of the plant hormone auxin by *Salmonella* and its role in the interactions with plants and animals. *Frontiers in Microbiology*, 1, 2668. <https://doi.org/10.3389/fmicb.2017.02668>

Van Tol, H. M., Amin, S. A., & Armbrust, E. V. (2017). Ubiquitous marine bacterium inhibits diatom cell division. *ISME Journal*, 11(1), 31–42. <https://doi.org/10.1038/ismej.2016.112>

Vardi, A., Van Mooy, B. A. S., Fredricks, H. F., Popendorf, K. J., Ossolinski, J. E., Haramaty, L., & Bidle, K. D. (2009). Viral glycosphingolipids induce lytic infection and

cell death in marine phytoplankton. *Science*, 326(5954), 861–865. <https://doi.org/10.1126/science.1177322>

Wilkinson, S., & Davies, W. J. (2010). Drought, ozone, ABA, and ethylene: New insights from cell to plant to community. *Plant, Cell & Environment*, 33(4), 510–525. <https://doi.org/10.1111/J.1365-3040.2009.02052.X>

Yang, J., Kloepper, J. W., & Ryu, C. M. (2009). Rhizosphere bacteria help plants tolerate abiotic stress. *Trends in Plant Science*, 14(1), 1–4. <https://doi.org/10.1016/j.tplants.2008.10.004>

Yeh, Y. C., & Fuhrman, J. A. (2022). Effects of phytoplankton, viral communities, and warming on free-living and particle-associated marine prokaryotic community structure. *Nature Communications*, 13(1), 1-13. <https://doi.org/10.1038/S41467-022-35551-4>

Yu, J., Ding, B., Li, R., Chen, X., Yin, D., Song, M., & Ye, X. (2024). The efficient capture of polysaccharides in *Tetradesmus obliquus* of indole-3-acetic acid coupling sludge extraction. *Science of The Total Environment*, 912, 168963. <https://doi.org/10.1016/J.SCITOTENV.2023.168963>

Zhang, B., Chen, J., Su, Y., Sun, W., & Zhang, A. (2022). Utilization of indole-3-acetic acid-secreting bacteria in algal environment to increase biomass accumulation of *Ochromonas* and *Chlorella*. *Bioenergy Research*, 15(1), 242–252. <https://doi.org/10.1007/S12155-021-10246-8/FIGURES/3>

Zhao, Y. (2010a). Auxin biosynthesis and its role in plant development. *Annual Review of Plant Biology*, 61, 49–64. <https://doi.org/10.1146/ANNUREV-ARPLANT-042809-112308>

Zhou, J. L., Vadiveloo, A., Chen, D. Z., & Gao, F. (2024). Regulation effects of indoleacetic acid on lipid production and nutrient removal of *Chlorella pyrenoidosa* in seawater-containing wastewater. *Water Research*, 248, 120864. <https://doi.org/10.1016/J.WATRES.2023.120864>